DISCUSSION PAPER SERIES

DP18210

THE SOCIAL COST OF CARBON UNDER CLIMATE VOLATILITY RISK

Xu Lin and Sweder van Wijnbergen

ASSET PRICING

CEPR

THE SOCIAL COST OF CARBON UNDER CLIMATE VOLATILITY RISK

Xu Lin and Sweder van Wijnbergen

This Discussion Paper is issued under the auspices of the Centre's research programmes:

- Asset Pricing

Any opinions expressed here are those of the author(s) and not those of the Centre for Economic Policy Research. Research disseminated by CEPR may include views on policy, but the Centre itself takes no institutional policy positions.

The Centre for Economic Policy Research was established in 1983 as an educational charity, to promote independent analysis and public discussion of open economies and the relations among them. It is pluralist and non-partisan, bringing economic research to bear on the analysis of medium- and long-run policy questions.

These Discussion Papers often represent preliminary or incomplete work, circulated to encourage discussion and comment. Citation and use of such a paper should take account of its provisional character.

THE SOCIAL COST OF CARBON UNDER CLIMATE VOLATILITY RISK

Abstract

We calculate the social cost of carbon (SCC) under stochastic climate volatility resulting from uncertainty about future climate risk regimes where weather extremes are becoming more frequent and intense. Using a stochastic dynamic integrated climate-economy model where representative agents are endowed with Duffie-Epstein recursive preferences, we find that climate volatility risks substantially increase the SCC both in the business-as-usual and optimal abatement policy scenario. We also show that switching to a regime with more intense disasters increases the SCC more than a switch to a regime with more frequent disasters for equal expected value. Overall we show that \textit{stochastic volatility} has a major impact on the SCC.

Xu Lin - x.lin@uva.nl
Amsterdam School Of Economics University Of Amsterdam

Sweder van Wijnbergen - s.j.g.vanwijnbergen@uva.nl
Amsterdam School of Economics and Tinbergen Institute, University of Amsterdam and CEPR

The Social Cost of Carbon under Climate Volatility Risk

Xu Lin [*]   Sweder van Wijnbergen [†]

June 9, 2023

Abstract

We calculate the social cost of carbon (SCC) under stochastic climate volatility resulting from uncertainty about future climate risk regimes where weather extremes are becoming more frequent and intense. Using a stochastic dynamic integrated climate-economy model where representative agents are endowed with Duffie-Epstein recursive preferences, we find that climate volatility risks substantially increase the SCC both in the business-as-usual and optimal abatement policy scenario. We also show that switching to a regime with more intense disasters increases the SCC more than a switch to a regime with more frequent disasters for equal expected value. Overall we show that *stochastic volatility* has a major impact on the SCC.

---

[*]Amsterdam School of Economics, University of Amsterdam and Tinbergen Institute.
[†]Amsterdam School of Economics, University of Amsterdam, Tinbergen Institute and CEPR.

1 Introduction

Recent years have witnessed increasing volatility of climate disasters. As the global temperature rises, extreme weather events once considered rare are becoming more prevalent. More extreme deviations from climatological normals, such as the record-breaking North American heatwaves in 2021, are happening. Climate scientists and meteorologists have warned that extreme weather events will become more frequent and more intense with human-induced climate change (Reidmiller et al. (2018), IPCC (2021)). Moreover, climate disasters and the damages they inflict are not only becoming more frequent but also more volatile over time. Uncertainty about the timing and size of increasing climate volatility has inspired climatologists to develop models to predict unprecedented extremes (Thompson et al. (2017), Kelder et al. (2020)), but the implications of the risk that such distributional changes may occur have not been studied by climate economists. Current climate-economy models incorporate only the uncertainty about climate damage itself, by assuming that climate damage is a stochastic process with known drift and volatility. Different from these existing models, our paper focuses on higher-order climate uncertainty – the risk of changes in climate volatility – a risk that has been pointed out by climate scientists. In particular we study how uncertainty about climate volatility affects the social cost of carbon (SCC). In our model we emphasize that climate volatility itself is subject to stochastic change, which has not been discussed in the climate economics literature.

The SCC estimates the marginal economic damages resulting from one additional unit of carbon emission into the atmosphere. It measures negative externalities of climate change and has been adopted by many governments to motivate climate policies. In the US, the SCC has been widely used in regulatory analysis, federal carbon tax legislation, and developing energy efficiency standards for appliances (Rennert et al. (2022)). Basic economic theory suggests that an optimal carbon tax be set equal to the SCC, although this may be an oversimplified answer to a complex policy problem involving global coordination and undesirable distributional consequences. We will not address these challenges in this paper,

although they are of vital importance in policy discourse. Our focus is on climate volatility risk and on its implications for the SCC.

There is a large literature on estimating the SCC under various aspects of uncertainty such as economic fluctuations and shocks to cumulative atmospheric carbon concentration (see for example Cai and Lontzek (2019), Van den Bremer and Van der Ploeg (2021), Hambel et al. (2021), Jensen and Traeger (2021)). But climate economists have not paid attention yet to the fact that climate volatility itself is subject to uncertainty. Bansal et al. (2017) introduced endogenous volatility in their model by assuming that both the frequency and damage sizes of climate disasters increase once temperature reaches a tipping point, but did not study the impact of climate volatility risk explicitly. Their main focus is on the long-run impact of temperature on consumption growth and asset prices. The lack of explicit attention to stochastic climate volatility is maybe to be expected: more frequent record-setting weathers have only materialized recently and climate research on predicting future climate volatility is still at its infancy. Nevertheless, given the irreversibility of shifting to a climate regime with higher volatility and its ramifications for welfare, we consider it important to assess this potential risk explicitly, no matter how limited our current knowledge is.

We set up a continuous-time integrated climate-economy model and compute the SCC under a stylized but general equilibrium asset pricing framework. The economy is modeled as a pure-exchange economy so we abstract from the production process: agents receive endowments over time. Endowments cannot be stored and therefore must be spent on either consumption or abatement. Their growth is affected by economic fluctuations, economic crises and climate damages. Climate conditions are characterized by the mean global surface temperature and the distribution of climate damages. The mean global surface temperature is assumed to increase linearly in cumulative carbon emissions, following Dietz et al. (2021). Climate damages are induced solely by climate-related natural disasters. The arrival of climate disasters follows a Poisson process and the economic damage from such a disaster event

2

is a stochastic variable itself. Therefore the distribution of climate damage is characterized both by the arrival rate of climate disasters and by the distribution of the size of a given disaster event once it arrives (i.e. once the Poisson shock hits).

To introduce climate volatility risk, we consider two climate risk regimes, the current one and one with more frequent and extreme climate disasters which will arrive in the future but with uncertain severity and timing. Little is known about the severity of climate disasters in the new regime, so we solve the model under two assumptions about this new climate regime: (A) climate disasters happen more frequently, and (B) climate disasters become more extreme. And given our limited knowledge on the timing of the regime shift, we assume in the main part of this paper that the arrival of the new climate risk regime follows a Poisson process with arrival rate 0.01 so that the expected arrival time is 100 years. [The 100 year time horizon is primarily chosen by the first IPCC reports. This choice is close to the atmospheric lifetimes of greenhouse gases and avoids distortions of socioeconomic scenarios in distant future (Abernethy and Jackson (2022)).[1]] For simplicity, the climate regime shift is regarded as a one-off event and is irreversible: climate change is irreversible. In the main part of the paper we assume that climate volatility increases abruptly upon a regime shift; towards the end of the paper, in Section 6, we also consider a more gradual alternative where the long run volatility jumps instantaneously but actual volatility catches up with that shift only gradually over time after the arrival of the new regime. In addition, we examine the effect of abatement policies on the SCC by comparing two policy scenarios. The first policy scenario is the business-as-usual (BAU) case where little or no effort is made on reducing greenhouse gas emissions. The second one implements optimal abatement policy which aims to maximize total welfare through reducing carbon emissions.

We find that stochastic climate volatility leads to substantially higher risk premia but also that it nevertheless leads to a significantly higher SCC. And the climate-volatility risk premium is of the same order of magnitude as the risk premium stemming from climate

---

[1]Some criticize the use of 100-year horizon as unjustified. Therefore, we also show the numerical results under other possible values of arrival rates in Appendix C.

volatility itself. The climate-volatility risk premium increases with the frequency and intensity of the climate disasters in the new climate regime, as well as with the arrival rate of the new climate regime. Climate volatility risk also has an impact on the equilibrium risk-free rates but overall discount rates go up. Climate volatility risk influences the SCC through two channels: (a) the discount rate of future consumption and (b) the certainty equivalent expected value of the consumption flows being discounted. The two channels work in opposite direction but we unambiguously show that the stochasticity of climate volatility leads to a higher SCC. Furthermore we also show that for given climate severity in the new climate regime, the SCC under a stochastic regime shift expected to arrive in 2115 is much larger than the SCC under a similar but deterministic climate regime shift arriving with certainty in 2115.

And finally we establish that switching to a regime with more intense and less frequent climate disasters induces a higher SCC than shifting to a regime with more frequent but correspondingly less intense climate disasters for equal expected value of annual climate damages under both regimes.[2] Also the response of the SCC to changes in the characteristics of the new regime is stronger under stringent emission control than it is in the Business-As-Usual scenario. For example, doubling the arrival rate of climate disasters in the new climate risk regime for given intensity raises the average SCC in 2025 from $376 to $505 per ton of carbon in the business-as-usual scenario (up by 34%), but with optimal abatement it rises from $385 to $548 per ton of carbon (up by 42%). And by considering a new climate risk regime where climate disasters are twice as intense for equal arrival rate, the average social cost of carbon in 2025 will rise from $376 to $522 (up by 39%) in the business-as-usual scenario but from $395 to $574 per ton of carbon in optimal abatement scenario (up by 45%).

We obtain similar implications from several alternative model assumptions. First, we repeat the same numerical exercises under endogenous emissions. The results show that

---

[2]This holds in our model and for our parameter specifications, but may not generalise to other specifications or parameter values.

endogenizing carbon emissions does not qualitatively change the results obtained under exogenous emissions. Second, we find that smoothing the increase in climate volatility does not have a major impact on the SCC. This contributes to the discussion on whether inadequately capturing the geophysical processes of irreversible phase changes in the climate system would lead to lower economic costs of climate damages (Dietz et al. (2021)). In prior studies on climate tipping, some explicitly model the corresponding geographical processes, leading to gradual tipping processes. Others adopt more reduced-form climate models where tipping processes are abrupt. Our paper considers both gradual and abrupt changes in climate volatility. We show that smoothing the tipping processes generates lower SCCs, since a more gradual response to a positive shock in the long run value of climate volatility implies a lower time path for volatility after the shock has arrived.

Stochastic regime shifts have been studied earlier in the more general macroeconomic literature. For example, Lettau et al. (2008) explain the persistent above-norm US aggregate stock prices by a shift to a lower macroeconomic volatility regime in the 1990s. They model the transitions between a high and a low macroeconomic volatility state as a Markov switching process. Our model has a similar structure. We assume that the transition from a low-volatility to a high-volatility regime follows a Poisson process, but we differ from Lettau et al. (2008) in that the climate regime shift is one-off and irreversible: once the stochastic regime shifts, climate volatility rises abruptly and irreversibly.

Modelling stochastic transitions among different regimes is a simplified way to analyse volatility uncertainty and can be extended to richer risk structures. The modelling of volatility risk originates from financial economics and mathematical finance, where it has been used extensively to explain asset market features. A thorough discussion of stochastic volatility models is provided in Shephard and Andersen (2009). Also, already since the early 1970s various stochastic volatility models have been used to explain empirically observed departures from Black-Scholes, such as time-varying and non-stationary volatility processes (Clark (1973), Taylor (2018), Hull and White (1987), Wiggins (1987), Barndorff-Nielsen and

Shephard (2001), Eraker et al. (2003), etc.). More recent studies show that higher-order uncertainties such as the volatility of volatility and the volatility-of-volatility risk are themselves significant risk factors which affect option returns (Branger et al. (2018), Huang et al. (2019), Hu and Liu (2022), Eraker and Yang (2022), etc.). To check whether a richer risk structure of climate volatility leads to different model implications, we provide an alternative model of climate volatility risk in Section 6. There we assume that the climate disaster frequency follows a Cox–Ingersoll–Ross (CIR) process with its long-run value subject to a one-off irreversible Poisson jump upon the climate regime shift while the actual volatility shifts gradually towards its new long run value. Our numerical results suggest that climate volatility risk yields similar asset pricing implications under different specifications of volatility risk.

Our model of stochastic climate volatility differs from the climate tipping points discussed by many climate economists. In the current literature, climate tipping has a broad definition including nonlinear geophysical feedbacks and abrupt phase changes (Kopp et al. (2016)). Dietz et al. (2021) provides a unified estimate of economic impacts of eight climate tipping points covered in the economic literature using a meta-analytic integrated assessment model. Tipping points considered in their paper can be broadly divided into three categories: positive feedbacks between the carbon cycle and temperature, ice shelf disintegration, and changes in large-scale circulation. However, most economic studies represent climate tipping points in a highly stylized way. For example, Gjerde et al. (1999) models the costs of climate tipping directly as a utility loss. Lemoine and Traeger (2014) models climate tipping as abrupt irreversible shifts in system dynamics and studies the impact of uncertain climate tipping on the optimal carbon tax. They consider two types of climate tipping points: an increase in the strength of temperature feedbacks and a decrease in the ability of the earth system to remove carbon. Lontzek et al. (2015) point out that these assumptions on climate tipping are scientifically questionable. To study the impact of climate tipping on optimal policy choice, Lontzek et al. (2015) model climate tipping points as abrupt reductions in GDP. In

our baseline model, stochastic climate volatility is modelled as a one-off irreversible increase in climate volatility which falls into the broad definition of climate tipping but so far has not been discussed in the literature. Like climate tipping points, climate volatility risk is not really reflected in current policy advice, presumably because its economic consequences are subject to considerable uncertainty, and relevant parameters are nearly impossible to calibrate.

Our stochastic dynamic integrated assessment model (IAM) builds on Olijslagers (2020) which estimates the social cost of carbon under rare disaster risks using a high-dimensional stochastic dynamic IAM with a realistic climate model in a continuous-time framework. Our model includes rare disasters both from economic disruptions and climate change. These disasters are modelled as discrete shocks to economic outputs as in Barro (2006), Barro (2009) and Pindyck and Wang (2013). Since disaster risk can generate the high equity premia and low risk-free rates observed in the data, it is of vital importance to include disaster shocks in the model, because the SCC is essentially the expected discounted future damages from climate change. To get a clear picture of how the stochastic climate regime shift affects the social cost of carbon, we use a simplified climate model where temperature is approximately linear in cumulative carbon emissions (as in Matthews et al. (2009) and Van den Bremer and Van der Ploeg (2021)), and do not model explicitly other determinants of global warming such as atmospheric carbon decay, the earth's heat radiation, radiative forcing, and heat absorption by the ocean. In contrast, Hambel et al. (2021) models the dynamics of atmospheric carbon concentration with unexpected environmental shocks and accounts for the amount of carbon absorbed by natural sinks. Temperature follows a self-exciting process which captures the delayed climate feedback effects (IPCC (2007)) and the right-skewed distribution of future temperatures (Roe and Baker (2007)). Olijslagers and van Wijnbergen (2019) use the IPCC AR5 impulse-response model discussed in Mattauch et al. (2018). This model accounts for the nonlinear response of temperature to carbon emission. We use a simpler structure than those detailed climate models, temperature changes in our

model are linear in emission flows. This simplification buys computational convenience at the expense of a slight distortion of climate dynamics.

The rest of the paper is structured as follows: Section 2 describes the stochastic IAM and Section 3 outlines the model calibration. Section 4 shows the numerical results under different types of climate regime shifts. Section 5 compares the numerical implications under exogenous and endogenous emissions. Section 6 provides an alternative model of climate volatility risk and compares its numerical results with those from Section 4 under the BAU scenario. Section 7 concludes.

2 The Model

In this section, we describe the stochastic integrated climate and economic model for estimating the social cost of carbon. It consists of two blocks: an endowment economy where representative agents are endowed with recursive preferences, and a climate system characterized by the temperature and climate risk regime.

2.1 The Climate Model

While climate change has a broader meaning, here we focus on anthropogenic global warming due to the increasing atmospheric carbon concentration caused by fossil fuel combustion during manufacturing. Initially, in Section 4 we assume for computational convenience that carbon emissions E are exogenous Without abatement, like in Olijslagers (2020). E increases annually with economic growth but starts to decline at the beginning of the next century as fossil fuel stocks are exhausted.

Of course in reality, carbon emissions are stochastic and dependent on aggregate economic output. We therefore provide a more realistic model in Section 5 where endogenous emissions are a function of aggregate endowment and carbon intensity. We show that both the exogenous and the endogenous setups generate similar implications on how climate volatility risk

affects the SCC. We focus initially on the exogenous case because only with that simplification the model allows for analytical results. In the more general model with endogenous and stochastic emissions used in Section 5 we show numerically that whether carbon emissions are exogenous or endogenous does not matter much for our conclusions.

The growth rate $r_{E,t}$ of emission is given by $r_{E,t} = e^{-\delta_E t} r_{E,0} + \left(1 - e^{-\delta_E t}\right) r_{E,\infty}$. Its initial value $r_{E,0}$ moves slowly to its long-run level $r_{E,\infty}$ at the rate δ_E. Without abatement, the emission dynamics are given by $dE_t = r_{E,t} E_t dt$, starting from the initial emission level E_0. In Section 5 we link emissions the stochastic output process. Let $u_t \in [0, 1]$ be the emission control rate at t, then the actual carbon emission $\tilde{E}_t := (1 - u_t) E_t$. Since large scale carbon capture and storage seems to be out of reach technologically, the emission control rate in our model cannot exceed 100%.

Changes in mean global surface temperature T_t are linearly dependent on the emission flow because of our assumption that the total carbon concentration in the atmosphere affects temperature linearly and decays slowly over time. The dynamics of temperature are then given by

$$dT_t = \chi(1 - u_t) E_t dt$$

where χ is the transient climate response to cumulative carbon emissions. For the sake of computational simplicity we take temperature as a deterministic process increasing linearly in carbon emission, and do not model explicitly the more complex dynamics of atmospheric carbon concentration and temperature used in Olijslagers (2020).

We model the stochastics of climate volatility as a one-off irreversible switch of climate regime from a low-volatility to a high-volatility one. This irreversible regime shift is modelled as a one-off Poisson shock N_0 to climate volatility with arrival rate λ_0. Given limited knowledge about more extreme scenarios in the new climate regime at the current stage, we focus on the simple case where λ_0 is exogenously given and is independent of climate con-

ditions. Two different types of regime shift are considered, under which the climate system will switch to a new regime where climate disasters either (A) happen more frequently but at the same scale as in the current regime, or (B) become more extreme but happen at the same frequency as in the current regime. In Section 4, we compare regime shifts where the frequency or the expected scale of climate disasters are respectively doubled and quadrupled, and compare the SCCs under these different climate regimes.

In particular Dietz et al. (2021) has argued that tipping points are unlikely to occur instantaneously in real time. Therefore we provide in Section 6 an alternative model of climate volatility risk where climate volatility increases gradually over time. Numerical results from this alternative model shows that smoothing the response to the positive shock in the long-run climate volatility implies a lower time path for the SCC, because a more gradual response implies a lower time path for climate volatility after the shock arrives. For now we simplify the risk of climate volatility as a one-off stochastic jump as described above. Such simplification enables us to obtain clear analytical expressions for the pricing effect of stochastic climate volatility, and is consistent with the shift in the long run distribution of climate disasters used in Section 6.

2.2   The Economic Model

We consider a continuous-time stochastic pure exchange economy in order to generate analytical results and maintain tractability. A representative agent owns an asset which pays a flow of dividends (endowments) at any time t. The time-t endowment flow Y_t is affected by diffusion risks and occasional crises in the economic system as well as damages from climate disasters. Its dynamic is given by

$$dY_t = \mu Y_t dt + \sigma Y_t dZ_t - J_1 Y_{t-} dN_{1,t} - J_2 Y_{t-} dN_{2,t}$$

where μ and σ are the growth rate and volatility of the endowment, Z_t is a standard Brownian motion representing the diffusion economic risks. Economic disasters such as financial crises are introduced by the Poisson process N_1 like in Barro (2009), which is necessary to generate empirically plausible discount rates for future payoffs which in turn is essential for the calculation of the SCC. The Poisson process N_1 has a constant arrival intensity λ_1 and reduces the endowment flow by $J_1 \in (0, 1)$ upon each arrival. We assume $X := 1 - J_1$ is a random variable with density $f(x) = \alpha_1 x^{\alpha_1 - 1}$, which implies an average economic disaster size $\mathbb{E}J_1 = \frac{1}{\alpha_1 + 1}$. Endowments are also negatively affected by damages from climate disasters which we capture by the Poisson process N_2 with arrival rate $\lambda_{2,t} := \bar{\lambda}_t T_t$. The size of climate damage is characterized by the random variable J_2 following the same distribution as J_1 but with a different parameter $\alpha_{2,t}$, like in Olijslagers (2020).

Climate volatility is characterized by the frequency parameter $\lambda_{2,t}$ and expected damage size $\mathbb{E}_t J_2 := \frac{1}{\alpha_{2,t} + 1}$ of climate disasters; both parameters together determine how uncertain climate damages are. Upon the Poisson climate regime shift with rate λ_0, $\lambda_{2,t}$ and $\alpha_{2,t}$ might increase, which correspond to the two types of climate volatility risks, Type (A) and Type (B), that we discussed in Section 2.1. We assume that for Type (A) the value of $\bar{\lambda}_t$ jumps upwards from $\bar{\lambda}^{(L)}$ to $\bar{\lambda}^{(H)}$ upon the regime shift. For (B), the expected damage size of one climate disaster $\mathbb{E}J_2$ increases from $\mathbb{E}J_2^{(L)} := \frac{1}{\alpha_2^{(o)} + 1}$ to $\mathbb{E}J_2^{(H)} := \frac{1}{\alpha_2^{(n)} + 1}$ upon the one-off climate regime shift, which is equivalent to a decrease of $\alpha_{2,t}$ from $\alpha_2^{(o)}$ to $\alpha_2^{(n)}$. In this model, climate volatility risk is characterized by λ_0, $\frac{\bar{\lambda}^{(H)}}{\bar{\lambda}^{(L)}}$ and $\frac{\mathbb{E}J_2^{(H)}}{\mathbb{E}J_2^{(L)}}$, where λ_0 stands for the timing risk, $\frac{\bar{\lambda}^{(H)}}{\bar{\lambda}^{(L)}}$ represents the increase in disasters frequency, and $\frac{\mathbb{E}J_2^{(H)}}{\mathbb{E}J_2^{(L)}}$ captures the increase in disasters intensity in the new regime.

The endowment Y_t cannot be stored for future expenditure and has to be spent on either consumption C_t or abatement A_t at time t. The abatement costs follows the same structure as in Nordhaus (2017) and are given by $A_t = c_{1,t} u_t^{c_2} Y_t$, where $c_{1,t}$ captures the effect of technology process on abatement cost and declines over time and $c_2 > 1$ characterizes the increase of marginal cost in the emission control rate u_t. The consumption flow is then given

by

$$C_t = Y_t - A_t = (1 - c_{1,t}u_t^{c_2})Y_t := \xi_t Y_t$$

where $\xi_t = \frac{C_t}{Y_t} = (1 - c_{1,t}u_t^{c_2})$ is the consumption-endowment ratio.

We model the preferences of the representative agent by stochastic differential utility (Duffie and Epstein (1992)) which is the continuous-time version of Epstein-Zin preferences. This allows us to separately vary risk aversion γ and the elasticity of intertemporal substitution (EIS) ϵ. By separating risk aversion and EIS, such preference can generate non-trivial and empirically plausible risk premia by increasing risk aversion without compromising the model's explanatory power on historical financial data. Moreover, the value of these preference parameters affects agents' attitude towards temporal resolution of uncertainty which in turn is critical to explain the dynamics under expected future regime shift risks. When $\gamma > \frac{1}{\epsilon}$, agents prefer an early resolution of uncertainty about future consumption. If $\gamma = \frac{1}{\epsilon}$, this boils down to the power utility and the timing of resolution of uncertainty becomes irrelevant.

Representative agents face a trade-off between less consumption today under abatement or lower consumption in the future under more severe climate damages. Formally, agents' value function is defined recursively as

$$V_0 = \max_{u_t} \mathbb{E}_0 \int_0^\infty f(C_t, V_t)dt$$

with $f(C,V) = \frac{\beta}{1-\frac{1}{\epsilon}} \frac{C^{1-\frac{1}{\epsilon}} - [(1-\gamma)V]^{\frac{1}{\zeta}}}{[(1-\gamma)V]^{\frac{1}{\zeta}-1}}$ as in Duffie and Epstein (1992), $\epsilon \neq 1$, $\zeta = \frac{1-\gamma}{1-\frac{1}{\epsilon}}$, and β the time discount rate. Appendix A provides the numerical procedures we use to solve this optimization problem.

2.3 The Social Cost of Carbon

The social cost of carbon (SCC) measures the marginal cost of carbon emission. It is the present value of damages due to a marginal increase in carbon emissions today. Formally,

SCC is defined as the marginal utility of carbon emissions scaled by marginal utility of consumption, which allows us to express SCC in terms of units of current consumption goods. At time 0, SCC can be written as

$$SCC_0 = -\chi \frac{\partial V_0 / \partial T_0}{f_C(C_0, V_0)} \tag{1}$$

where $f_C(C_0, V_0)$ is the marginal utility of consumption at time 0.

3 Calibration

Following Johansson et al. (2012), we set the endowment growth rate at $\mu = 3\%$ and endowment volatility at $\sigma = 2.5\%$. Barro and Jin (2011) estimates that rare economic disasters arrive at rate 0.035 with size parameter $\alpha_1 = 6.5$, which generates an estimate of risk aversion γ around 4 by approximating the observed risk premium in the market. Olijslagers (2020) calibrates $\epsilon = 1.5$ and $\beta = 0.025$, which, together with risk aversion $\gamma = 4.3$, yields reasonable approximations of the estimated worldwide average risk-free rate and equity risk premium during the period 1900-2010 in Dimson et al. (2011). Given that the arrival rate of climate disasters is linear in temperature, we follow Karydas and Xepapadeas (2019) who find that the arrival rate increases by $\bar{\lambda}^{(L)} = 6\%$ if temperature rises by $1°C$ in the current climate regime. The mean disaster size is 1.5% which implies $\alpha_2^{(o)} = 65$ before the regime shift.

Parameters of carbon emission under BAU scenario are set to resemble the projected industrial carbon emissions in the baseline scenario in Nordhaus (2017). Taking 2015 as the starting point of our simulation, we set the initial CO_2 emission level at 35.6 gigatonnes with initial growth rate $r_{E,0} = 1.7\%$. The growth rate of carbon emission decreases over time at an annual rate 0.75% until reaching its long-run level -2%. The abatement cost function follows the same as in the RICE-2010 model (Nordhaus (2010)) with time-decreasing technology effect $c_{1,t} = 0.074e^{-0.019t}$ and cost nonlinearity $c_2 = 2.8$. The mean global mean

surface temperature is approximately 0.83°C in 2015 (source: NASA) and gradually rises as cumulative carbon increases. Matthews et al. (2012) shows that the 90% confidence interval of transient climate response (TCR) to carbon emissions is between 1°C and 2.5°C per teraton of carbon. We take $\chi = 1.8°C/TtC$ in the simulation as in Olijslagers et al. (2023).

Calibrating climate volatility risk is difficult for lack of time series data. Since the negative impact of climate change is going up fast over time, climate volatility in the future cannot be predicted using historical climate data. In the next section we therefore run simulations for several possible values of $\bar{\lambda}^{(H)}$ and $\alpha_2^{(n)}$ to characterize the post-shift climate regime. In Appendix C, we provide numerical results under different arrival rate λ_0 of the shocks to climate volatility.

4   The SCC and Climate Volatility Risk: Numerical results

We numerically solve the integrated assessment model of Section 2 under two different type of shocks to the volatility process and two different assumptions about economic policy, so we present four scenario's. First we distinguish a new climate regime characterized by a higher arrival rate of the Poisson shock versus one with a shift towards a bigger shock conditional on arrival but for given arrival rate. And second we analyse both types of shocks under a Business As Usual (BAU) scenario and under optimal abatement.[3]

Research has to date not told us much about higher-order uncertainties in the climate system, in particular little is known about the timing and the scale of a future climate regime shift. We assume that the base case climate regime shift has an arrival rate $\lambda_0 = 0.01$. This implies an expected arrival time of 100 years, which is close to the atmospheric lifetimes of greenhouse gases and avoids distortions of socioeconomic scenarios in distant

---

[3]All scenario's are solved for using finite difference methods with 2015 as the initial year of simulation and number of simulation $K = 5000$. Time range of the simulation is 500 years, and results are provided up to Year 2100.

14

future (Abernethy and Jackson (2022)).[4]

We now turn to analyzing the two different types of regime shift: (A) an increase in the frequency of climate disasters (Section 4.1) and (B) a rise in their intensities (Section 4.2). For (A) we present numerical results for $\bar{\lambda}^{(H)}/\bar{\lambda}^{(L)} = 1, 2$ and 4, i.e. a base case where the arrival rate does not change and two cases where the arrival rate respectively doubles and quadruples. For the scenario's under (B), we apply the same multipliers but with respect to the expected size of climate disasters in the new regime.

4.1 The New Climate Regime (A): a Higher Disaster Frequency

We first consider the case where under climate volatility risk the frequency of climate disasters increases in the new regime while their intensity does not change. Call this regime (A). Since the SCC depends on future consumption flows under climate damages but also on discount rates, calculating its value fits well into the regular asset pricing framework: the SCC can be taken as the current price of an asset which pays the amount of climate-induced future losses in consumption flow as "dividend" in each period. The risk-free rate and the risk premium of this asset are key components of the consumption discount rate, so we present the impact of climate volatility risk on them first, before turning to the SCC itself.

4.1.1 The risk-free rate, climate risks and climate volatility risk

The model without regime shift allows for analytical solutions: see the first three terms of Equation 2 for the risk-free rate r_t^f. The fourth term represents the impact of the regime shift on the risk-free rate and requires numerical procedures for evaluation (the derivation is

---

[4]In Appendix C we present numerical results for different values of λ_0.

in Appendix A). So the instantaneous risk-free rate at time t is given by

$$r_t^f = \underbrace{\beta + \frac{\mu_{C,t}}{\epsilon} - \frac{\gamma}{2}\left(1 + \frac{1}{\epsilon}\right)\sigma^2}_{Standard} + \underbrace{\lambda_1\left(\frac{\gamma - 1/\epsilon}{\alpha_1 + 1 - \gamma} - \frac{\gamma}{\alpha_1 - \gamma}\right)}_{Econ.\ disasters} + \underbrace{\lambda_{2,t}\left(\frac{\gamma - 1/\epsilon}{\alpha_2 + 1 - \gamma} - \frac{\gamma}{\alpha_2 - \gamma}\right)}_{Clim.\ disasters}$$

$$+ \underbrace{\lambda_{0,t}\mathcal{J}_{f,t}}_{Regime\ shift} . \tag{2}$$

where $\mu_{C,t}$ is the consumption growth rate (see Appendix A for detail), $\lambda_{0,t} := \lambda_0\left(1 - N_{0,t-}\right)$ is the arrival rate of a new climate regime, $N_{0,t-}$ is the corresponding Poisson variable equal to 0 before and to 1 after the shock has occurred, and $\mathcal{J}_{f,t}$ captures the effect of climate volatility risk due to the uncertain regime switch. Equation (2) is similar to the expression for risk-free rate in Olijslagers (2020), except for the last term $\lambda_{0,t}\mathcal{J}_{f,t}$ which is due to the climate volatility risk analyzed in this paper.

The first component of Equation (2) is the standard expression for the risk-free rate when disaster risks are absent. β represents time preference, $\frac{\mu_{C,t}}{\epsilon}$ captures the intertemporal smoothing effect, and $-\frac{\gamma}{2}\left(1 + \frac{1}{\epsilon}\right)\sigma^2$ captures the precautionary saving effect. The second and third component represent the impact of rare economic and climate disaster risks respectively. Both depend on their respective arrival rate λ_1 and $\lambda_{2,t}$ and corresponding disaster intensities α_1 and $\alpha_{2,t}$. We assume without loss of generality that the parameters for the economic disaster process are time-invariant. Both the second and the third term are negative for the parameters chosen in Section 3: disaster risks always reduce the risk-free rate given that we have chosen $\epsilon > 1$. In particular climate volatility is characterized by $\lambda_{2,t}$ and $\alpha_{2,t}$ and thus also has a negative impact on the risk-free rate.

The fourth and last component captures the impact of climate volatility risk, which affects the risk-free rate through two channels: (a) the risk of a new climate shift leads to higher *expected* climate damages in the future, which leads to a lower safe real rate now, (b) the risk of a new climate shift represents an additional source of risk. Both channels lead to higher prices of future goods or, equivalently, a lower safe rate of interest. We refer

to these two channels as the expectation effect and the risk effect of climate volatility risk. Intuitively, we can take the one-off stochastic regime shift as a compound Poisson process with its jump process characterized by N_0 and its jump size captured by the climate severity in the new regime. Then the expected value of the compound Poisson process can under mild conditions (independence of the arrival rate and the jump size) be decomposed into two parts using Wald's equation: the jump risk (i.e. the risk effect) and the expected size of each jump (i.e. the expectation effect).

The expectation effect is the difference between the effects of climate disasters with and without regime shift risk on r^f (the third term in Equation (2)). Mathematically, it is given by

$$\lambda_{2,t}\left(\frac{\gamma - 1/\epsilon}{\alpha_{2,t} + 1 - \gamma} - \frac{\gamma}{\alpha_{2,t} - \gamma}\right) - \bar{\lambda}^{(L)}T_t\left(\frac{\gamma - 1/\epsilon}{\alpha_{2,0} + 1 - \gamma} - \frac{\gamma}{\alpha_{2,0} - \gamma}\right) \tag{3}$$

where the climate disaster frequency $\lambda_{2,t} = \bar{\lambda}_t T_t$ is the product of frequency parameter $\bar{\lambda}_t$ and temperature T_t, the first term is the same as the effect of climate disasters on r^f in Equation (2), and the second term is the effect of climate disasters on r^f without climate volatility risk. Under stochastic climate volatility, the value of $\bar{\lambda}_t$ (or $\alpha_{2,t}$) jumps from its initial value $\bar{\lambda}^{(L)}$ (or $\alpha_2^{(o)}$) to $\bar{\lambda}^{(H)}$ (or $\alpha_2^{(n)}$) upon regime shift of Type (A) (or Type (B)). The formula also shows that the impact depends on the temperature anomaly T_t in a predictable way. The magnitude of the expectation effect depends on the frequency and intensity of climate disasters in the new climate regime. Figures 1 and 2 show the magnitudes of these two effects under different abatement policies.

The risk-free rate in the business-as-usual scenario Figure 1 shows the decomposition of the risk-free rate in the business-as-usual scenario based on Equation (2). Panel (a) and (b) show how much risk-free rates are affected by stochastic climate volatility through the expectation channel of Equation (3) and the risk channel ($\lambda_{0,t}\mathcal{J}_{f,t}$) respectively. Panel (c) shows the effect of climate disaster risk on the risk-free rate r^f, and Panel (d) shows the

time paths of the risk-free rates. Comparing Panel (a), (b) and (c), we find that climate volatility risk affects the risk-free rate mainly through the expectation channel, which is as important as the effect of climate disaster.
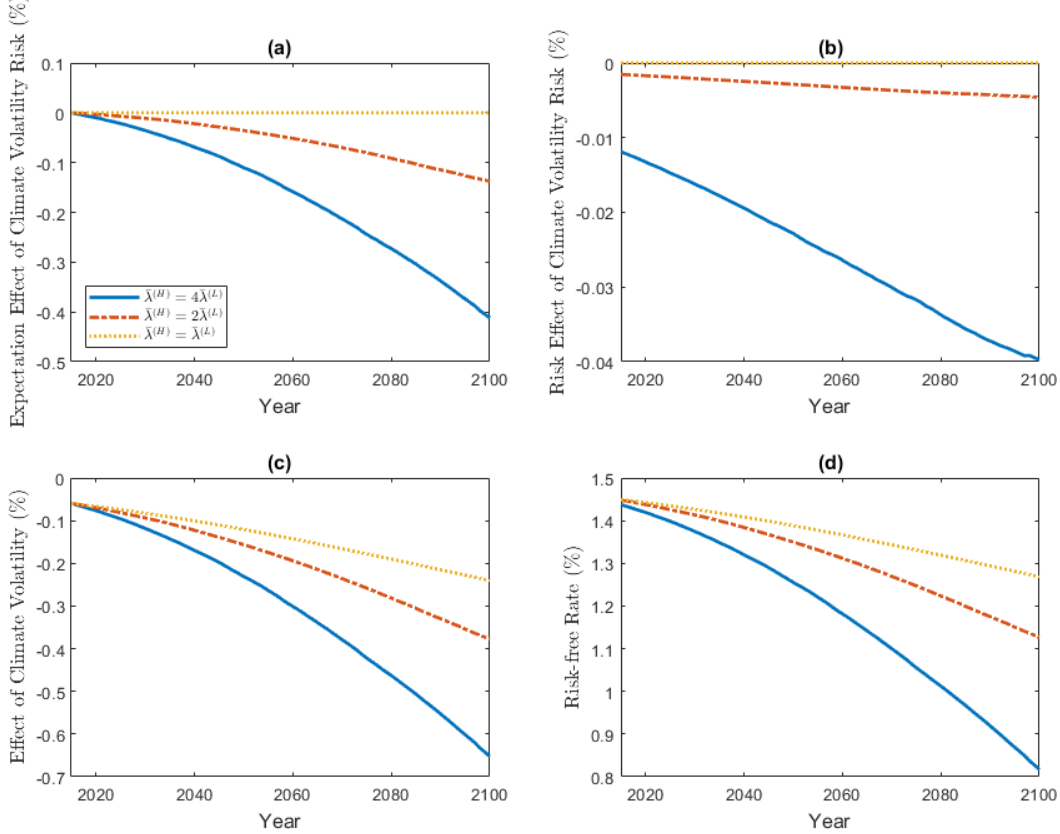

Figure 1: Decomposition of (average) risk-free rates in the BAU scenario under different $\bar{\lambda}^{(H)}$ in the new regime. The legends correspond to $\bar{\lambda}^{(H)} = 4\bar{\lambda}^{(L)}$, $2\bar{\lambda}^{(L)}$ and $\bar{\lambda}^{(L)}$. Panel (a) and (b) present the expectation effect (Equation (3)) and the risk effect (the last term in Equation (2)) describing the impact of stochastic climate volatility on the risk-free rate. Panel (c) shows the effect of climate disaster risk itself, and Panel (d) shows the risk-free rate over time.

Panel (a) and (b) imply that climate volatility risk negatively affects the risk-free rate through both channels. The magnitude of the expectation effect of climate volatility risk increases both in the frequency of climate disasters and over time. This is because both the temperature T_t and the expected value of $\bar{\lambda}_t$ increase over time. Therefore, the expected climate disaster frequency $\lambda_{2,t} = \bar{\lambda}_t T_t$ increases over time. Agents expect higher climate disaster risks in the future, and thus the time path of the impact through the expectation

18

channel is downward sloping. The magnitude of the risk effect of climate volatility is downward sloping over the entire period as a climate regime shift is increasingly likely to have happened as time goes by. But in the very far future, the risk effect shown in Panel (b) will converge to zero as the uncertainty about climate volatility is eventually resolved.

Panel (c) shows that climate disaster risks affect r^f negatively with its magnitude increasing over time. Since both the temperature T_t and the climate disaster frequency parameter $\bar{\lambda}_t$ increase over time, the frequency of climate disasters $\lambda_{2,t}$ also increases. More frequent climate disasters in the future lead to more damages and thus a stronger precautionary saving effect (a greater scarcity of future goods) which results in lower risk-free rates.

The risk-free rate under optimal abatement   Next we repeat the numerical exercise but now under optimal abatement. In this scenario, the average risk-free rate and its decomposition are shown in Figure 2. Panel (a) and (b) again measure the effects of climate volatility risk through the expectation and the risk channels, Panel (c) shows the effect of climate disaster risks, and Panel (d) shows the time path of risk-free rates under different climate disaster frequencies in the new climate regime.

Compared with the business-as-usual scenario, both climate disaster risk and climate volatility risk have a smaller impact on the risk-free rate. This is because temperature rises more slowly under abatement and thus extreme weather events are less likely to happen.

Comparing the magnitudes in Panel (a), (b) and (c), we find that climate volatility risk has a significant impact on risk-free rates. It affects the risk-free rate largely through the expectation effect shown in Panel (a), although the risk effect in Panel (b) is also non-negligible. The risk effect of climate volatility risk is positive before the emission control rate reaches 100% but declines below zero afterwards. Intuitively, abatement cannot be more stringent in the future after the emission control rate reaches its maximum, and this causes a stronger precautionary saving effect which leads to a sharp decline in the risk effect in Panel (b). As the uncertainty about climate regime shift resolves over time, the risk effect
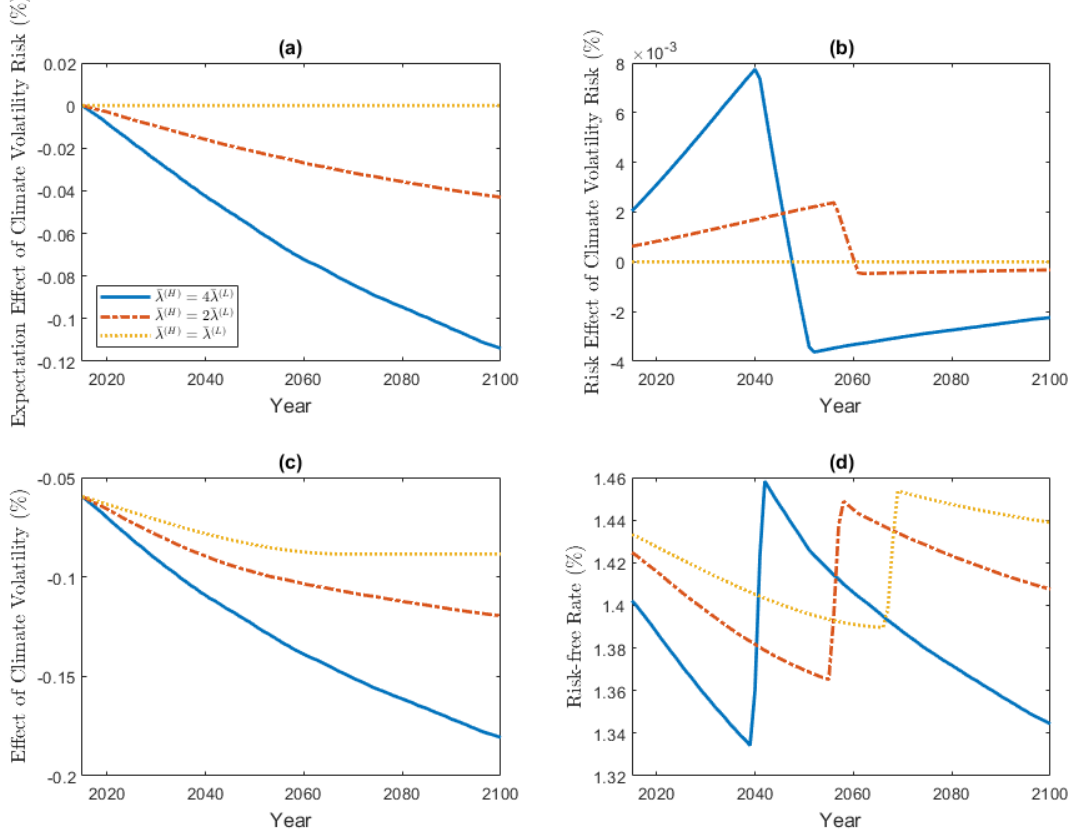
19

Figure 2: Decomposition of (average) risk-free rates under optimal abatement policies. The legends correspond to $\bar{\lambda}^{(H)} = 4\bar{\lambda}^{(L)}$, $2\bar{\lambda}^{(L)}$, and $\bar{\lambda}^{(L)}$. Panel (a) and (b) present the expectation effect (Expression (3)) and the risk effect (i.e. the last term in Equation (2)) of stochastic climate volatility on the risk-free rate. Panel (c) shows the effect of climate disaster risk, and Panel (d) shows the risk-free rate over time.

will gradually converge to zero, but this happens way beyond our window of time displayed in the figures.

Panel (d) shows that under any assumption of climate disaster frequency in the new regime, the risk-free rate will decline in the short run and in the long run, as climate conditions deteriorate under global warming and more frequent disasters. In the medium run, the risk-free rate jumps upwards when the emission control rate reaches its maximum 100%. Since abatement costs stop increasing afterwards, consumption growth will no longer be negatively affected by increasing abatement costs, and thus the precautionary saving effect becomes weaker. Therefore, the risk-free rate experiences a sharp increase at this point.

20

4.1.2 The risk premium

In Appendix A, we show that the risk premium is given by

$$
r_{p,t} = \underbrace{\gamma\sigma^2}_{Standard} + \underbrace{\lambda_1 \left[\frac{-1}{\alpha_1 + 1} + \frac{\gamma}{\alpha_1 - \gamma} + \frac{1 - \gamma}{\alpha_1 + 1 - \gamma} \right]}_{Econ.\ disasters} + \underbrace{\lambda_{2,t} \left[\frac{-1}{\alpha_2 + 1} + \frac{\gamma}{\alpha_2 - \gamma} + \frac{1 - \gamma}{\alpha_2 + 1 - \gamma} \right]}_{Clim.\ disasters}
$$

$$
+ \underbrace{\lambda_{0,t} \mathcal{J}_{rp,t}}_{Regime\ shift} \tag{4}
$$

which again can be decomposed into four parts. The first component, $\gamma\sigma^2$, represents the standard constant relative risk aversion (CRRA) risk premium arising from diffusive risk in the endowment process. The second and the third terms capture the risk compensations for economic and climate disasters; both are positive. The last term stands for the compensation for climate volatility risk due to the uncertain one-off regime shift, where $\lambda_{0,t}$ is the arrival rate of a new regime and $J_{rp,t}$ is the instantaneous effect of the regime shift on r_p. Appendix A shows that $J_{rp,t}$ has no analytical expression, so we solve this numerically.

Similar to the discussion on the risk-free rate in Section 4.1.1, the effect of climate volatility risk on risk premia can also be decomposed into two parts: the expectation effect and the risk effect. The expectation effect comes from an increase in the expected future climate damage under volatility risk. It is given by

$$
\lambda_{2,t} \left[\frac{-1}{\alpha_{2,t} + 1} + \frac{\gamma}{\alpha_{2,t} - \gamma} + \frac{1 - \gamma}{\alpha_{2,t} + 1 - \gamma} \right] - \bar{\lambda}^{(L)} T_t \left[\frac{-1}{\alpha_2^{(o)} + 1} + \frac{\gamma}{\alpha_2^{(o)} - \gamma} + \frac{1 - \gamma}{\alpha_2^{(o)} + 1 - \gamma} \right] \tag{5}
$$

which is the difference between the third term in Equation (4) and its counterpart when the climate disaster frequency does not change in the new regime. The risk effect is captured by the last term $\lambda_{0,t} \mathcal{J}_{rp,t}$ in Equation (4), which measures how much climate volatility risk affects the risk premium. Figure 3 and 4 show the relative size of these two components.

The risk premia in the business-as-usual scenario Figure 3 shows how much the risk premium is affected by climate disaster risks and stochastic volatility in the business-as-usual (BAU) scenario. Panel (a) and (b) shows the expectation effect and the risk effect of climate volatility risk, respectively. Panel (c) shows how much the risk premium is affected by climate disaster risk, and Panel (d) shows the time paths of risk premia. Both types of climate risks affect risk premia positively. Comparing the magnitudes in Panel (a), (b) and (c), we find that the climate disaster effect, the expectation effect and the risk effect of climate volatility risk are of the same order of magnitude. This implies that climate volatility risk is as important as climate volatility itself when calculating risk premia.
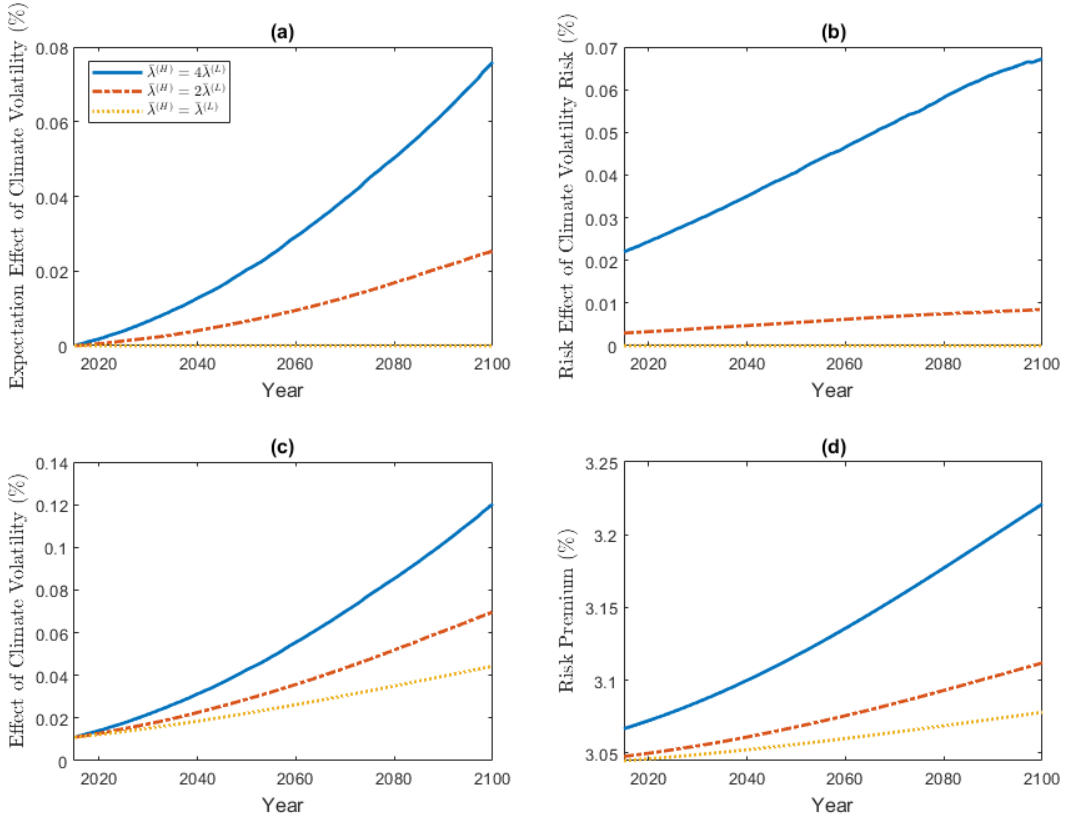

Figure 3: Decomposition of risk premia in the BAU scenario under different $\bar{\lambda}^{(H)}$ in the new regime. The legends correspond to $\bar{\lambda}^{(H)} = 4\bar{\lambda}^{(L)}$, $2\bar{\lambda}^{(L)}$, and $\bar{\lambda}^{(L)}$. Panel (a) and (b) present the expectation effect (Expression (5)) and the risk effect (the last term in Equation (4)) of stochastic climate volatility on risk premia. Panel (c) shows the effect of climate disaster risk, and Panel (d) shows the risk premia over time.

The climate disaster effect (Panel (c)) and the expectation effect of volatility risk (Panel (a)) both increase over time. This is because global warming is irreversible and causes more frequent climate disasters over time. Meanwhile, the positive shock to disaster frequency upon a regime shift further deteriorates the climate conditions. Under the threat of more frequent disasters in the future, agents require higher risk compensation. The risk effect of stochastic climate volatility shown in Panel (b) increases in disaster frequency, because a new regime with more frequent disasters poses larger threats to the economic growth and thus the risk compensation required by agents increases correspondingly. In addition, the risk effect of climate volatility risk on risk premia increases over time under the risk of a positive shock to climate volatility. But far outside our time window the risk effect will eventually converge to zero as the uncertainty about a regime shift gradually resolves over time.

The risk premia under optimal abatement   Figure 4 shows how much the risk premium is affected by climate disasters and volatility risks under optimal abatement. Panel (a) and (b) show the expectation effect and the risk effect of climate volatility risk, respectively. Panel (c) shows the effect of climate disaster risk on the risk premium, and Panel (d) plots the time paths of the risk premium.

Compared with the BAU scenario, the effects of climate volatility risk and climate disasters on the risk premium are smaller under optimal abatement because of the stringent abatement policies. Nevertheless, they are of the same order of magnitude. This implies that climate volatility risk is as important as climate volatility itself when calculating risk premia, regardless of abatement policy stringency.

Panel (a), (b) and (c) in Figure 4 imply that both the climate disaster risk and the climate volatility risk increase the risk compensation required by agents as the deteriorating climate condition poses larger threat to economic growth over time. In Panel (b), the short-run and the long-run risk effects of climate volatility risk decrease over time as the uncertainty about climate volatility resolve over time. The sharp increase in the middle happens when the
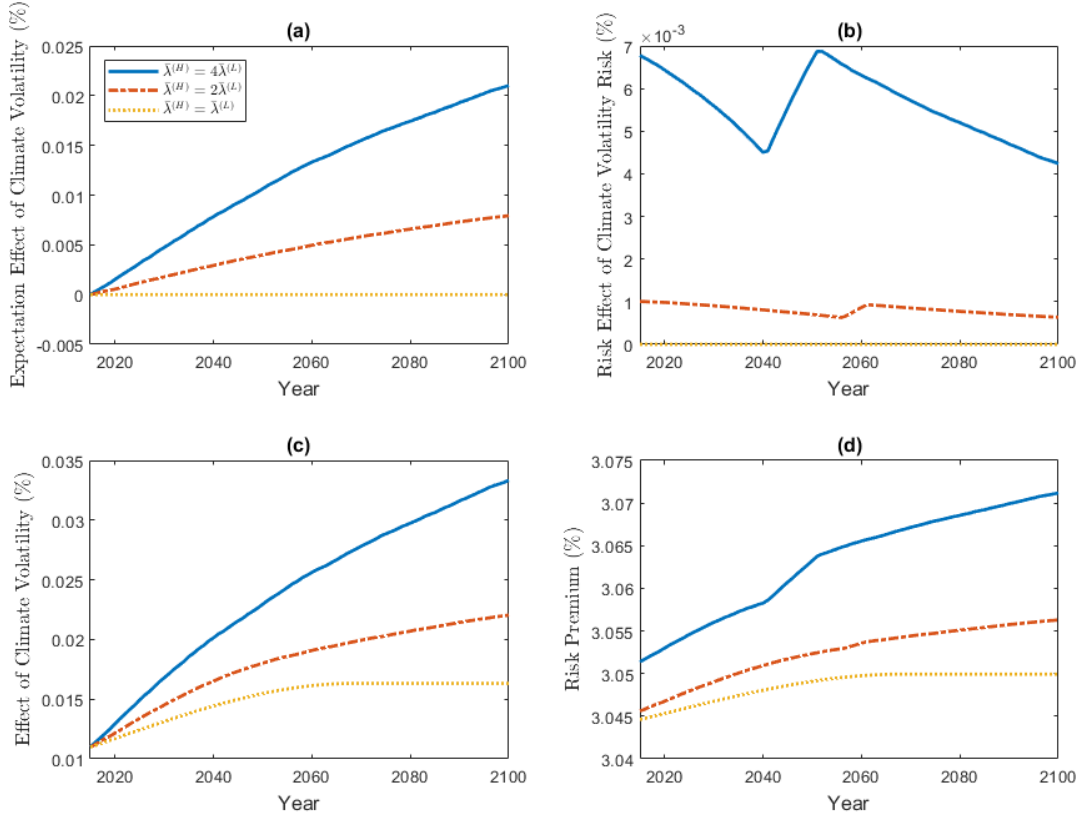
23

Figure 4: Decomposition of risk premia in the optimal abatement policy scenario under different $\bar{\lambda}^{(H)}$ in the new regime. The legends correspond to $\bar{\lambda}^{(H)} = 4\bar{\lambda}^{(L)}$, $2\bar{\lambda}^{(L)}$, and $\bar{\lambda}^{(L)}$. Panel (a) and (b) present the expectation effect (Expression (5)) and the risk effect (the last term in Equation (4)) of stochastic climate volatility on the risk premium. Panel (c) shows the effect of climate disaster risk, and Panel (d) shows the time paths of the risk premium.

emission control rate reaches its maximum of 100%. Since emission control cannot be more stringent afterwards, more severe climate conditions in the future cannot be mitigated by abatement. This leads to a sharp increase in the risk compensation required by the agents, which is reflected as the sudden increase in Panel (b).

In Panel (d), we find that the risk premium does not differ much under different specifications of climate condition in the new regime. This is because stringent emission control effectively decelerates global warming and postpones the negative impact of climate change on the economy. Therefore, agents require less compensation for climate risks than in the BAU scenario shown in Figure 3.

4.1.3 The stochastic discount factor

The dynamics of the stochastic discount factor π_t are essential for understanding the sources and consequences of risks in our model. Using Ito's lemma, we show in Appendix A that

$$\frac{d\pi_t}{\pi_{t-}} = \mu_{\pi,t}dt - \gamma\sigma dZ_t + \left[(1-J_1)^{-\gamma} - 1\right]dN_{1,t} + \left[(1-J_2)^{-\gamma} - 1\right]dN_{2,t} + \mathcal{J}_{\pi,t}dN_{0,t}$$

where $\mu_{\pi,t} = -r_t^f - \lambda_1\frac{\gamma}{\alpha_1-\gamma} - \lambda_{2,t}\frac{\gamma}{\alpha_2-\gamma} - \lambda_{0,t}\mathcal{J}_{\pi,t}$. The stochastic discount factor prices diffusive risks of the economy (dZ_t), disaster risks from the economy (N_1) and climate (N_2), and the risk of climate regime shift (N_0). The price of economic diffusive risk is $\gamma\sigma$ and positive. The sensitivity of the stochastic discount factor with respect to economic and climate disasters is measured by $\left[(1-J_1)^{-\gamma} - 1\right]$ and $\left[(1-J_2)^{-\gamma} - 1\right]$ respectively, both taking positive values. $\mathcal{J}_{\pi,t}$ captures the exposure to regime shift risk, which is positive under either policy scenario, as shown in Figure 5. In line with intuition, it is higher without climate mitigation or if future climate is more volatile.
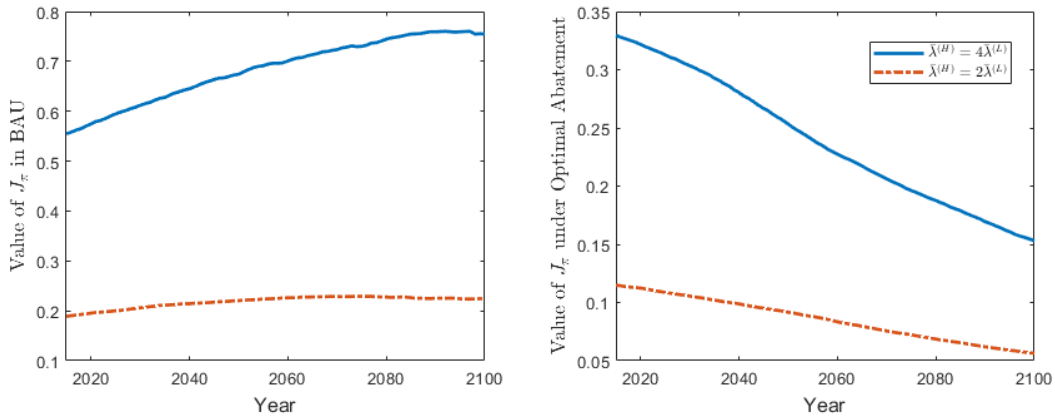

Figure 5: Exposure to the climate regime shift risk $\mathcal{J}_{\pi,t}$ under BAU (left) and optimal abatement (right). The legends correspond to $\bar{\lambda}^{(H)} = 4\bar{\lambda}^{(L)}$ and $2\bar{\lambda}^{(L)}$.

4.1.4 The Social Cost of Carbon and Volatility Risk

We now pull everything together and check how climate volatility risk affects the SCC under different abatement policies. To explain the mechanisms in detail, we first rewrite the social

cost of carbon at time 0 using the following expression derived in Appendix A:

$$SCC_0 \approx \int_0^\infty \underbrace{\left(\int_0^t \chi \frac{\partial \lambda_{2,s}}{\partial T_0} \frac{1}{\alpha_2 + 1 - \gamma} ds \right) \mathbb{E}_0 C_t}_{(i)} \cdot \underbrace{\exp\left(-\int_0^t r_s^{(CDR)} ds \right)}_{(ii)} dt \qquad (6)$$

which is an integral of the product of two terms (A) and (B) from initial time 0 to infinity. Note that Equation (6) is not easy to evaluate numerically and thus we will use Equation (1) to compute the SCC instead. However, Equation (6) provides an intuitive decomposition which will be analysed next. This decomposition facilitates our analysis and helps identify the channels through which the climate volatility risk affects the SCC.

Term (i) captures the marginal welfare loss induced by an increase in the current carbon emissions. An extra unit of carbon emitted to the atmosphere accelerates global warming, and subsequently increases the frequency of climate disasters $\lambda_{2,s}$. The marginal increase in the arrival rate of climate disaster $\lambda_{2,s}$ with one unit extra carbon emission today is captured by $\chi \frac{\partial \lambda_{2,s}}{\partial T_0}$, which will jump from $\chi \bar{\lambda}^{(L)}$ to $\chi \bar{\lambda}^{(H)}$ upon the regime shift. The certainty equivalent of damage from one climate disaster is measured by $\frac{1}{\alpha_2 + 1 - \gamma}$, which is constant since the expected damage from climate disasters does not change over time under the assumption of Type (A) regime shift. Since the intensity of climate disasters is defined as a percentage of consumption, the integral in Term (i) is multiplied by the expected consumption $\mathbb{E}_0 C_t$.

We show in Appendix A that the expected consumption flow $\mathbb{E}_0 C_t$ can be written as

$$\mathbb{E}_0 C_t = C_0 \exp\left\{ \int_0^t \left[\mu_{C,s} - \frac{\lambda_1}{\alpha_1 + 1} - \frac{\lambda_{2,s}}{\alpha_2 + 1} + \lambda_{0,s} \left(\frac{\xi_s}{\xi_{s-}} - 1 \right) \right] ds \right\} \qquad (7)$$

where μ_C is the consumption growth rate with detailed expression provided in Appendix A. It equals to the endowment growth rate μ plus a correction term for the abatement cost. The last term in the integrand, $\frac{\xi_s}{\xi_{s-}} - 1$, is the percentage change in the consumption-endowment ratio ξ once the new regime arrives at time s.

Equation (7) shows that $\mathbb{E}_0 C_t$ is influenced by climate volatility risk through three terms

in the integrand: $\mu_{C,s}$, $-\frac{\lambda_{2,s}}{\alpha_2 + 1}$ and $\lambda_{0,s}\left(\frac{\xi_s}{\xi_{s-}} - 1\right)$. The term $-\frac{\lambda_{2,s}}{\alpha_2 + 1}$, implies that $\mathbb{E}_0 C_t$ is affected by the expectation effect of climate volatility risk through $\lambda_{2,s}$. It captures the fact that consumption flows in the future are expected to grow slowly under high expected climate damages in the new regime. The other two terms, $\mu_{C,s}$ and $\lambda_{0,s}\left(\frac{\xi_s}{\xi_{s-}} - 1\right)$, capture the risk effect of climate volatility risk on expected consumption growth. Intuitively, consumption growth depends on the emission control rate u and thus the consumption-endowment ratio ξ. Upon the climate regime shift, the consumption growth rate jumps because both u and ξ change discontinuously. To see this, note that the regime shift leads to a sudden increase in the climate disaster frequency and thus a discontinuous increase in the marginal damage from carbon emissions. Since the optimal emission control rate equates the marginal abatement cost and the marginal damage, the emission control rate and thus also the consumption-endowment ratio ξ change discontinuously once the regime shift actually happens.

In the business-as-usual scenario, consumption equals endowment and Equation (7) boils down to

$$\mathbb{E}_0 C_t = C_0 \exp\left[\int_0^t \left(\mu - \frac{\lambda_1}{\alpha_1 + 1} - \frac{\lambda_{2,t}}{\alpha_2 + 1}\right) dt\right] \tag{8}$$

which implies that climate volatility risk affects $\mathbb{E}_0 C_t$ only through the expectation channel without abatement. Without abatement, consumption growth rate is not directly exposed to the jump risk of regime shift in Equation (7) discussed above.

Term (ii) is the discount factor for climate damages measured by Term (i), where $r_s^{(CDR)}$ is the consumption growth-adjusted discount rate. Appendix A shows that

$$r_t^{(CDR)} = r_t^f + r_{p,t} + r_{J,t}. \tag{9}$$

where r_t^f is the risk-free rate, $r_{p,t}$ is the risk premium, and $r_{J,t}$ is an additional term introduced by the risk effect of stochastic climate volatility compared with the consumption discount rate provided in Olijslagers (2020). The value of $r^{(CDR)}$ depends on the preference parameters

27

γ and ϵ. To explain how different values of γ and ϵ affect the discount rate, we simplify the setup by considering the business-as-usual scenario where disaster risks are absent. Without abatement, the consumption growth rate $\mu_{C,t}$ equals the endowment growth rate μ, so the risk-free rate becomes $\beta + \frac{\mu}{\epsilon} - \frac{\gamma}{2}\left(1 + \frac{1}{\epsilon}\right)\sigma^2$, the risk premia equals $\gamma\sigma^2$, and $r_J \equiv 0$. Summing up all these terms and subtracting μ yield the growth-adjusted discount rate

$$\beta + \left(\frac{1}{\epsilon} - 1\right)\left(\mu - \frac{1}{2}\gamma\sigma^2\right)$$

which increases in risk aversion γ when $\epsilon > 1$, and decreases in γ if $\epsilon < 1$. As higher γ leads to lower risk-free rates but larger risk premia, its effect on the growth-adjusted discount rate depends on the relative importance of risk-free rate and risk premium effects determined by ϵ. Intuitively, when ϵ is small, higher γ means a stronger precautionary saving effects and the risk-free rate effect dominates. When ϵ is large, the precautionary saving effect plays a less important role than risk premia in determining the discount rate.

The SCC in the business-as-usual scenario   Before looking at the SCC in the business-as-usual scenario, we present the time paths of the growth-adjusted consumption discount rate $r^{(CDR)}$ and the growth rate of expected consumption given in Equation (7). Since neither of them can be evaluated analytically, we show the numerical results from our simulation to show how climate volatility risk affects each term.

Figure 6 shows the expectation effect (Panel (a)) and the risk effect (Panel (b)) of stochastic climate volatility, the effect of climate disaster risk on the growth-adjusted consumption discount rate $r^{(CDR)}$ (Panel (c)), as well as the time paths of $r^{(CDR)}$ (Panel (d)) in the business-as-usual scenario. Given that $r^{(CDR)}$ is the sum of the risk-free rate r^f, risk premium r_p and r_J, the size of the expectation effect in Panel (a) is the sum of corresponding terms in r^f and r_p, or formally, it can be calculated by the sum of (3) and (5). Likewise, the risk effect of stochastic climate volatility in Panel (b) can be calculated by $\lambda_{0,t}\mathcal{J}_{f,t} + \lambda_{0,t}\mathcal{J}_{rp,t} + r_J$.

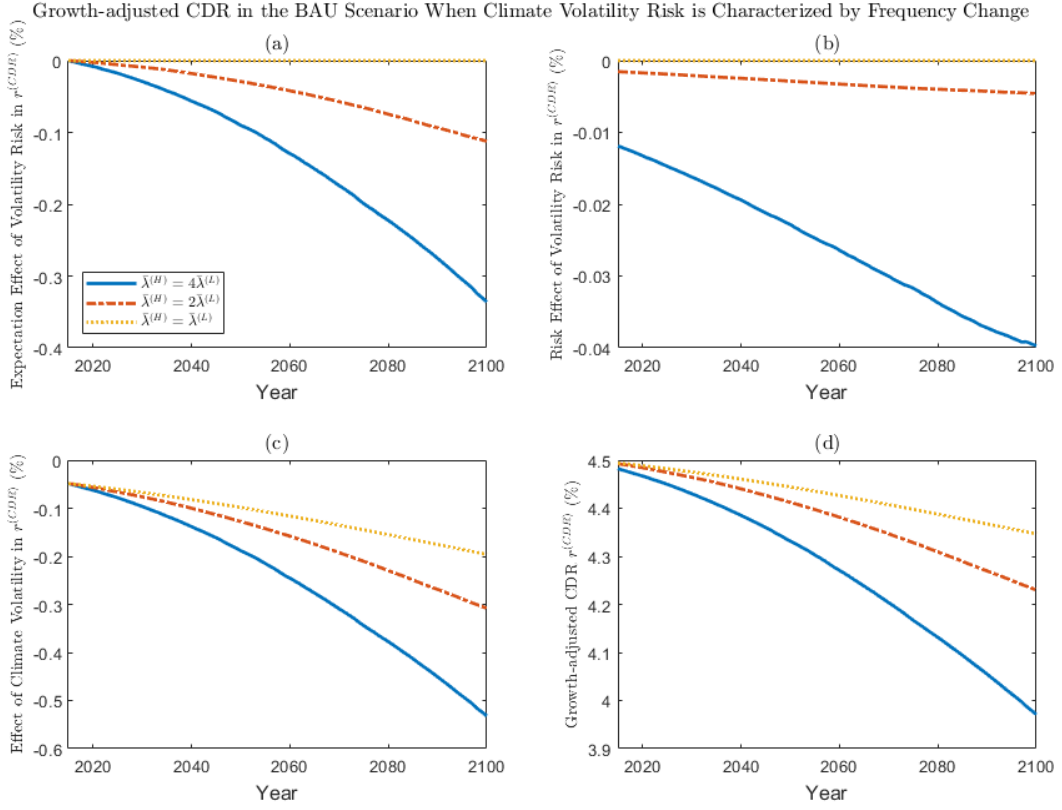Negative values in Panel (a), (b) and (c) imply that both climate disaster risk and

Figure 6: The expectation effect (Panel (a)) and the risk effect (Panel (b)) of stochastic climate volatility, the effect of climate disaster risk (Panel (c)) in the growth-adjusted consumption discount rate $r^{(CDR)}$, and the time paths of $r^{(CDR)}$ (Panel (d)) under BAU. The legends correspond to $\bar{\lambda}^{(H)} = 4\bar{\lambda}^{(L)}$, $2\bar{\lambda}^{(L)}$, and $\bar{\lambda}^{(L)}$.

stochastic climate volatility reduce the growth-adjusted consumption discount rate $r^{(CDR)}$, which pushes up the SCC. The negative impact of stochastic climate volatility increases over time since rising temperature increases the frequency of climate disasters and the new climate regime is more likely to arrive as time proceeds. Comparing the magnitudes in Panel (a) and (b), we find that the expectation effect outweighs the risk effect in terms of determining the growth-adjusted consumption discount rate. Panel (d) shows that our model generates declining growth-adjusted consumption discount rates over time, due to the climate risk effects in Panel (a), (b) and (c).

Figure 7 shows the expected consumption growth over time in the business-as-usual scenario which is the integrand in Equation (8). As suggested by the analytical expression,

the expected growth of future consumption is affected by climate volatility risk only through the expectation channel characterized by the increasing climate disaster frequency $\lambda_{2,t}$. If climate volatility risk does not exist and the frequency parameter remains time invariant, then the expected consumption growth still declines over time but more slowly because global warming increases the probability of climate disasters.
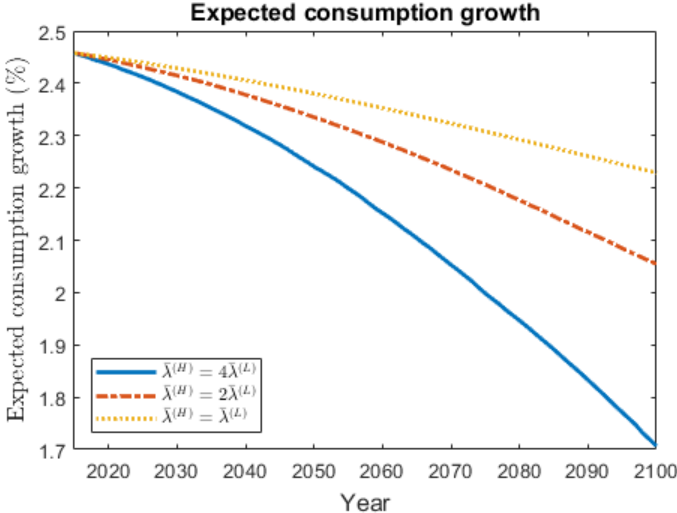

Figure 7: The expected consumption growth rate in the business-as-usual scenario when $\bar{\lambda}^{(H)} = 4\bar{\lambda}^{(L)}$, $2\bar{\lambda}^{(L)}$, and $\bar{\lambda}^{(L)}$.

The average social cost of carbon and mean global surface temperature from Year 2015 to 2100 are shown in Figure 8. Since total carbon emissions are exogenously given and independent of the scale of climate damage in the business-as-usual scenario, changes in temperature are deterministic too and the same under all assumptions on the disaster frequency in the new regime, as shown in the right panel. Without abatement, the mean global surface temperature will rise to 3.35°C by the end of this century. The left panel of Figure 8 shows the time paths of SCC. At time 0, the initial social cost of carbon rises to \$385.06 and \$574.41 per ton of carbon if the climate disasters are expected to happen two and four times as frequent in the new climate regime, compared with \$298.05 per ton of carbon[5] when the regime shift

---

[5]Compared with Olijslagers (2020), our estimate for the (initial) SCC is larger because the climate model in Olijslagers (2020) features atmospheric carbon decay and a concave radiative forcing function; both slow down the impact of carbon emissions on global warming. Our model ignores such delays, and thus leads to more rapid global warming and more frequent (or intense) climate damages in the future.
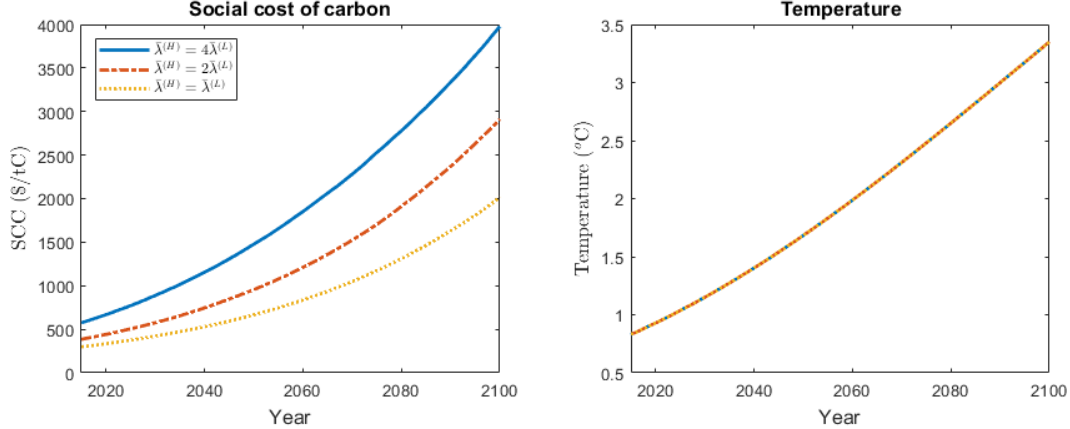
Figure 8: Social cost of carbon (US dollar per ton of carbon, or \$/tC) and mean global surface temperature (°C) in the business-as-usual (BAU) scenario from 2015 to 2100, when climate disaster frequency in the new regime rises to $4\bar{\lambda}^{(L)}$, $2\bar{\lambda}^{(L)}$, or remains unchanged.

is not considered. As Equation (6) implies, the social cost of carbon is substantially affected by the climate volatility risk through the certainty equivalent of climate disasters and the growth-adjusted consumption discount rate in the business-as-usual scenario. With climate disasters happening more frequently in the new regime, the certainty equivalent of climate disasters in Term (i) increases and the growth-adjusted consumption discount rate in Term (ii) decrease, which leads to a rise in SCC.

We saw already in Equation (6) that stochastic climate volatility affects the certainty equivalent of climate disasters through the expectation channel and the growth-adjusted consumption discount rate through both the expectation channel and the risk channel. Next we separate effects of both channels on SCC and show how they interact with preference parameters. To see how much SCC are affected by these two channels, we calculate SCC under two different assumptions on the regime shift: (a) it arrives as a Poisson process with rate $\lambda_0 = 0.01$ (and thus with expected arrival time 100 years), and (b) it arrives deterministically in the 100th year. Table 1 reports the numerical results under the assumption that climate disaster frequency doubles in the new regime (i.e. $\bar{\lambda}^{(H)} = 2\bar{\lambda}^{(L)}$). Since the SCC under deterministic regime shift captures the expectation effect of stochastic climate volatility but are not exposed to volatility risk, the difference between values in Column (a) and (b)

measures how much stochastic climate volatility affects the SCC through the risk channel. The certainty equivalent component in the SCC are equal under both types of regime shift but volatility risk has a negative effect on the growth-adjusted consumption discount rate, which leads to higher SCCs when regime shift is stochastic.

γ	ϵ	(a) Stochastic regime shift	(b) Deterministic regime shift
6	1.5	359.23	268.17
4.3	1.5	504.68	377.02
6	0.75	360.07	242.49
4.3	0.75	243.37	172.76

Table 1: The business-as-usual social cost of carbon (\$/tC) in Year 2025 as a function of risk aversion γ, EIS ϵ with and without the risk effect of climate volatility. The parameter set $(\gamma, \epsilon) = (4.3, 1.5)$ is the calibrated values in Section 3. Here we assume that climate disaster frequency doubles ($\bar{\lambda}^{(H)} = 2\bar{\lambda}^{(L)}$) but its size remains unchanged in the new climate regime.

As shown in Table 1, the risk channel of stochastic climate volatility leads to significant increases in the SCC under all combinations of preference parameters γ and ϵ. Higher risk aversion increases in the certainty equivalent of climate disasters, but its effect on the growth-adjusted consumption discount rate $r^{(CDR)}$ and SCC depends on the value of ϵ. To see this, Figure 9 presents time paths of $r^{(CDR)}$ under different combinations of preference parameters when the regime shift is deterministic. When $\epsilon > 1$, the growth-adjusted consumption discount rate $r^{(CDR)}$ increases if risk aversion γ is larger; when $\epsilon < 1$, $r^{(CDR)}$ decreases in γ. Table 1 shows that the SCC goes down with higher risk aversion when $\epsilon > 1$, and increases in risk aversion when $\epsilon < 1$. This implies that the discount effect dominates the certainty equivalent effect and is in line with results in Cai and Lontzek (2019) and Olijslagers and van Wijnbergen (2019).

The SCC under optimal abatement   We now study the effect of climate volatility risk on the social cost of carbon in an economy under optimal abatement policies. As before, we first check the dynamics of growth-adjusted consumption discount rates $r^{(CDR)}$ and the growth rate of expected consumption, since both play an important role in determining the
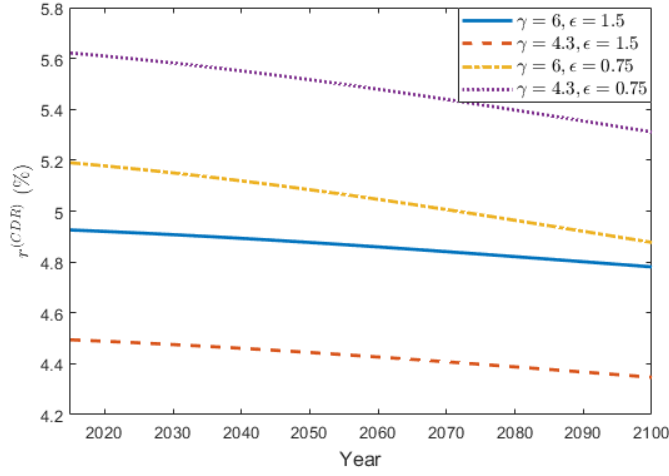
Figure 9: Growth-adjusted consumption discount rate under different risk aversion γ and EIS ϵ when regime shift is deterministic and $\bar{\lambda}^{(H)} = 2\bar{\lambda}^{(L)}$.

SCC. We do this numerically, analytical solution is not possible.

The growth-adjusted consumption discount rate $r^{(CDR)}$ and its climate risk components under optimal abatement is shown in Figure 10. Panel (a) and (b) show the expectation effect and the risk effect of stochastic climate volatility on $r^{(CDR)}$, both being smaller than those in the business-as-usual scenario because abatement mitigates the impact of climate volatility risk on climate change. The expectation effect in Panel (a) always takes negative values and its magnitude increases over time due to the rising probability of climate disasters under volatility risk and global warming. The risk effect in Panel (b) rises over time initially as the probability of climate disasters increases, and converges to zero in the long run as the uncertainty about climate volatility resolves. In line with Figure 2 and Figure 4, it decreases sharply in the medium run when the emission control rate reaches its maximum. Compared with the business-as-usual scenario, the growth-adjusted consumption discount rate in Panel (d) changes little over time. It jumps upwards in the medium run when emission control reaches its maximum as has been observed also in the time paths of risk-free rates (Figure 2) and risk premia (Figure 4).

The comparison of Figure 11 with the corresponding figure for the BAU scenario (Figure 7) shows that expected consumption growth is much less affected under optimal abatement

Growth-adjusted CDR in the OPT Scenario When Climate Volatility Risk is Characterized by Frequency Change
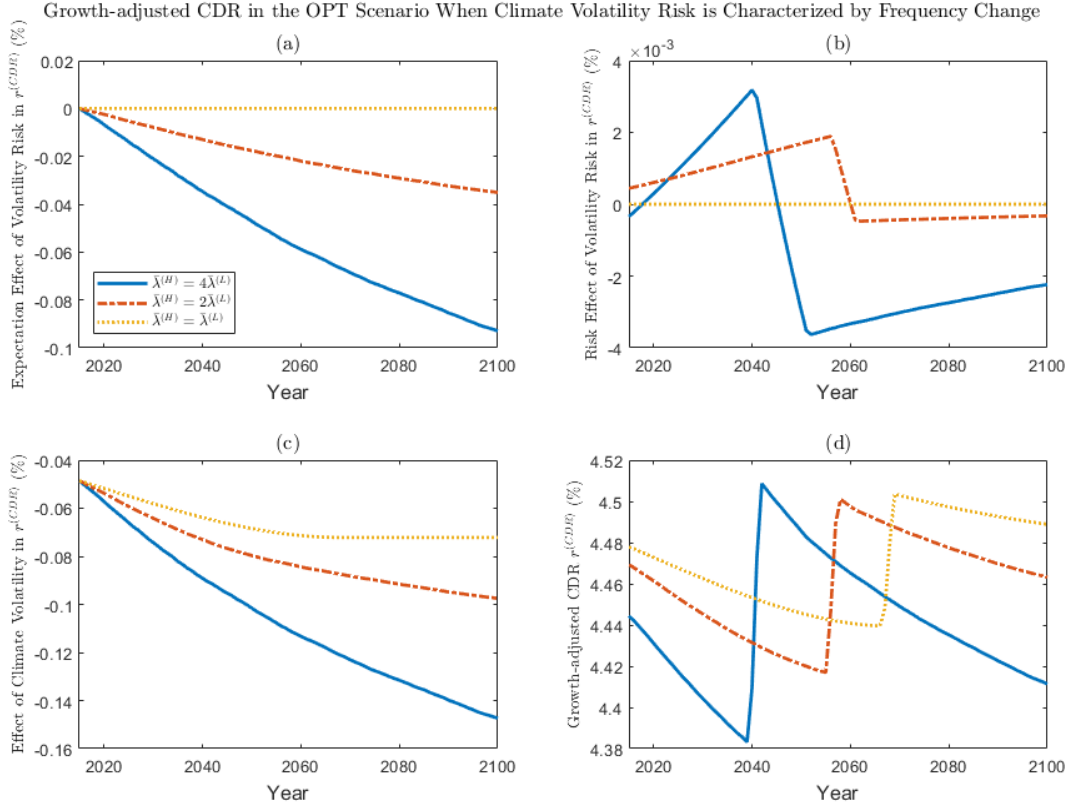
Figure 10: The expectation effect (Panel (a)), the risk effect (Panel (b)) of stochastic climate volatility, the effect of climate disaster (Panel (c)) on growth-adjusted consumption discount rate, and the time paths of the discount rate (Panel (d)) under optimal abatement policies (OPT). In the new regime, climate disaster frequency rises to $4\bar{\lambda}^{(L)}$, $2\bar{\lambda}^{(L)}$, or remains unchanged.

than it is under the business-as-usual scenario. This is because although abatement costs take up a proportion of the endowment in each period, they also substantially reduce the future damage from climate disasters on consumption flows because abatement leads to a slower increase in temperature.

Expected consumption growth rate jumps up halfway the century when the emission control rate u hits its maximum of 100%. Since the marginal damage of carbon emission rises over time, the optimal emission control rate also increases over time. Since we do not incorporate the possibility of carbon capture, the emission control rate stops increasing after reaching 100% and remains at this maximum level afterwards (see Figure 12). The expected

34

consumption growth rate depends on both the expected endowment growth rate and the growth rate of abatement cost, so the sudden stop of the growth rate of abatement costs leads to a discrete upward jump in the expected consumption growth rate.

In the short run, the decline in the expected consumption growth rate is due to expected climate damages under regime shift risk but also to increasingly stringent emission controls over time. In the long run, abatement is stuck at its maximum value of 100% and the consumption growth rate is expected to decline again but this time only because *expected* damages from climate disasters to aggregate endowment and consumption are expected to be more severe over time under the regime shift risk.
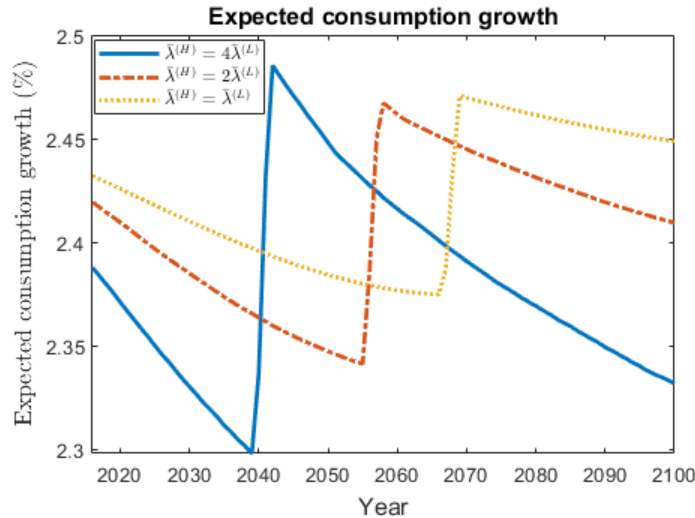

Figure 11: Expected consumption growth rate under optimal abatement policies when $\bar{\lambda}^{(H)} = 4\bar{\lambda}^{(L)}$, $2\bar{\lambda}^{(L)}$ and $\bar{\lambda}^{(L)}$.

Also we find that when $\bar{\lambda}^{(H)}$ is larger, the *expected* consumption growth is lower both in the short run and long run. This is because the frequency of climate disasters in the new climate regime $\lambda_{2,t} = \bar{\lambda}^{(H)} T_t$ increases in $\bar{\lambda}^{(H)}$. Although more abatement effort made under a higher $\bar{\lambda}^{(H)}$ leads to a lower temperature T in the long run, such mitigation effect on global warming is insufficient to counteract the increase in $\bar{\lambda}^{(H)}$. As can be seen in Figure 12, under optimal abatement, emission control under the threat of twice as frequent climate disasters in the new regime (i.e. when $\bar{\lambda}^{(H)} = 2\bar{\lambda}^{(L)}$) leads to only about 16% decline of temperature

in the long run. Therefore, more severe climate conditions in the new regime leads to slower expected consumption growth under optimal abatement.

Figure 12 presents the time path of the SCC, the mean global surface temperature, the emission control rate, annual carbon emissions and the consumption-endowment ratio under optimal abatement policies. Under any assumption on $\bar{\lambda}^{(H)}$, the SCC increases over time since it is proportional to consumption which increases over time. Moreover, the SCC becomes larger if climate disasters are expected to be more frequent in the new regime: discount rates are lower and the certainty equivalent of climate damages is higher under more variable weather in the future. Given that climate disasters will happen two and four times as frequent in the new regime, the initial SCC rises to \$413.64 and \$637.94 per ton of carbon, in contrast with \$311.06 per ton of carbon without a climate regime shift.
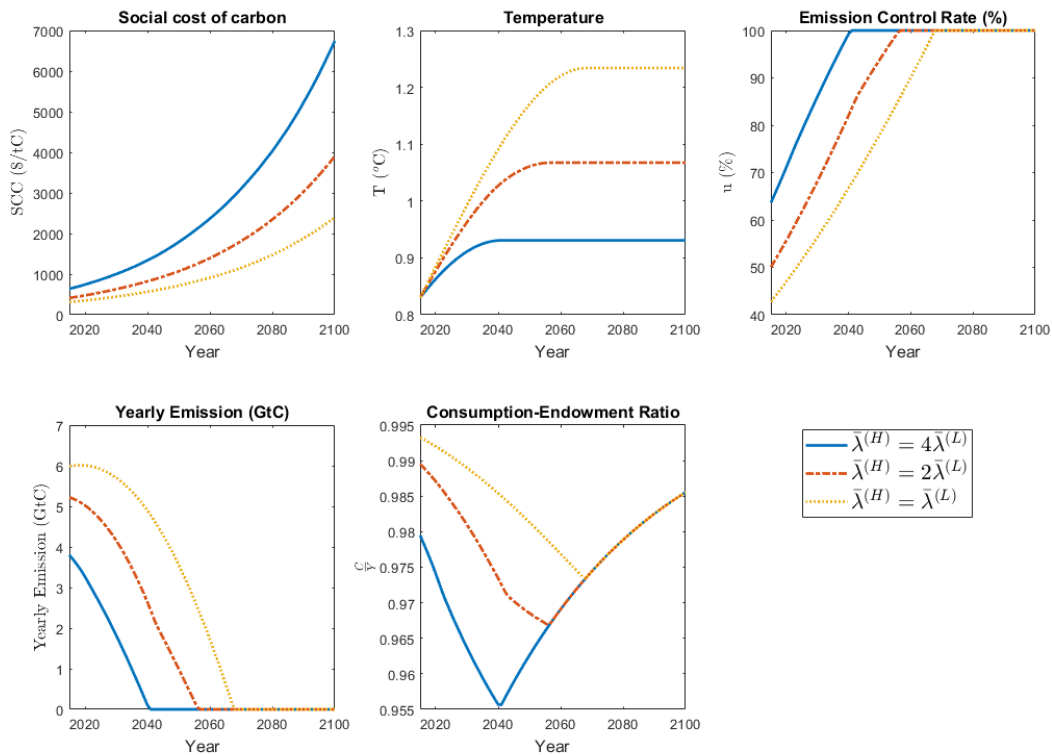

Figure 12: Social cost of carbon, mean global surface temperature, emission control rate, yearly carbon emissions and consumption-endowment ratio from Year 2015 to 2100 under optimal abatement, when $\bar{\lambda}^{(H)} = 4\bar{\lambda}^{(L)}$, $2\bar{\lambda}^{(L)}$ and $\bar{\lambda}^{(L)}$.

The dynamics of emission control, yearly emission, temperature, and consumption-endowment ratio vary under different $\bar{\lambda}^{(H)}$. More stringent emission control under higher $\bar{\lambda}^{(H)}$ leads to lower yearly emissions and a slower increase in temperature T. Meanwhile, through climate disaster frequency $\lambda_{2,t} := \bar{\lambda}_t T_t$, temperature T affects the marginal damage of carbon emissions and thus the stringency of emission control. Initially, temperatures are the same under different values of $\bar{\lambda}^{(H)}$ but emission control is stricter for higher $\bar{\lambda}^{(H)}$, which leads to a slower increase in T under higher $\bar{\lambda}^{(H)}$. The slower temperature rise mitigates the impact of $\bar{\lambda}^{(H)}$ on climate disaster frequency $\lambda_{2,t}$. However, as can be seen in Figure 12, stricter emission control rates under both $\bar{\lambda}^{(H)} = 2\bar{\lambda}^{(L)}$ and $\bar{\lambda}^{(H)} = 4\bar{\lambda}^{(L)}$ lead to less than 20% decline in the long-run temperature than we get when $\bar{\lambda}^{(H)} = \bar{\lambda}^{(L)}$. This implies that the mitigation effect of temperature on future disaster frequency is insufficient to counteract the direct effect of $\bar{\lambda}^{(H)}$. Therefore, a higher $\bar{\lambda}^{(H)}$ leads to higher marginal damage of emissions and stricter emission control. Indeed, without climate volatility risk, the optimal abatement rate in 2015 is slightly over 40%. With more frequent disasters in the new regime, the optimal emission control rate increases and reaches its maximum of 100% earlier. Since the emission control rate cannot exceed 100%, it will remain at this maximum level thereafter. With decreasing marginal abatement cost due to technological progress, the consumption-endowment ratio increases in the long run.

Compared with the BAU scenario, the SCC is larger under optimal abatement policy. This comes from the joint effects of certainty equivalent of climate damages and discount effects, as suggested in Equation (6). On the one hand, emission abatement decelerates global warming, so future aggregate endowment and consumption are less affected by climate damages, implying a larger certainty equivalent effect (Term (i) in Equation (6)). On the other hand, however, the discount rate under optimal abatement (Figure 10) is larger than in the BAU scenario (Figure 6). Intuitively, since future consumption suffers less from climate damages under high abatement efforts, the discount factor is lower or equivalently the discount rate becomes larger. From the observed higher SCCs under optimal abatement

policy, we infer that the certainty equivalent effect dominates the discount effect.

Finally, we find that there is considerable uncertainty about the SCC in the future under both policies, because the endowment process is stochastic and the climate regime shift is uncertain. Table 2(a) lists the means and standard deviations of the social costs of carbon in the BAU scenario in 2025, 2050 and 2100. Under any assumption of the new regime, the mean and the standard deviation increase over time. This is consistent with the fact that the SCC is a geometric Brownian motion (GBM) because it is a function of aggregate endowment which is also a GBM process (Shephard and Andersen (2009)), and that both the mean and the standard deviation of a GBM increases over time. Of course, under the optimal abatement scenario there is uncertainty about future SCCs too: see Table 2(b), where we compare the BAU and the optimal abatement scenario. Both the means and the standard deviations are larger than in the BAU case under the same assumption on the new climate regime, which is because of the differences in the certainty equivalent effects and the discount effect of climate volatility risk on SCC, as has been discussed in the last paragraph. Under optimal abatement, the certainty equivalent effect is larger but the discount effect is smaller than the BAU case. Higher SCC under optimal abatement implies that the certainty equivalent effect dominates the discount effect.

New Regime	Year	(a) Business as usual		(b) Optimal abatement	
		Mean	Standard Deviation	Mean	Standard Deviation
$\frac{\bar{\lambda}^{(H)}}{\bar{\lambda}^{(L)}} = 1$	2025	375.79	49.12	395.19	51.89
	2050	666.22	166.46	717.51	177.09
	2100	2013.39	804.42	2393.98	942.04
$\frac{\bar{\lambda}^{(H)}}{\bar{\lambda}^{(L)}} = 2$	2025	504.68	87.11	548.38	100.82
	2050	955.47	281.33	1070.20	323.57
	2100	2911.38	1208.18	3900.78	1666.68
$\frac{\bar{\lambda}^{(H)}}{\bar{\lambda}^{(L)}} = 4$	2025	770.80	164.00	863.49	204.97
	2050	1475.99	457.98	1788.28	666.13
	2100	3976.36	1679.76	6741.11	3120.43

Table 2: Means and standard deviations of SCC ($/tC) in Year 2025, 2050 and 2100 from Monte Carlo simulations.

4.2 The New Climate Regime (B): a Higher Disaster Intensity

We now introduce climate volatility risk by assuming that in the new climate regime, climate disasters become more intense instead of more frequent. Upon the arrival of the new regime, the expected size of damages from one extreme weather event will increase immediately to $\mathbb{E}J_2^{(H)}$ from the current value $\mathbb{E}J_2^{(L)}$. We call this regime (B). To compare the numerical results under different types of climate volatility risk, we apply the same multipliers (2 and 4) to the post-shift expected damage size, in other words, when $\frac{\mathbb{E}J_2^{(H)}}{\mathbb{E}J_2^{(L)}} = 2$ and 4[6]. We consider the BAU scenario first and then for comparison the optimal abatement (OA) scenario.

Business-as-Usual Scenario Consider first the business-as-usual scenario, still with exogenous emissions, and assuming the stochastic shock structure of Regime (B). We remind the reader that we run the same numerical exercises but with endogenous and thus stochastic carbon emissions in Section 5.

Without abatement effort and with deterministic emissions, the emissions are the same under all possible values of the expected disaster size $\mathbb{E}J_2^{(H)}$ in the new regime. As a consequence in the BAU scenario and the non-stochastic emissions case, temperature T follows the same dynamic path also under all assumptions on $\mathbb{E}J_2^{(H)}$.[7] Therefore, the expected annual climate damages are also the same after regime shifts of both types as long as $\frac{\mathbb{E}J_2^{(H)}}{\mathbb{E}J_2^{(L)}}$ in Regime (B) equals $\frac{\bar{\lambda}^{(H)}}{\bar{\lambda}^{(L)}}$ in Regime (A). However, we will show that the SCC that comes out is different in the two regimes (A) and (B) even though expected damages are the same.

Consider first the effect on the SCC through the Consumption Discount Rate (see the analytical expression of the SCC (Equation (6)). Figure 13 shows the growth-adjusted consumption discount rate $r^{(CDR)}$ and its components introduced by climate disaster risk and climate volatility risk in the business-as-usual scenario. Panel (a) and (b) show the

---

[6]We quantify the impact of climate volatility risk on risk-free rates and risk premia under Regime (B) in Appendix B.

[7]This is not necessarily true under optimal abatement since optimal abatement does depend on the size and the type of shocks. And (the change in) carbon concentration is influenced by $(1 - u_t)E_t$, so different emission and temperature patterns will emerge when abatement u_t varies.

expectation effect and the risk effect of stochastic climate volatility on $r^{(CDR)}$, Panel (c) shows the effect of climate disasters on $r^{(CDR)}$, and Panel (d) shows the dynamic of $r^{(CDR)}$ under different assumptions on the disaster intensity $\mathbb{E}J_2^{(H)}$ in the new regime. The magnitudes in all these panels do not differ much from those in Figure 6 under Regime (A) in the BAU scenario. Negative values in Panel (a), (b) and (c) imply that both climate disaster risk and climate volatility risk reduce the growth-adjusted consumption discount rate $r^{(CDR)}$. A lower CDR obviously implies a higher Consumption Discount Factor which in turn implies a higher SCC as future damages are discounted less. The expectation effect of climate volatility risk (see Panel (a)) and the effect of climate disaster risk (see Panel (c)) are of the same order, and both are larger than the risk effect of climate volatility risk shown in Panel (b).

Next, we check the certainty equivalent effect on the SCC which consists of two parts according to Equation (6): the expected future consumption flow $\mathbb{E}_0 C_t$ and the marginal increase in the certainty equivalent of climate damages on $\mathbb{E}_0 C_t$ under one extra unit of emission today. Figure 14 shows the growth rate of expected consumption $\mathbb{E}_0 C_t$ under Regime (B) (see for the analytical expression Equation (8)). Consumption growth is expected to decline as climate damages become more severe under global warming. Moreover, a higher disaster intensity $\mathbb{E}J_2^{(H)}$ in the new regime leads to an even lower time path of expected consumption growth because more damaging climate disasters hinder the economic growth to a larger extent. Comparison with Figure 7 shows that the dynamic response of expected consumption growth is almost the same under Regime (A) and (B).

But the marginal increase in the certainty equivalent component of climate damages on expected consumption at time t, $\int_0^t \chi \frac{\partial \lambda_{2,s}}{\partial T_0} \frac{1}{\alpha_{2,s}+1-\gamma} ds$, is larger in Regime (B) than Regime (A) even when the *expected* climate damages are the same in both new regimes (i.e. when the multipliers on disaster frequency and intensity are the same in the new regime). Utility is concave under risk aversion, therefore, when climate disasters become more intense, the certainty equivalent of the marginal increase in climate damage is larger although the expected climate damages are the same under both regimes.
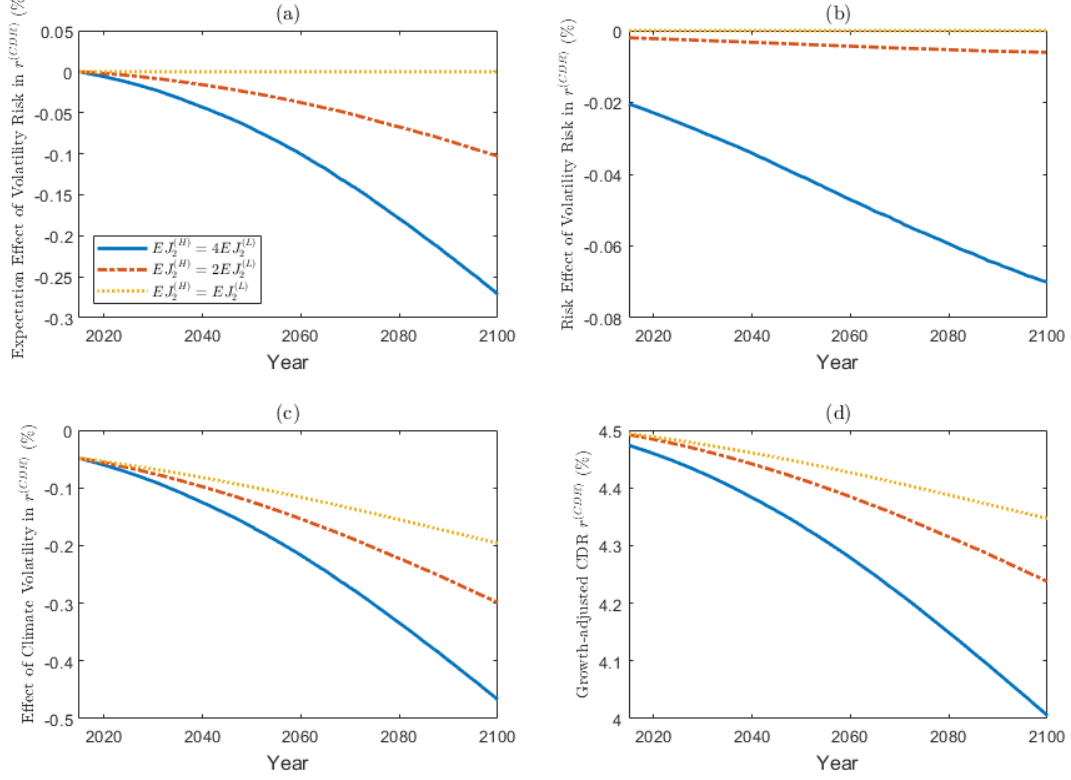
Figure 13: The expectation effect of climate volatility risk (Panel (a)), the risk effect of climate volatility risk (Panel (b)) and the effect of climate disaster risk (Panel (c)) on the growth-adjusted consumption discount rate $r^{(CDR)}$, as well as the time paths of $r^{(CDR)}$ (Panel (d)) in the BAU scenario. The expected intensity of one climate disaster in the new regime rises to $4\mathbb{E}J_2^{(L)}$, $2\mathbb{E}J_2^{(L)}$, or remains unchanged.

As a numerical example, consider the regime shift arrives at the same date τ under both regimes when the multiplier is 2. Then

$$
\begin{aligned}
CE_t(B) &= \left(\int_0^\tau \chi \bar{\lambda}^{(L)} \frac{1}{\alpha_2^{(o)} + 1 - \gamma} ds + \int_\tau^t \chi \bar{\lambda}^{(L)} \frac{1}{\alpha_2^{(n)} + 1 - \gamma} ds \right) \mathbb{E}_0 C_t \\
&> \left(\int_0^\tau \chi \bar{\lambda}^{(L)} \frac{1}{\alpha_2^{(o)} + 1 - \gamma} ds + 2 \int_\tau^t \chi \bar{\lambda}^{(L)} \frac{1}{\alpha_2^{(o)} + 1 - \gamma} ds \right) \mathbb{E}_0 C_t \\
&= \left(\int_0^t \chi \frac{\partial \lambda_{2,s}}{\partial T_0} \frac{1}{\alpha_{2,s} + 1 - \gamma} ds \right) \mathbb{E}_0 C_t = CE_t(A)
\end{aligned}
$$

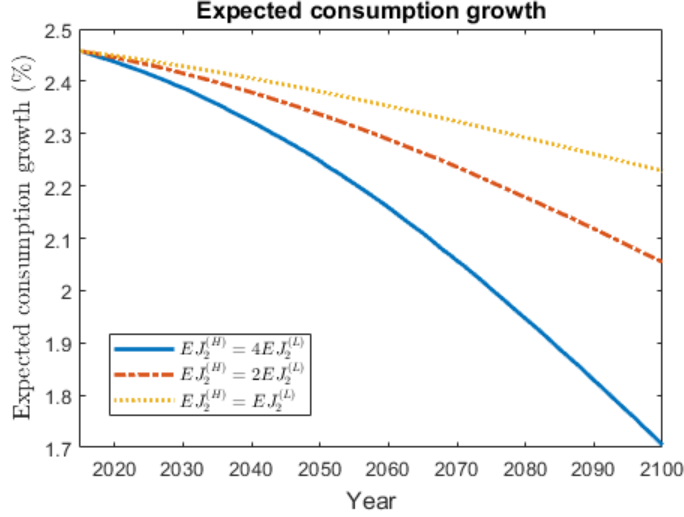where $CE_t(A)$ and $CE_t(B)$ are the certainty equivalent term at t in Equation (6) under

41

Figure 14: Expected consumption growth in the BAU scenario when the expected size of one climate disaster in the new regime rises to $4\mathbb{E}J_2^{(L)}$, $2\mathbb{E}J_2^{(L)}$, or remains unchanged.

regime (A) and (B). The inequality holds because the disaster intensity in the new regime $\mathbb{E}J_2^{(H)} := \frac{1}{\alpha_2^{(n)}+1}$ is double the current disaster intensity $\mathbb{E}J_2^{(L)} := \frac{1}{\alpha_2^{(o)}+1}$, and thus $\frac{1}{\alpha_2^{(n)}+1-\gamma} > 2 \cdot \frac{1}{\alpha_2^{(o)}+1-\gamma}$ given $\gamma > 0$.

Finally consider the dynamics of SCC. Figure 15 shows the time paths of the SCC and temperature in the BAU scenario under Regime (B). We already saw that temperature follows the same dynamic under any assumption of $\mathbb{E}J_2^{(H)}$ with deterministic emissions. But the SCC is larger when shocks follow regime (B). As we saw, the growth-adjusted discount rates are similar under both regimes but the certainty equivalent effect of climate damages in (B) is larger than in regime (A): SCC_0 equals \$298.05 per ton of carbon without climate volatility risk, but rises rises to \$398.88 per ton of carbon if the intensity of one climate disaster is twice the current level and and \$673.73 when the disaster multiplier equals four.

Optimal Abatement Policy Consider next the SCC under optimal abatement policy. As before, we first show how climate volatility risk affects the SCC through the discount effect and the certainty equivalent effect.

We again decompose the growth-adjusted consumption discount rate $r^{(CDR)}$ into an expectation effect (Panel (a)), a risk effect (Panel (b)) and a risk effect due to volatility risk
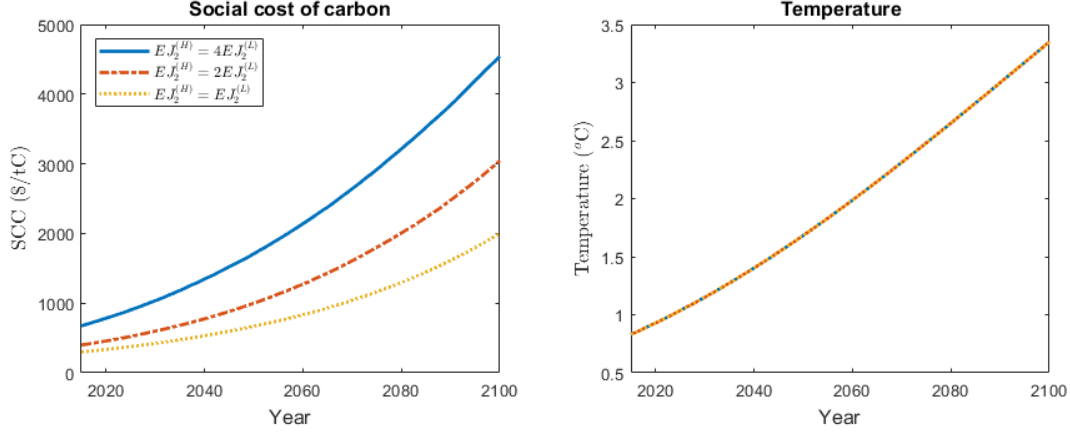
Figure 15: SCC ($/tC$) and mean global surface temperature (°C) in the BAU scenario from 2015 to 2100. The expected size of one climate disaster in the new regime rises to $4\mathbb{E}J_2^{(L)}$, $2\mathbb{E}J_2^{(L)}$, or remains unchanged.

rather than due to volatility itself (panel (c)). Panel (d) shows the net result of climate disasters under optimal abatement on the CDR itself. Comparison of the graphs with the corresponding ones under the BAU scenario (**??**) indicates that the magnitudes of climate risks in Panel (a), (b) and (c) do not differ much from what they are under Regime (A), and so is the time path of the growth-adjusted consumption discount rates, as can be seen in Figure 10. Comparison with the BAU scenario implies that both the expectation effect (Panel (a)) and the risk effect (Panel (b)) of stochastic climate volatility are smaller under emission control, because abatement mitigates climate change and thus weakens the impact of climate volatility risk on the discount factor.

We then check the certainty equivalent effect in SCC (Equation (6)) which consists of two parts: the expected future consumption $\mathbb{E}_0 C_t$ and the marginal increase in the certainty equivalent of climate damages on $\mathbb{E}_0 C_t$ under one extra unit of emission today. The growth rate of expected future consumption $\mathbb{E}_0 C_t$ is shown in Figure 17, which resembles Figure 11 under optimal abatement in Regime (A). In the short run, it declines over time as climate damages become more severe under global warming and emission control becomes more stringent. In the short run, it declines over time only because expected damages from climate disasters to aggregate endowment and consumption become more severe. In the
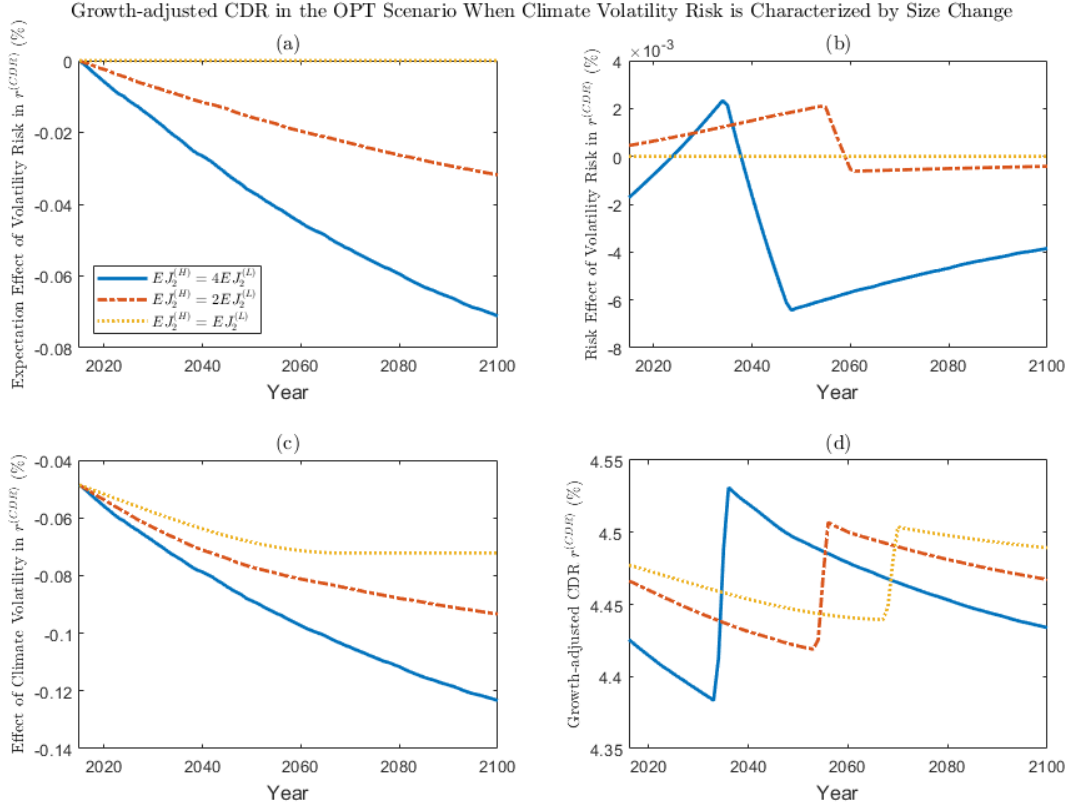
Figure 16: The effect of climate volatility risk on growth-adjusted consumption discount rate through the expectation channel (Panel (a)) and the risk channel (Panel (b)), the effect of climate disaster risk (Panel (c)), and the discount rate (Panel (d)) under optimal abatement policy. In the new climate regime, the expected damage size of one climate disaster increases to $4\mathbb{E}J_2^{(L)}$, $2\mathbb{E}J_2^{(L)}$, or remains unchanged in the new regime.

medium run, the expected consumption growth increases discontinuously when the emission control rate u hits its maximum 100% and remains at this maximum level afterwards. Since the expected consumption growth depends on the growth of both endowment and abatement, the sudden stop of the growth of abatement costs leads to a discrete upward jump in the expected consumption growth. Furthermore, the growth in expected consumption under optimal abatement is less affected by climate change than in the BAU scenario because abatement mitigates the negative impact of climate change on the economic growth. Although abatement comprises a proportion of endowment in each period, it substantially reduces the damage from climate disasters on consumption, leading to a higher long-run

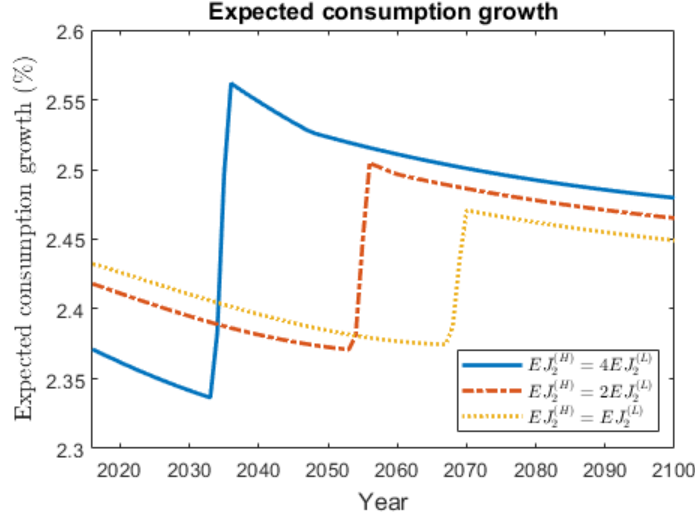endowment and consumption growth.

Figure 17: Expected consumption growth rate under optimal abatement if the expected damage size of one climate disaster increases to $6\mathbb{E}J_2^{(L)}$, $4\mathbb{E}J_2^{(L)}$, $2\mathbb{E}J_2^{(L)}$, or remains unchanged in the new regime.

Figure 18 shows the time paths of the SCC, mean global surface temperature, emission control rate, annual carbon emissions and consumption-endowment ratio under optimal abatement policies in Regime (B). As in Regime (A), the SCC increases over time since it is proportional to consumption which increases over time. Moreover, when the disaster intensity in the new regime is larger, the SCC is higher because of lower discount rates and higher certainty equivalent of climate damages. Given that the average intensity of climate disasters are twice and four times as large in the new regime, the initial SCCs rise to \$429.71 and \$762.70 per ton of carbon, in contrast with \$311.06 per ton of carbon if climate volatility risk is not considered. The dynamics of emission control, yearly emission, temperature, and consumption-endowment ratio vary under different specifications of the disaster intensity $\mathbb{E}J_2^{(H)}$ in the new regime. Emission control becomes more strict under larger $\mathbb{E}J_2^{(H)}$, which therefore leads to a lower consumption-endowment ratio, less yearly emissions and a slower increase in temperature.

When comparing regime (B) with the results under Regime (A) (Figure 12), we find that emission control under Regime (B) is more strict. This is because the certainty equivalent

45

of climate damage increases more under Regime (B) than (A), as discussed earlier in this section. More stringent emission control explains the lower consumption-endowment ratio, faster decline in annual emissions and slower increase in temperature under Regime (B).
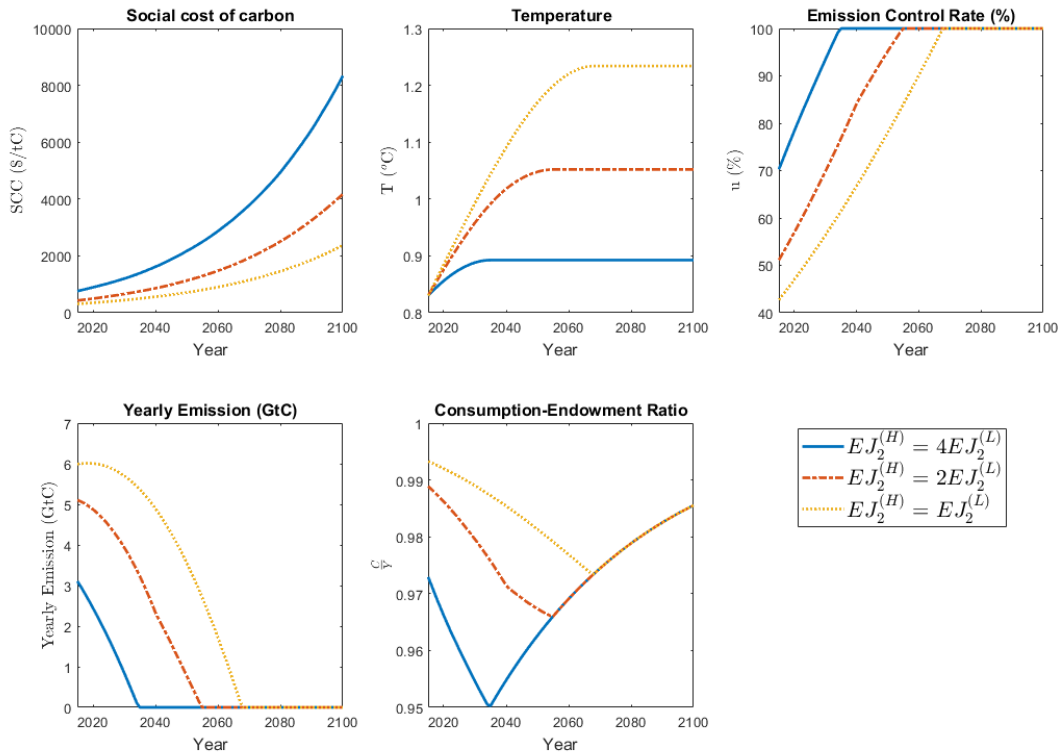

Figure 18: Social cost of carbon, mean global surface temperature, emission control rate, yearly carbon emissions and consumption-endowment ratio from Year 2015 to 2100 under optimal abatement in Regime (B) of climate volatility risk, where the expected size of one climate disaster in the new regime rises to $4\mathbb{E}J_2^{(L)}$, $2\mathbb{E}J_2^{(L)}$, or remains unchanged.

For completeness, we provide the means and standard deviations of SCCs under both policy scenarios in Table 3. The Table shows that under both policy scenarios the mean and the standard deviation of SCCs are increasing over time. But comparison with Table 2 shows that a new climate regime with more intense disasters increases the SCC more than a switch to a regime with more frequent disasters for equal expected damage value.

46

New Regime	Year	(a) Business as usual		(b) Optimal abatement	
		Mean	Standard Deviation	Mean	Standard Deviation
$\frac{\mathbb{E}J_2^{(H)}}{\mathbb{E}J_2^{(L)}} = 1$	2025	375.79	49.12	395.19	51.89
	2050	666.22	166.46	717.51	177.09
	2100	2013.39	804.42	2393.98	942.04
$\frac{\mathbb{E}J_2^{(H)}}{\mathbb{E}J_2^{(L)}} = 2$	2025	521.70	93.18	573.66	109.66
	2050	997.56	300.53	1130.65	357.51
	2100	3043.94	1276.30	4176.99	1804.32
$\frac{\mathbb{E}J_2^{(H)}}{\mathbb{E}J_2^{(L)}} = 4$	2025	901.94	196.30	1036.46	260.80
	2050	1706.84	540.31	2168.28	840.28
	2100	4542.63	2009.69	8332.87	4026.95

Table 3: Means and standard deviations of SCC ($/tC) in Year 2025, 2050 and 2100 when climate disasters become more intense in the new regime.

5   Endogenous Carbon Emissions

So far we have for analytical convenience assumed that business-as-usual carbon emissions are exogenous and deterministic, increasing initially over time but declining eventually as fossil fuel depletion and renewable energy development kick in. This simplification allowed us to almost completely decompose the expression of SCC analytically (cf Equation (6)) and to analyse the climate risk impact of each component separately. But there is an obvious cost to this simplification, in reality emissions are related to the output process and as such a stochastic process themselves. To assess how limiting this simplification really is we redo much of the analysis but now with emissions modeled as a stochastic process linked to the output process.

So we now model emissions E_t as

$$E_t = \psi_t Y_t$$

where Y_t is the endowment process that characterizes the intensity of economic activities at t, and ψ_t is the carbon intensity: the amount of carbon produced per dollar of GDP. The carbon intensity is calibrated such that *expected* emissions are close to those assumed in the

exogenous base emission case, as in Olijslagers (2020). We assume that ψ_t declines over time due to technological improvements in production processes and renewable energies:

$$d\psi_t = -\delta_t \psi_t dt$$

where δ_t increases over time and follows the dynamic

$$d(\delta_t - \delta_\infty) = -\alpha_\psi(\delta_t - \delta_\infty)dt, \ \alpha_\psi > 0$$

with initial value δ_0 and long-run value δ_∞, or equivalently, $\delta_t = \delta_\infty + e^{-\alpha t}(\delta_0 - \delta_\infty)$. So initially, carbon intensity declines at a rate smaller than the economic growth rate, and emissions are driven up as the endowments grow. But in the long run the carbon intensity declines at a rate δ_∞ larger than the rate of economic growth, so carbon emissions eventually decline and converge to zero. We set $\delta_0 = -0.5\%$, $\delta_\infty = -6.5\%$ and $\alpha = 0.25\%$. The key difference with the exogenous emission case is that carbon emissions are now stochastic due to the volatility of the output process to which they are linked. This introduces a new source of risk, realistically so but this also makes it impossible to generate analytical expressions for SCC. We therefore just present the numerical outcomes.

5.1 Endogenous emissions and arrival rate climate shocks

Table 4 reports the numerical results under the assumption that the climate disaster frequency doubles in the new regime (i.e. $\lambda^{(H)} = 2\lambda^{(L)}$) but now with endogenous carbon emissions. As in Table 1, we calculate the SCC under two different assumptions on the climate regime shift: Column (a) assumes the arrival of the regime shift follows a Poisson process with rate $\lambda_0 = 0.01$ (and thus with expected arrival time 100 years); Column (b) assumes the regime shift arrives exactly in 2115 (i.e. 100 years from 2015, the starting point of our simulation). Also we compare the SCC under different preference parameter values for γ and ϵ.

γ	ϵ	(a) Stochastic regime shift	(b) Deterministic regime shift
6	1.5	345.18	256.82
4.3	1.5	439.65	347.77
6	0.75	347.71	237.83
4.3	0.75	232.16	171.51

Table 4: The business-as-usual social cost of carbon (\$/tC) in Year 2025 as a function of risk aversion γ, EIS ϵ with and without the risk effect of climate volatility. Assume that in the new regime climate disaster frequency doubles ($\lambda^{(H)} = 2\lambda^{(L)}$) but its size remains unchanged. Carbon emission is a function of aggregate endowment and carbon intensity.

As in the exogenous emission setup of Table 1, the SCC is significantly larger in Column (a) than Column (b) under the same preference parameters, implying that the stochasticity of climate volatility substantially increases the SCC and thus cannot be ignored for an adequate assessment of the SCC. We also find the same pattern as in Table 1 regarding SCCs under different values of γ and ϵ, which can be explained likewise.

Carbon emissions are now proportional to aggregate endowment which introduces an additional source of stochasticity to the extended model. Not surprisingly given that representative agents are risk averse, accounting for endogenous carbon emissions magnifies the risk effect of stochastic climate volatility on social costs of carbon.

Figure 19 and 20 show the time path of the SCC and of temperature T, respectively under the BAU and the optimal abatement scenario, but now with endogenous and therefore stochastic emissions. In the BAU scenario, the dynamics of temperature no longer coincide under different specifications of climate volatility risk, contrary to what they did under the exogenous emissions assumption. This is because now emissions depend on the aggregate endowment which is affected by higher climate disaster arrival rates.

An increase in $\bar{\lambda}^{(H)}$ leads to a lower temperature T because a higher $\bar{\lambda}^{(H)}$ generates larger economic losses, therefore lower future endowments, as a consequence less emissions and hence a slower increase in temperature. The effect of $\bar{\lambda}^{(H)}$ on the SCC comes from two channels. First, an increase in $\bar{\lambda}^{(H)}$ leads to a higher Expected Loss effect as we just discussed (see Term (i) in Equation (6)) and thus a larger SCC. Second, the aggregate endowment and
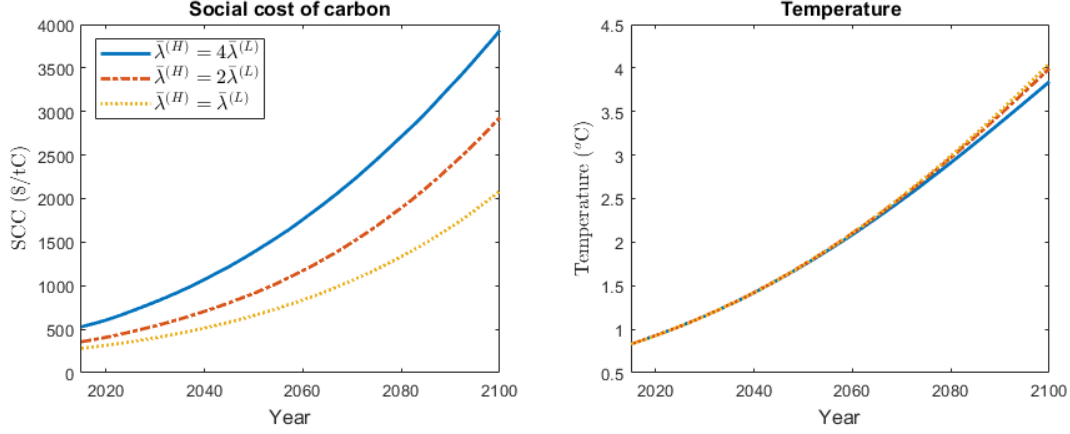
Figure 19: Social cost of carbon (US dollar per ton of carbon, or \$/tC) and mean global surface temperature (°C) in the business-as-usual (BAU) scenario when carbon emission is endogenous. The frequency of climate disasters in the new regime rises to $4\bar{\lambda}^{(L)}$, $2\bar{\lambda}^{(L)}$, or remains unchanged.

consumption in the future are expected to decrease under larger $\bar{\lambda}^{(H)}$, which leads to a higher price of future goods or, equivalently, a higher stochastic discount factor (SDF)/lower CDR. And that in turn also leads to a higher SCC. Figure 19 demonstrates the positive impact of a higher $\bar{\lambda}^{(H)}$ on the SCC numerically.

Under optimal abatement, the SCC, temperature and emission control rate follow the same pattern as in the exogenous emission setup shown in Figure 12. When $\bar{\lambda}^{(H)}$ is higher, the expected marginal damage from climate disasters becomes larger, which leads to more stringent optimal emission control and therefore a lower (future) temperature. A higher climate disaster frequency increases the SCC through both a larger certainty equivalent effect (Term (i) in Equation (6)) and a lower discount rate (Term (ii) in Equation (6)). Under a higher $\bar{\lambda}^{(H)}$, the certainty equivalent of climate damage is expected to be larger. Meanwhile, aggregate endowment and consumption become lower in a world with more frequent climate disasters. And lower future consumption implies a higher stochastic discount factor and a lower discount rate. Both the increase in the certainty equivalent of climate damage and the decrease in discount rates lead to higher values for the SCC.
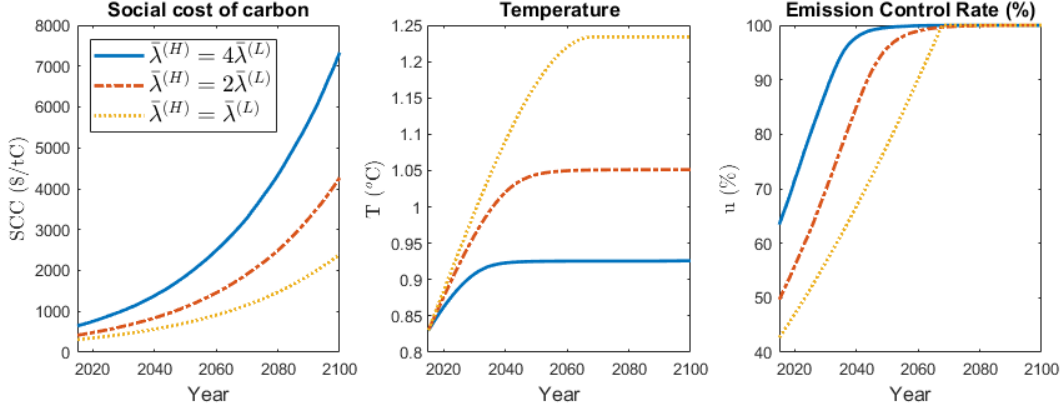
Figure 20: Social cost of carbon, mean global surface temperature, emission control rate, yearly carbon emissions and consumption-endowment ratio from Year 2015 to 2100 under optimal abatement, where carbon emission is endogenous. The frequency of climate disasters in the new regime rises to $4\bar{\lambda}^{(L)}$, $2\bar{\lambda}^{(L)}$, or remains unchanged.

5.2 Endogenous emissions and jump-size climate shocks

Next we show the SCCs, temperature and emission control rates in Figure 21 and 22 under both scenarios when the climate regime shift is of Type (B), that is, the climate disaster intensity increases in the new regime but the disaster frequency remains unchanged.

In the BAU scenario, the SCC increases in the climate disaster intensity $\mathbb{E}J_2^{(H)}$, although temperature is lower under higher disaster intensity. Like in the higher frequency scenario's (cf Figure 19) this follows because with larger disasters output is lower and so are therefore emissions, with a slightly lower increase in T as a result.

The effect of disaster intensity on the SCC also depends on the expected loss effect and the discount effect. First, an increase in $\mathbb{E}J_2^{(H)}$ leads to larger economic losses in the future. Second, the decline in aggregate consumption under larger climate damages leads to a higher stochastic discount factor (or a lower discount rate), which in turn increases the SCC.

Figure 22 shows the SCC, temperature and the emission control rate under optimal abatement policy. Their dynamics follow the same patterns as in Figure 12 under optimal abatement and exogenous emissions. When climate disasters become more intense in the new climate regime, the expected marginal damage from climate disasters increases, leading to stricter emission controls, less emissions and a slower increase in temperature over time.
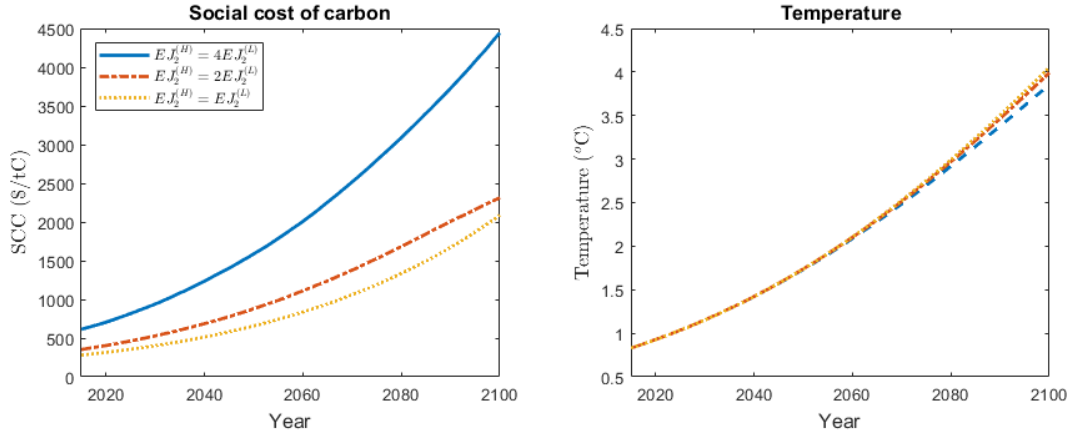
51

Figure 21: Social cost of carbon (US dollar per ton of carbon, or $\$/tC$) and mean global surface temperature (°C) in the business-as-usual scenario when carbon emission is endogenous. The expected size of one climate disaster in the new regime rises to $4\mathbb{E}J_2^{(L)}$, $2\mathbb{E}J_2^{(L)}$, or remains unchanged.

The SCC increases in the intensity of climate disasters. Like in Section 4.2, under a larger $\mathbb{E}J_2^{(H)}$, the expected losses from climate disasters increase, so the certainty equivalent effect of climate volatility risk on the SCC increases. Moreover, higher abatement efforts leave less of any given endowment for consumption as abatement costs rise. Also lower aggregate endowment and consumption due to higher climate damages and higher abatement costs imply a higher discount factor, or equivalently, a lower discount rate. Both the higher certainty equivalent of climate damage and the lower discount rate lead to larger SCCs.

6 An alternative Model of Climate Volatility Risk: Gradually Unfolding Tipping Points

In the climate literature, tipping points play a large role, as we discuss in our survey in Section 1. But in particular Dietz et al. (2021) and Lontzek et al. (2015) have argued that what looks like an instantaneous jump on a geographical time scale unfolds much more gradually on a regular timescale (see also Lenton and Ciscar (2013)). Therefore in this section, we provide an alternative model of climate volatility risk. Instead of an immediate increase in
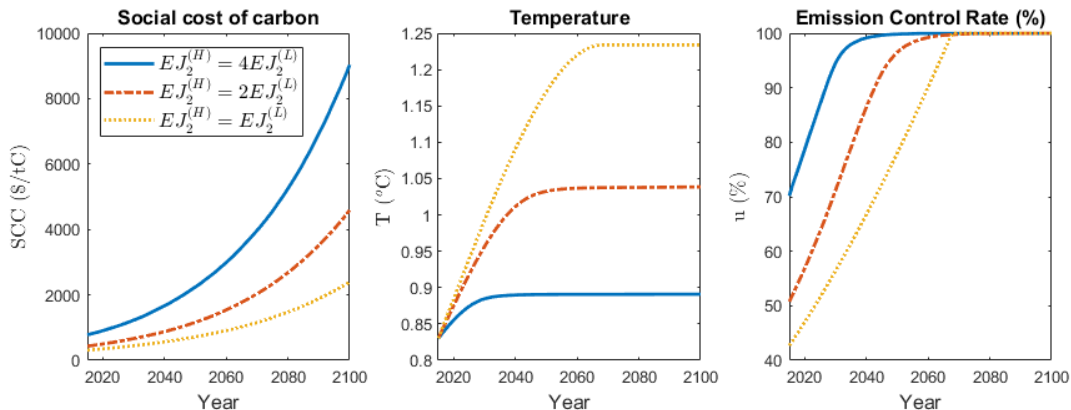
Figure 22: Social cost of carbon, mean global surface temperature, emission control rate, yearly carbon emissions and consumption-endowment ratio from Year 2015 to 2100 under optimal abatement when carbon emission is endogenous. The expected size of one climate disaster in the new regime rises to $4\mathbb{E}J_2^{(L)}$, $2\mathbb{E}J_2^{(L)}$, or remains unchanged.

climate volatility upon a regime shift, we model climate volatility as a Cox–Ingersoll–Ross (CIR) process as in Eraker and Yang (2022). We assume that its long-run value is subject to the one-off jump risk, and the climate volatility rises gradually to its long-run level after a regime shift. This assumption is more realistic than the baseline model, because actual jumps in the climate system unfolds more gradually over time. We find that this alternative model of climate volatility risk yields similar asset pricing implications, which implies that gradual climate regime shift matters little for the SCC and the long-run impact of the regime shift dominates.

All else the same as in Section 2, except that we now assume that the climate disaster frequency parameter $\bar{\lambda}_t$ follows a Cox–Ingersoll–Ross (CIR) process where its long-run value is subject to a one-off irreversible Poisson jump (i.e. climate regime shift) N_0 at rate λ_0. Formally,

$$d\bar{\lambda}_t = \theta \left(\bar{\bar{\lambda}}_t - \bar{\lambda}_t \right) dt + \sigma_\lambda \sqrt{\bar{\lambda}_t} dZ_{\lambda,t},$$

$$\bar{\bar{\lambda}}_t = (1 - N_{0,t}) \bar{\lambda}^{(L)} + N_{0,t} \bar{\lambda}^{(H)}$$

where $\bar{\bar{\lambda}}_t$ is the long-run value of $\bar{\lambda}_t$ which jumps from $\bar{\lambda}^{(L)}$ to $\bar{\lambda}^{(H)}$ upon the regime shift, θ

is the mean-reversion speed, $\sigma_\lambda \sqrt{\bar{\lambda}_t}$ is the standard deviation and Z_λ is a Brownian motion independent of the economic fluctuation risk Z. We impose the Feller condition (Feller (1951))

$$2\theta\bar{\bar{\lambda}}_t \geq \sigma_\lambda^2$$

to ensure $\bar{\lambda}_t > 0$.

To check whether different risk structures of climate volatility affects the SCC, we next compare the time paths of SCCs under the CIR model and the baseline one-off jump model in Figure 23, where no abatement policy is implemented (BAU) and carbon emissions are exogenous. We can expect similar results for the stochastic emissions model we analyzed in Section 5.

In our simulation we use the same values of $\bar{\lambda}^{(L)}$ and $\bar{\lambda}^{(H)}$ as before. For illustrative purpose we set the speed of volatility increase $\theta = 0.1$ so climate volatility rises to the new level in around 10 years in our simulation. To compare with the results from the baseline model, we set $\sigma_\lambda = 0$ so the SCCs are not affected by the stochasticity from the Brownian term of $\bar{\lambda}_t$ in the CIR process.

Figure 23 shows that for the same long run value of $\bar{\lambda}_t$ in the new climate regime, the SCC is larger in the one-off jump model than in the CIR model. In other words, the SCC is larger if climate volatility increases faster after the regime shift. This should not come as a surprise: a more gradual response to a positive shock in the long run value of volatility implies a lower time path for volatility after the shock has arrived.

Figure 24 shows how the speed of climate volatility increase affects the SCCs. We assume that the climate disaster frequency parameter is doubled in the new regime, i.e. $\bar{\lambda}^{(H)} = 2\bar{\lambda}^{(L)}$. In this plot, we compare the SCCs when θ takes different values (0.5 and 0.05) in the CIR model, as well as the SCC when climate volatility increases immediately in the baseline model. Consistent with the intuition above, we find that a more gradual response of climate volatility to the regime shift shock leads to a lower SCC, although the difference between SCCs is relatively small under different θ. When θ is large, climate disaster frequency
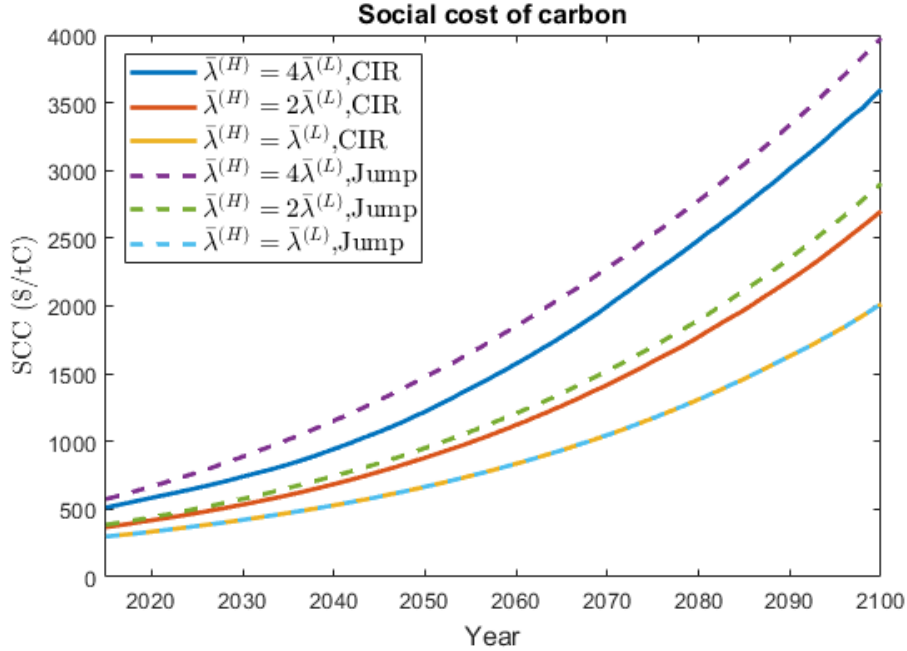
Figure 23: Social costs of carbon in the BAU scenario when $\bar{\lambda}_t$ follows an CIR process ("CIR") and when $\bar{\lambda}_t$ is subject to a one-off Poisson jump ("Jump"), where $\theta = 0.1$ and $\sigma_\lambda = 0$.

increases faster to the new long-run level after the regime shift, which implies larger marginal damages of carbon emissions and thus higher SCCs in the long run. The differences in SCCs at the beginning of our simulation are trivial. This is because the climate volatility increases only after the uncertainty about regime shift is resolved later, and the differences in future climate damages under different θ become smaller after having been discounted back to today's value.
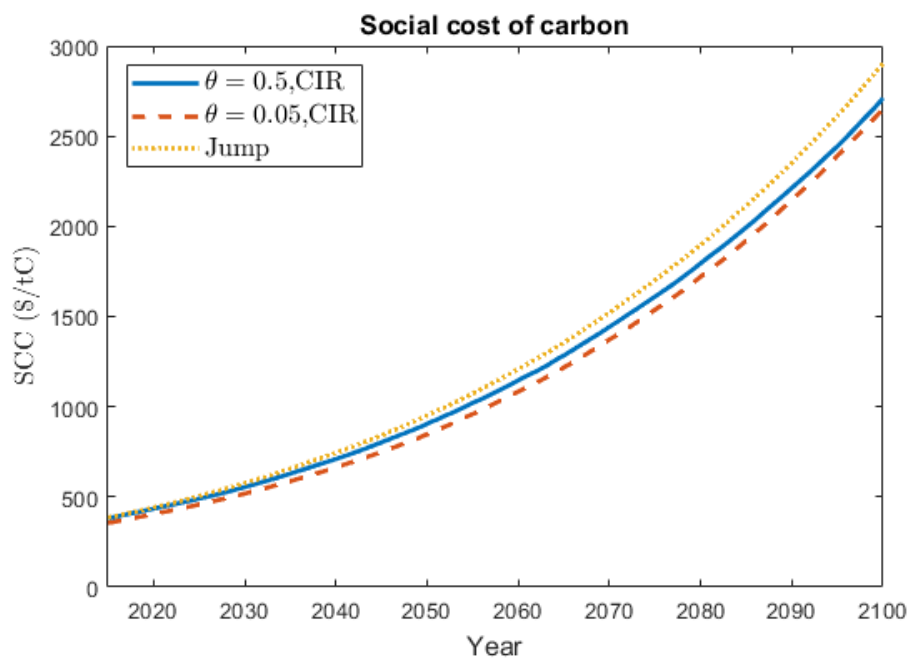
Figure 24: Social costs of carbon in the BAU scenario when $\bar{\lambda}_t$ either jumps immediately ("Jump") or follows an CIR process ("CIR") under $\sigma_\lambda = 0$ and different speed θ.

7 Conclusion

In this paper we have focused on stochastic climate volatility, a second-order uncertainty in the climate system that has not yet been studied in the climate economic literature. We show that under plausible calibrations the impact of volatility risk on the SCC is certainly not of second order. This matters since climate scientists have argued that global warming will bring irreversible and potentially permanent increases in climate volatility as part of a switch to a new climate risk regime, possibly already in the near future. However, when exactly such a shift to a new regime will take place is unknown and we do not know either how severe climate damages will be in the new regime. All this implies that climate volatility itself should be considered as a stochastic process, thereby introducing a new source of climate risk that we show affects the social cost of carbon significantly.

Using a dynamic stochastic integrated climate-economic model where representative agents are endowed with Duffie-Epstein recursive preferences, we examine how and by how much stochastic climate volatility affects the social cost of carbon under different abatement policies. We model the climate volatility risk as an irreversible one-off jump in climate volatility arriving as a Poisson process. We also test the robustness of the results using an alternative model of the volatility process, where actual climate volatility rises slowly after a Poisson shock to its long run value. This more realistic assumption is shown to not materially affect any of our conclusions.

First of all we find that climate volatility risk is as important as the climate volatility itself in terms of its impact on the Social Cost of Carbon (SCC), risk premia and the safe rate of interest. Climate volatility risk increases equilibrium risk premia on the same scale as climate volatility, and in spite of the higher risk premia also leads to a higher social cost of carbon. The impact of higher expected losses following climate volatility shocks more than offsets the impact of higher risk premia. As a consequence, and this is our second key conclusion, the stochasticity of climate volatility substantially increases the SCC, and thus deserves explicit analysis and inclusion in climate-economy models. We demonstrate this by also analyzing a

volatility shock that arrives at a known date and is of a known size. In that deterministic case both the certainty equivalent of climate damage and the stochastic discount factor will be smaller than they are when climate volatility risk is present. Therefore, failing to account for the stochasticity of climate volatility results in estimates of the SCC that are too low.

Third, we demonstrate that increases in the frequency and intensity of climate disasters affect the social cost of carbon in different ways. Both type of shocks lead to a higher social cost of carbon, but the marginal impact differs. For equal expected climate damage, both types of climate volatility shocks have a similar effect on the discount factor. However, the certainty equivalent effect of climate damages increases proportionally under a shock to disaster frequency, but more than proportionally under a shock to disaster intensity. This is possible for equal expected damages because of risk aversion. Therefore, a regime with more intense disasters increases the certainty equivalent of climate damages more and thus leads to a higher SCC than a switch to a regime with more frequent disasters does.

Conclusion number four is that endogenizing carbon emissions by linking them to the output process, thereby making emissions a stochastic process themselves, adds realism but changes none of the conclusions. Of course adding stochasticity does lead to a higher SCC, in line with our earlier results, but does not qualitatively change any of the results obtained under exogenous emissions. In the first part of this paper, we focused on the exogenous emission setup because it enabled us to obtain analytical expressions which cannot be derived under endogenous emissions, and these analytical expressions help in gaining intuition for the results obtained numerically. But when the exogenous emission flows are calibrated to match the endogenous emissions in expected value terms, they have the same impact on temperature and climate change as the endogenous emissions setup. Hence, the asset pricing implications and the SCCs are similar under both model specifications of carbon emissions.

Finally conclusion number five: we show that smoothing the increase in climate volatility leads to lower time paths of the SCC but does not generate qualitatively different implications from the response to the possibility of instantaneous shocks. A gradual unfolding of a

volatility tipping point slows down the increase in climate volatility and thus the SCC over time, but does not lead to different implications regarding the effect of climate volatility risk on the SCC.

Of course shocks on climate volatility are mostly yet to come; therefore there is lack of time-series data that could help in calibrating the stochastic volatility process. That makes the impact of volatility risk a natural candidate for the multiple prior/ambiguity aversion approach advocated by Chen and Epstein (2002) and Klibanoff et al. (2005), an issue we intend to take up in future work.

References

Abernethy, S. and Jackson, R. B. (2022). Global temperature goals should determine the time horizons for greenhouse gas emission metrics. *Environmental Research Letters*, 17(2):024019.

Bansal, R., Ochoa, M., and Kiku, D. (2017). Climate change and growth risks. Technical report, National Bureau of Economic Research.

Barndorff-Nielsen, O. E. and Shephard, N. (2001). Non-gaussian ornstein–uhlenbeck-based models and some of their uses in financial economics. *Journal of the Royal Statistical Society: Series B (Statistical Methodology)*, 63(2):167–241.

Barro, R. J. (2006). Rare disasters and asset markets in the twentieth century. *The Quarterly Journal of Economics*, 121(3):823–866.

Barro, R. J. (2009). Rare disasters, asset prices, and welfare costs. *American Economic Review*, 99(1):243–264.

Barro, R. J. and Jin, T. (2011). On the size distribution of macroeconomic disasters. *Econometrica*, 79(5):1567–1589.

Branger, N., Hülsbusch, H., and Kraftschik, A. (2018). The volatility-of-volatility term structure. In *Paris December 2017 Finance Meeting EUROFIDAI-AFFI*.

Cai, Y. and Lontzek, T. S. (2019). The social cost of carbon with economic and climate risks. *Journal of Political Economy*, 127(6):2684–2734.

Chen, Z. and Epstein, L. (2002). Ambiguity, risk, and asset returns in continuous time. *Econometrica*, 70(4):1403–1443.

Clark, P. K. (1973). A subordinated stochastic process model with finite variance for speculative prices. *Econometrica: journal of the Econometric Society*, pages 135–155.

Dietz, S., Rising, J., Stoerk, T., and Wagner, G. (2021). Economic impacts of tipping points in the climate system. *Proceedings of the National Academy of Sciences*, 118(34):e2103081118.

Dimson, E., Marsh, P., and Staunton, M. (2011). Equity premia around the world. *Available at SSRN 1940165*.

Duffie, D. and Epstein, L. G. (1992). Stochastic differential utility. *Econometrica: Journal of the Econometric Society*, pages 353–394.

Eraker, B., Johannes, M., and Polson, N. (2003). The impact of jumps in volatility and returns. *The Journal of Finance*, 58(3):1269–1300.

Eraker, B. and Yang, A. (2022). The price of higher order catastrophe insurance: The case of vix options. *The Journal of Finance*, 77(6):3289–3337.

Feller, W. (1951). Two singular diffusion problems. *Annals of mathematics*, pages 173–182.

Gjerde, J., Grepperud, S., and Kverndokk, S. (1999). Optimal climate policy under the possibility of a catastrophe. *Resource and energy economics*, 21(3-4):289–317.

Hambel, C., Kraft, H., and Schwartz, E. (2021). Optimal carbon abatement in a stochastic equilibrium model with climate change. *European Economic Review*, 132:103642.

Hu, G. and Liu, Y. (2022). The pricing of volatility and jump risks in the cross-section of index option returns. *Journal of Financial and Quantitative Analysis*, 57(6):2385–2411.

Huang, D., Schlag, C., Shaliastovich, I., and Thimme, J. (2019). Volatility-of-volatility risk. *Journal of Financial and Quantitative Analysis*, 54(6):2423–2452.

Hull, J. and White, A. (1987). The pricing of options on assets with stochastic volatilities. *The journal of finance*, 42(2):281–300.

IPCC (2007). The physical science basis. contribution of working group i to the fourth assessment report of the intergovernmental panel on climate change. *Cambridge University Press, Cambridge, United Kingdom and New York, NY, USA*, 996(2007):113–119.

IPCC (2021). *Climate Change 2021: The Physical Science Basis. Contribution of Working Group I to the Sixth Assessment Report of the Intergovernmental Panel on Climate Change*, volume In Press. Cambridge University Press, Cambridge, United Kingdom and New York, NY, USA.

Jensen, S. and Traeger, C. P. (2021). Pricing climate risk.

Johansson, Å., Guillemette, Y., Murtin, F., Turner, D., Nicoletti, G., de la Maisonneuve, C., Bousquet, G., and Spinelli, F. (2012). Looking to 2060: Long-term global growth prospects: A going for growth report.

Karydas, C. and Xepapadeas, A. (2019). Pricing climate change risks: Capm with rare disasters and stochastic probabilities. *CER-ETH Working Paper Series Working Paper*, 19:311.

Kelder, T., Müller, M., Slater, L., Marjoribanks, T., Wilby, R., Prudhomme, C., Bohlinger, P., Ferranti, L., and Nipen, T. (2020). Using unseen trends to detect decadal changes in 100-year precipitation extremes. *npj Climate and Atmospheric Science*, 3(1):47.

Klibanoff, P., Marinacci, M., and Mukerji, S. (2005). A smooth model of decision making under ambiguity. *Econometrica*, 73(6):1849–1892.

Kopp, R. E., Shwom, R. L., Wagner, G., and Yuan, J. (2016). Tipping elements and climate–economic shocks: Pathways toward integrated assessment. *Earth's Future*, 4(8):346–372.

Lemoine, D. and Traeger, C. (2014). Watch your step: optimal policy in a tipping climate. *American Economic Journal: Economic Policy*, 6(1):137–166.

Lenton, T. and Ciscar, J. (2013). Integrating tipping points into climate impact assessments. *Climate Change*, pages 585–597.

Lettau, M., Ludvigson, S. C., and Wachter, J. A. (2008). The declining equity premium: What role does macroeconomic risk play? *The Review of Financial Studies*, 21(4):1653–1687.

Lontzek, T. S., Cai, Y., Judd, K. L., and Lenton, T. M. (2015). Stochastic integrated assessment of climate tipping points indicates the need for strict climate policy. *Nature Climate Change*, 5(5):441–444.

Mattauch, L., Millar, R., van der Ploeg, R., Rezai, A., Schultes, A., Venmans, F., Bauer, N., Dietz, S., Edenhofer, O., Farrell, N., et al. (2018). Steering the climate system: an extended comment.

Matthews, H. D., Gillett, N. P., Stott, P. A., and Zickfeld, K. (2009). The proportionality of global warming to cumulative carbon emissions. *Nature*, 459(7248):829–832.

Matthews, H. D., Solomon, S., and Pierrehumbert, R. (2012). Cumulative carbon as a policy framework for achieving climate stabilization. *Philosophical Transactions of the Royal Society A: Mathematical, Physical and Engineering Sciences*, 370(1974):4365–4379.

Nordhaus, W. D. (2010). Economic aspects of global warming in a post-copenhagen environment. *Proceedings of the National Academy of Sciences*, 107(26):11721–11726.

Nordhaus, W. D. (2017). Revisiting the social cost of carbon. *Proceedings of the National Academy of Sciences*, 114(7):1518–1523.

Olijslagers, S. (2020). The social cost of carbon: Optimal policy versus business-asusual.

Olijslagers, S., van der Ploeg, F., and van Wijnbergen, S. (2023). On current and future carbon prices in a risky world. *Journal of Economic Dynamics and Control*, 146:104569.

Olijslagers, S. and van Wijnbergen, S. (2019). Discounting the future: on climate change, ambiguity aversion and epstein-zin preferences.

Pindyck, R. S. and Wang, N. (2013). The economic and policy consequences of catastrophes. *American Economic Journal: Economic Policy*, 5(4):306–339.

Reidmiller, D., Avery, C. W., Easterling, D. R., Kunkel, K. E., Lewis, K., Maycock, T. K., and Stewart, B. C. (2018). Fourth national climate assessment. *Volume II: Impacts, Risks, and Adaptation in the United States*, 440.

Rennert, K., Errickson, F., Prest, B. C., Rennels, L., Newell, R. G., Pizer, W., Kingdon, C., Wingenroth, J., Cooke, R., Parthum, B., et al. (2022). Comprehensive evidence implies a higher social cost of co2. *Nature*, 610(7933):687–692.

Roe, G. H. and Baker, M. B. (2007). Why is climate sensitivity so unpredictable? *Science*, 318(5850):629–632.

Shephard, N. and Andersen, T. G. (2009). Stochastic volatility: origins and overview. In *Handbook of financial time series*, pages 233–254. Springer.

Taylor, S. (2018). *Financial returns modelled by the product of two stochastic processes, a study of daily sugar prices*, pages 423–446. The International Library of Critical Writings in Economics. Edward Elgar. Reprinted, original publication 1982, in Time Series Analysis: Theory and Practice 1.

Thompson, V., Dunstone, N. J., Scaife, A. A., Smith, D. M., Slingo, J. M., Brown, S., and Belcher, S. E. (2017). High risk of unprecedented uk rainfall in the current climate. *Nature communications*, 8(1):107.

Tsai, J. and Wachter, J. A. (2015). Disaster risk and its implications for asset pricing. *Annual Review of Financial Economics*, 7:219–252.

Van den Bremer, T. S. and Van der Ploeg, F. (2021). The risk-adjusted carbon price. *American Economic Review*, 111(9):2782–2810.

Wiggins, J. B. (1987). Option values under stochastic volatility: Theory and empirical estimates. *Journal of financial economics*, 19(2):351–372.

A   Solution to the Optimization Problem and SCC

We describe details on solving the optimization problem of the representative agent in Section 2, where climate volatility risk is modelled by a stochastic arrival of a new regime in which climate disasters happen more frequently (Type (A)). Then we provide analytical expression of SCC. Under the other type of climate volatility risk (Type (B)), optimization problems can be solved analogously so we will not provide the details.

The following steps follow Tsai and Wachter (2015) and Olijslagers (2020). Let V_t be the total welfare which is a function of time t and state variables $(Y_t, T_t, \bar{\lambda}_t)$ with dynamics

$$dY_t = \mu Y_t dt + \sigma Y_t dZ_t - J_1 Y_t dN_{1,t} - J_2 Y_t dN_{2,t},$$
$$dT_t = \chi(1-u_t)E_t dt,$$
$$d\bar{\lambda}_t = \left(\bar{\lambda}^{(H)} - \bar{\lambda}^{(L)}\right) dN_{0,t}$$

Then the Hamilton–Jacobi–Bellman (HJB) equation is given by

$$
0 = \max_{u_t} \Bigg\{ f(C_t, V_t) + \frac{\partial V}{\partial t} + \mu Y_t V_Y + \mu_{T,t} V_T + \frac{1}{2}\sigma^2 Y_t^2 V_{YY}
$$
$$
+ \lambda_1 \mathbb{E}\left[V\left((1-J_1)Y_{t-}, T_t, \bar{\lambda}_t, t\right) - V(Y_{t-}, T_t, \bar{\lambda}_t, t)\right]
$$
$$
+ \lambda_{2,t} \mathbb{E}\left[V\left((1-J_2)Y_{t-}, T_t, \bar{\lambda}_t, t\right) - V(Y_{t-}, T_t, \bar{\lambda}_t, t)\right]
$$
$$
+ \lambda_0(1 - N_{0,t-})\mathbb{E}\left[V\left(Y_t, T_t, \bar{\lambda}^{(H)}, t\right) - V(Y_t, T_t, \bar{\lambda}^{(L)}, t-)\right] \Bigg\}
$$

where $\mu_{T,t} = \chi(1-u_t)E_t$, $\lambda_{2,t} = \bar{\lambda}_t T_t$, V_X and V_{XX} are the first- and second-order partial derivatives of variable X.

Tsai and Wachter (2015) showed that under this model setup, the conjecture $V = g\left(T, \bar{\lambda}_t, t\right)\frac{Y^{1-\gamma}}{1-\gamma}$ can be used to reduce the dimensionality of the state space and simplify the numerical procedure. Define $\xi_t := \frac{C_t}{Y_t}$ as the consumption-endowment ratio, then the flow utility can be rewritten as

$$f(C, V) = \beta\zeta\left(g^{-\frac{1}{\zeta}}\xi^{1-\frac{1}{\epsilon}} - 1\right)V$$

The HJB equation can then be rewritten as

$$
0 = \min_{u_t} \Bigg\{ \left[\beta\zeta\left(g_{t-}^{-\frac{1}{\zeta}}\xi_{t-}^{1-\frac{1}{\epsilon}} - 1\right) + (1-\gamma)\left(\mu - \frac{1}{2}\gamma\sigma^2 - \frac{\lambda_1}{\alpha_1 + 1 - \gamma} - \frac{\bar{\lambda}_t T_t}{\alpha_2 + 1 - \gamma}\right)\right]g_{t-}
$$
$$
+ \frac{\partial g}{\partial t} + \mu_{T,t}g_T + \lambda_0\left(1 - N_{0,t-}\right)\left(\frac{g_t}{g_{t-}} - 1\right) \Bigg\}
\tag{10}
$$

where $g_t = g(T_t, \bar{\lambda}_t, t)$ and $g_{t-} = g(T_t, \bar{\lambda}_{t-}, t)$. If the one-off jump N_0 does not happen at t, then we have $g_t = g_{t-}$. Equation 10 is a minimization problem because $\gamma > 1$.

The optimal abatement policy u_t^* satisfies the first order condition

$$\beta(1-\gamma)g_t^{1-1/\zeta}\xi_t^{-1/\epsilon}\frac{\partial\xi_t}{\partial u_t} - \chi E_t g_T = 0.$$

Stochastic discount factor To solve for the carbon price, we start with the stochastic discount factor which is given by $\pi_t = \exp\left[\int_0^t f_V(C_s, V_s)ds\right]f_C(C_t, V_t)$ (Duffie and Epstein (1992)). Taking derivatives of $f(C, V)$ with respect to C and V, we get $f_C(C, V) = \frac{\beta C^{-1/\epsilon}}{[(1-\gamma)V]^{1/\zeta-1}}$ and $f_V(C, V) = \beta\zeta\left[\left(1-\frac{1}{\zeta}\right)((1-\gamma)V)^{-1/\zeta}C^{1-1/\epsilon} - 1\right]$. Plugging $C_t = \xi_t Y_t$ and the conjecture $V_t = g_t\frac{Y_t^{1-\gamma}}{1-\gamma}$ into the derivatives above yields

$$f_C(C_t, V_t) = \beta g_t^{1-1/\zeta}\xi_t^{-1/\epsilon}Y_t^{-\gamma}, \quad f_V(C_t, V_t) = \beta\zeta\left[\left(1-\frac{1}{\zeta}\right)g_t^{-1/\zeta}\xi_t^{1-1/\epsilon} - 1\right].$$

Substituting $f_C(C, V)$ and $f_V(C, V)$ into the expression of stochastic discount factor π and using Ito's formula, we obtain the stochastic differential equation of π

$$\begin{aligned}
\frac{d\pi_t}{\pi_{t-}} =& \beta\zeta\left[\left(1-\frac{1}{\zeta}\right)g_{t-}^{-1/\zeta}\xi_{t-}^{1-1/\epsilon} - 1\right]dt + \frac{dY_t^{-\gamma}}{Y_{t-}^{-\gamma}} + \frac{dg_t^{1-1/\zeta}}{g_{t-}^{1-1/\zeta}} + \frac{d\xi_t^{-1/\epsilon}}{\xi_{t-}^{-1/\epsilon}} + \frac{dY_t^{-\gamma}dg_t^{1-1/\zeta}}{Y_{t-}^{-\gamma}g_{t-}^{1-1/\zeta}} \\
& + \frac{dY_t^{-\gamma}d\xi_t^{-1/\epsilon}}{Y_t^{-\gamma}g_{t-}^{1-1/\zeta}} + \frac{dg_t^{1-1/\zeta}d\xi_t^{-1/\epsilon}}{g_t^{1-1/\zeta}\xi_{t-}^{-1/\epsilon}}
\end{aligned}$$

where

$$\frac{dY_t^{-\gamma}}{Y_{t-}^{-\gamma}} = -\gamma\left(\mu - \frac{1}{2}(1+\gamma)\sigma^2\right)dt - \gamma\sigma dZ_t + \left[(1-J_1)^{-\gamma} - 1\right]dN_{1,t} + \left[(1-J_2)^{-\gamma} - 1\right]dN_{2,t}$$

$$\frac{dg_t^{1-\frac{1}{\zeta}}}{g_{t-}^{1-\frac{1}{\zeta}}} = \left(1-\frac{1}{\zeta}\right)\left(\frac{\partial g_t/\partial t}{g_{t-}} + \frac{g_T}{g_{t-}}\mu_T\right)dt + \left(\frac{g_t^{1-\frac{1}{\zeta}}}{g_{t-}^{1-\frac{1}{\zeta}}} - 1\right)dN_{0,t}$$

$$\frac{d\xi_t^{-\frac{1}{\epsilon}}}{\xi_{t-}^{-\frac{1}{\epsilon}}} = \left(-\frac{1}{\epsilon}\right)\left(\frac{\partial\xi_t/\partial t}{\xi_{t-}} + \frac{\xi_T}{\xi_{t-}}\mu_T\right)dt + \left(\frac{\xi_t^{-\frac{1}{\epsilon}}}{\xi_{t-}^{-\frac{1}{\epsilon}}} - 1\right)dN_{0,t}.$$

Plugging in yields

$$\begin{aligned}
\frac{d\pi_t}{\pi_{t-}} =& \left\{\beta\zeta\left[\left(1-\frac{1}{\zeta}\right)g_{t-}^{-1/\zeta}\xi_{t-}^{1-1/\epsilon} - 1\right] - \gamma\left(\mu - \frac{1}{2}(1+\gamma)\sigma^2\right) + \left(1-\frac{1}{\zeta}\right)\left(\frac{\partial g_t/\partial t}{g_{t-}} + \frac{g_T}{g_{t-}}\mu_T\right)\right. \\
& \left. + \left(-\frac{1}{\epsilon}\right)\left(\frac{\partial\xi_t/\partial t}{\xi_{t-}} + \frac{\xi_T}{\xi_{t-}}\mu_T\right)\right\}dt - \gamma\sigma dZ_t + \left[(1-J_1)^{-\gamma} - 1\right]dN_{1,t} + \left[(1-J_2)^{-\gamma} - 1\right]dN_{2,t} \\
& + \left[\left(\frac{g_t^{1-\frac{1}{\zeta}}}{g_{t-}^{1-\frac{1}{\zeta}}} - 1\right) + \left(\frac{\xi_t^{-\frac{1}{\epsilon}}}{\xi_{t-}^{-\frac{1}{\epsilon}}} - 1\right) + \left(\frac{g_t^{1-\frac{1}{\zeta}}}{g_{t-}^{1-\frac{1}{\zeta}}} - 1\right)\left(\frac{\xi_t^{-\frac{1}{\epsilon}}}{\xi_{t-}^{-\frac{1}{\epsilon}}} - 1\right)\right]dN_{0,t},
\end{aligned}$$

or

$$\frac{d\pi_t}{\pi_{t-}} = \left(\mu_{\pi,t} + r_t^f\right)dt - \gamma\sigma dZ_t + \left[(1-J_1)^{-\gamma} - 1\right]dN_{1,t} + \left[(1-J_2)^{-\gamma} - 1\right]dN_{2,t} + \mathcal{J}_{\pi,t}dN_{0,t},$$

(11)

where

$$\mu_{\pi,t} = \beta\zeta\left[\left(1-\frac{1}{\zeta}\right)g_{t-}^{-1/\zeta}\xi_{t-}^{1-1/\epsilon} - 1\right] - \gamma\left(\mu - \frac{1}{2}(1+\gamma)\sigma^2\right) + \left(1-\frac{1}{\zeta}\right)\left(\frac{\partial g_t/\partial t}{g_{t-}} + \frac{g_T}{g_{t-}}\mu_T\right)$$
$$-\frac{1}{\epsilon}\left(\frac{\partial \xi_t/\partial t}{\xi_{t-}} + \frac{\xi_T}{\xi_{t-}}\mu_T\right),$$

and

$$\mathcal{J}_{\pi,t} := \left(\frac{g_t^{1-\frac{1}{\zeta}}}{g_{t-}^{1-\frac{1}{\zeta}}} - 1\right) + \left(\frac{\xi_t^{-\frac{1}{\epsilon}}}{\xi_{t-}^{-\frac{1}{\epsilon}}} - 1\right) + \left(\frac{g_t^{1-\frac{1}{\zeta}}}{g_{t-}^{1-\frac{1}{\zeta}}} - 1\right)\left(\frac{\xi_t^{-\frac{1}{\epsilon}}}{\xi_{t-}^{-\frac{1}{\epsilon}}} - 1\right).$$

Equation (11) implies that the stochastic discount factor captures the exposure to economic diffusive risk dZ, economic disaster risk dN_1, climate disaster risk dN_2 and the climate volatility risk dN_0.

Risk-free rate Consider a risk-free bond B_t with return r_t^f. Let $\mu_{\pi,t}$ be the drift term in the stochastic differential equation of π at time t. Under no-arbitrage condition, $\pi_t B_t$ is a martingale, which implies

$$r_t^f = -\mu_{\pi,t} - \lambda_1\frac{\gamma}{\alpha_1 - \gamma} - \bar{\lambda}_t T_t\frac{\gamma}{\alpha_2 - \gamma} - \lambda_0\left(1 - N_{0,t-}\right)\mathcal{J}_{\pi,t}.$$

Note that the HJB equation (10) implies

$$\frac{\partial g_t/\partial t}{g_{t-}} + \mu_{T,t-}\frac{g_T}{g_{t-}} = -\beta\zeta\left(g_{t-}^{-1/\zeta}\xi_{t-}^{1-1/\epsilon} - 1\right) - (1-\gamma)\left(\mu - \frac{\gamma}{2}\sigma^2 - \frac{\lambda_1}{\alpha_1 + 1 - \gamma} - \frac{\bar{\lambda}_t T_t}{\alpha_2 + 1 - \gamma}\right)$$
$$- \lambda_0\left(1 - N_{0,t-}\right)\left(\frac{g_t}{g_{t-}} - 1\right)$$

Substituting the expression of $\frac{\partial g_t/\partial t}{g_{t-}} + \mu_{T,t-}\frac{g_T}{g_{t-}}$ above into $\mu_{\pi,t}$ yields the risk-free interest rate

$$r_t^f = \beta + \frac{\mu + \mu_{\xi,t}}{\epsilon} - \frac{\gamma}{2}\left(1+\frac{1}{\epsilon}\right)\sigma^2 + \lambda_1\left(\frac{\gamma - 1/\epsilon}{\alpha_1 + 1 - \gamma} - \frac{\gamma}{\alpha_1 - \gamma}\right) + \bar{\lambda}_t T_t\left(\frac{\gamma - 1/\epsilon}{\alpha_2 + 1 - \gamma} - \frac{\gamma}{\alpha_2 - \gamma}\right)$$
$$+ \lambda_0\left(1 - N_{0,t-}\right)\left[\left(1-\frac{1}{\zeta}\right)\left(\frac{g_t}{g_{t-}} - 1\right) - \mathcal{J}_{\pi,t}\right].$$

64

where $\mu_\xi = \frac{\partial \xi_t / \partial t}{\xi_{t-}} + \frac{\xi_T}{\xi_{t-}} \mu_T$. Note that the dynamic of consumption process C_t is given by

$$
\begin{aligned}
\frac{dC_t}{C_{t-}} &= \frac{d(\xi_t Y_t)}{\xi_{t-} Y_{t-}} = \frac{d\xi_t}{\xi_t} + \frac{dY_t}{Y_{t-}} + \frac{d\xi_t dY_t}{\xi_t Y_{t-}} \\
&= \mu_{C,t} dt + \sigma dZ_t - J_1 dN_{1,t} - J_2 dN_{2,t} + \left(\frac{\xi_t}{\xi_{t-}} - 1 \right) dN_{0,t} \qquad (12)
\end{aligned}
$$

where $\mu_{C,t} = \mu + \mu_{\xi,t}$. Therefore the risk-free rate is equivalent to

$$
\begin{aligned}
r_t^f = &\beta + \frac{\mu_{C,t}}{\epsilon} - \frac{\gamma}{2} \left(1 + \frac{1}{\epsilon} \right) \sigma^2 + \lambda_1 \left(\frac{\gamma - 1/\epsilon}{\alpha_1 + 1 - \gamma} - \frac{\gamma}{\alpha_1 - \gamma} \right) + \bar{\lambda}_t T_t \left(\frac{\gamma - 1/\epsilon}{\alpha_2 + 1 - \gamma} - \frac{\gamma}{\alpha_2 - \gamma} \right) \\
&+ \lambda_0 \left(1 - N_{0,t-} \right) \mathcal{J}_{f,t}
\end{aligned}
$$

where

$$
\mathcal{J}_{f,t} = \left(1 - \frac{1}{\zeta} \right) \left(\frac{g_t}{g_{t-}} - 1 \right) - \mathcal{J}_{\pi,t}.
$$

Risk premium   Consider an asset which pays continuous dividends equal to the consumption C_t, then its ex-dividend price S_t also measures the total wealth of the agent. The risk premium is given by the difference between the asset return and the risk-free rate r_t^f.

Let $\kappa_t := \frac{C_t}{S_t}$ be the consumption-wealth ratio (or price-dividend ratio). Given that $f_C = V_S$ under optimal condition (Tsai and Wachter (2015)) and $V_S = \kappa_t V_C$ (chain rule), we have $\kappa_t = \frac{f_C}{V_C} = \beta g_t^{-1/\zeta} \xi_t^{1-1/\epsilon}$ and thus the ex-dividend price of the asset is $S_t = \frac{C_t}{\kappa_t} = \beta^{-1} g_t^{1/\zeta} \xi_t^{1/\epsilon} Y_t$. Using Itô's lemma, we have

$$
\frac{dS_t}{S_{t-}} = \frac{dY_t}{Y_{t-}} + \frac{dg_t^{\frac{1}{\zeta}}}{g_{t-}^{\frac{1}{\zeta}}} + \frac{d\xi_t^{\frac{1}{\epsilon}}}{\xi_{t-}^{\frac{1}{\epsilon}}} + \frac{dY_t dg_t^{1/\zeta}}{Y_{t-} g_{t-}^{1/\zeta}} + \frac{dY_t d\xi_t^{1/\epsilon}}{Y_{t-} \xi_{t-}^{1/\epsilon}} + \frac{dg_t^{1/\zeta} d\xi_t^{1/\epsilon}}{g_{t-}^{1/\zeta} \xi_{t-}^{1/\epsilon}}
$$

where $\frac{dY_t}{Y_{t-}} = \mu dt + \sigma dZ_t - J_1 dN_{1,t} - J_2 dN_{2,t}$ is given, and by Itô's formula

$$
\begin{aligned}
\frac{dg_t^{1/\zeta}}{g_{t-}^{1/\zeta}} &= \frac{1}{\zeta} \mu_{g,t} dt + \left(\frac{g_t^{1/\zeta}}{g_{t-}^{1/\zeta}} - 1 \right) dN_{0,t}, \\
\frac{d\xi_t^{1/\epsilon}}{\xi_{t-}^{1/\epsilon}} &= \frac{1}{\epsilon} \mu_{\xi,t} dt + \left(\frac{\xi_t^{1/\epsilon}}{\xi_{t-}^{1/\epsilon}} - 1 \right) dN_{0,t}
\end{aligned}
$$

where $\mu_{g,t} = \frac{\partial g_t / \partial t}{g_{t-}} + \frac{g_T}{g_{t-}} \mu_T$ and $\mu_{\xi,t} = \frac{\partial \xi_t / \partial t}{\xi_{t-}} + \frac{\xi_T}{\xi_{t-}} \mu_T$. Then we can derive the dynamic of the cum-dividend price S_t^d

$$
\frac{dS_t^d}{S_{t-}} = \frac{dS_t}{S_{t-}} + \kappa_t dt = \mu_{S,t-} dt + \sigma dZ_t - J_1 dN_{1,t} - J_2 dN_{2,t} + \mathcal{J}_{S,t} dN_{0,t}
$$

where

$$\mu_{S,t-} = \beta + \frac{\mu_{C,t}}{\epsilon} + \frac{1}{2}\gamma\sigma^2\left(1 - \frac{1}{\epsilon}\right) + \lambda_1\frac{1 - 1/\epsilon}{\alpha_1 + 1 - \gamma} + \bar{\lambda}T_t\frac{1 - 1/\epsilon}{\alpha_2 + 1 - \gamma} - \lambda_0\left(1 - N_{0,t-}\right)\frac{1}{\zeta}\left(\frac{g_t}{g_{t-}} - 1\right),$$

$$\mathcal{J}_{S,t} = \left(\frac{g_t^{1/\zeta}}{g_{t-}^{1/\zeta}} - 1\right) + \left(\frac{\xi_t^{1/\epsilon}}{\xi_{t-}^{1/\epsilon}} - 1\right) + \left(\frac{g_t^{1/\zeta}}{g_{t-}^{1/\zeta}} - 1\right)\left(\frac{\xi_t^{1/\epsilon}}{\xi_{t-}^{1/\epsilon}} - 1\right).$$

Therefore the risk premium r_p is given by

$$r_{p,t} = \mu_{S,t} - r_t^f - \lambda_1\mathbb{E}J_1 - \bar{\lambda}_tT_t\mathbb{E}J_2 + \lambda_0(1 - N_{0,t-})\mathcal{J}_{S,t}$$

$$= \gamma\sigma^2 + \lambda_1\left[\frac{-1}{\alpha_1 + 1} + \frac{\gamma}{\alpha_1 - \gamma} + \frac{1 - \gamma}{\alpha_1 + 1 - \gamma}\right] + \bar{\lambda}_tT_t\left[\frac{-1}{\alpha_2 + 1} + \frac{\gamma}{\alpha_2 - \gamma} + \frac{1 - \gamma}{\alpha_2 + 1 - \gamma}\right]$$

$$+ \lambda_0\left(1 - N_{0,t-}\right)\left[-\frac{1}{\zeta}\left(\frac{g_t}{g_{t-}} - 1\right) - \mathcal{J}_{f,t} + \mathcal{J}_{S,t}\right]$$

$$= \gamma\sigma^2 + \lambda_1\left[\frac{-1}{\alpha_1 + 1} + \frac{\gamma}{\alpha_1 - \gamma} + \frac{1 - \gamma}{\alpha_1 + 1 - \gamma}\right] + \bar{\lambda}_tT_t\left[\frac{-1}{\alpha_2 + 1} + \frac{\gamma}{\alpha_2 - \gamma} + \frac{1 - \gamma}{\alpha_2 + 1 - \gamma}\right]$$

$$+ \lambda_0\left(1 - N_{0,t-}\right)\left[\mathcal{J}_{S,t} + \mathcal{J}_{\pi,t} - \left(\frac{g_t}{g_{t-}} - 1\right)\right]$$

SCC By definition, the social cost of carbon at time 0 is

$$SCC_0 = -\chi\frac{\partial V_0/\partial T_0}{f_C(C_0, V_0)} = -\frac{\chi Y_0}{\beta\left(1 - \gamma\right)g_0^{1 - \frac{1}{\zeta}}\xi_0^{-\frac{1}{\epsilon}}}g_{T,0} = -\frac{\chi C_0}{1 - 1/\epsilon}\frac{\partial(\kappa_0^{-1})}{\partial T_0} - \chi S_0\frac{\partial\xi_0/\partial T_0}{\xi_0} \quad (13)$$

where $\kappa_0^{-1} = \frac{S_0}{C_0}$ by definition, and the last line comes from the substitution $g_0 = \beta^\zeta\xi^{1-\gamma}\kappa_0^{-\zeta}$.
The second term in Equation (13) measures the effect of abatement on carbon price. The
first term can be further expanded as follows. Note that the initial asset price S_0 is the sum
of all future consumption flows discounted back to time 0, i.e. $S_0 = \int_0^\infty\mathbb{E}\left(\frac{\pi_sC_s}{\pi_0}\right)ds$, where
$\mathbb{E}\left(\frac{\pi_tC_t}{\pi_0}\right)$ is the time-0 value of time-t consumption C_t. Applying Ito's lemma on π_tC_t, we
have

$$\frac{d\left(\pi_tC_t\right)}{\pi_{t-}C_{t-}} = \left[\mu_{C,t} - r_t^f - \lambda_1\frac{\gamma}{\alpha_1 - \gamma} - \bar{\lambda}_tT_t\frac{\gamma}{\alpha_2 - \gamma} - \lambda_0\left(1 - N_{0,t-}\right)\mathcal{J}_{\pi,t} - \gamma\sigma^2\right]dt$$

$$+ (1 - \gamma)\sigma dZ_t + \left[(1 - J_1)^{1-\gamma} - 1\right]dN_{1,t} + \left[(1 - J_2)^{1-\gamma} - 1\right]dN_{2,t}$$

$$+ \left[\mathcal{J}_{\pi,t} + \left(\frac{\xi_t}{\xi_{t-}} - 1\right) + \left(\frac{\xi_t}{\xi_{t-}} - 1\right)\mathcal{J}_{\pi,t}\right]dN_{0,t}$$

which implies

$$\mathbb{E}_0 \frac{\pi_t C_t}{\pi_0 C_0} = \exp\left\{ \int_0^t \left[\mu_{C,s} - r_s^f - \frac{\lambda_1 \gamma}{\alpha_1 - \gamma} - \frac{\bar{\lambda}_s T_s \gamma}{\alpha_2 - \gamma} - \gamma \sigma^2 + \lambda_1 \frac{\gamma - 1}{\alpha_1 + 1 - \gamma} + \bar{\lambda}_s T_s \frac{\gamma - 1}{\alpha_2 + 1 - \gamma} \right. \right.$$

$$\left. \left. + \lambda_0 \left(1 - N_{0,s-}\right) \left(\left(\frac{\xi_s}{\xi_{s-}} - 1 \right) + \left(\frac{\xi_s}{\xi_{s-}} - 1 \right) \mathcal{J}_{\pi,s} \right) \right] ds \right\}$$

$$= \exp\left\{ -\int_0^t \left[r_s^f + r_{p,s} - \lambda_0 \left(1 - N_{0,s-}\right) \left(\frac{\xi_s}{\xi_{s-}} \mathcal{J}_{\pi,s} + \mathcal{J}_{S,s} - \left(\frac{g_s}{g_{s-}} - 1 \right) \right) \right. \right.$$

$$\left. \left. - \left(\mu_{C,s} - \frac{\lambda_1}{\alpha_1 + 1} - \frac{\bar{\lambda}_s T_s}{\alpha_2 + 1} + \lambda_0 \left(1 - N_{0,s-}\right) \left(\frac{\xi_s}{\xi_{s-}} - 1 \right) \right) \right] ds \right\}.$$

Given that $\mathbb{E}_0 C_t = C_0 \exp\left\{ \int_0^t \left[\mu_{C,s} - \frac{\lambda_1}{\alpha_1+1} - \frac{\bar{\lambda}_s T_s}{\alpha_2+1} + \lambda_0 \left(1 - N_{0,s-}\right) \left(\frac{\xi_s}{\xi_{s-}} - 1 \right) \right] ds \right\}$ from Equation (12), we can rewrite $\mathbb{E}_0 \frac{\pi_t C_t}{\pi_0 C_0}$ as

$$\mathbb{E}_0 \frac{\pi_t C_t}{\pi_0 C_0} = \exp\left\{ -\int_0^t \left[r_s^f + r_{p,s} + r_{J,s} \right] ds \right\} \frac{\mathbb{E}_0 C_t}{C_0}$$

where

$$r_{J,s} = -\lambda_0 \left(1 - N_{0,s-}\right) \left(\frac{\xi_s}{\xi_{s-}} \mathcal{J}_{\pi,s} + \mathcal{J}_{S,s} - \left(\frac{g_s}{g_{s-}} - 1 \right) \right)$$

$$= -\lambda_0 \left(1 - N_{0,s-}\right) \left(\frac{g_t^{1-1/\zeta}}{g_{t-}^{1-1/\zeta}} - \frac{\xi_t^{1/\epsilon}}{\xi_{t-}^{1/\epsilon}} \right) \left(\frac{\xi_t^{1-1/\epsilon}}{\xi_{t-}^{1-1/\epsilon}} - \frac{g_t^{1/\zeta}}{g_{t-}^{1/\zeta}} \right)$$

The numerical value of $r_{J,s}$ is much smaller than r^f and r_p because both $\frac{g_t^{1-1/\zeta}}{g_{t-}^{1-1/\zeta}} - \frac{\xi_t^{1/\epsilon}}{\xi_{t-}^{1/\epsilon}}$ and $\frac{\xi_t^{1-1/\epsilon}}{\xi_{t-}^{1-1/\epsilon}} - \frac{g_t^{1/\zeta}}{g_{t-}^{1/\zeta}}$ are approximately zero. The rate $r^f + r_p + r_J$ at which future consumption flows are discounted is called the (consumption) growth-adjusted consumption discount rate.

The inverse of consumption-wealth ratio is given by

$$\kappa_0^{-1} = \frac{S_0}{C_0} = \int_0^\infty \mathbb{E}\left(\frac{\pi_t C_t}{\pi_0 C_0} \right) dt = \int_0^\infty \exp\left[-\int_0^t \left(r_s^f + r_{p,s} + r_{J,s} \right) ds \right] \frac{\mathbb{E}_0 C_t}{C_0} dt \qquad (14)$$

Substituting Equation (14) into the first term in Equation (13) yields

$$-\frac{\chi C_0}{1-1/\epsilon}\frac{\partial(\kappa_0^{-1})}{\partial T_0} = -\frac{\chi}{1-1/\epsilon}\int_0^\infty \frac{\partial}{\partial T_0}\left\{\exp\left[-\int_0^t \left(r_s^f + r_{p,s} + r_{J,s}\right)ds\right]\mathbb{E}_0 C_t\right\}dt$$

$$=\frac{\chi}{1-1/\epsilon}\int_0^\infty\left\{\int_0^t \frac{\partial}{\partial T_0}\left[r_s^f + r_{p,s} + r_{J,s} - \left(\mu_{C,s} - \frac{\lambda_1}{\alpha_1+1} - \frac{\bar{\lambda}_s T_s}{\alpha_2+1}\right.\right.\right.$$

$$\left.\left.\left.+ \lambda_0\left(1-N_{0,s-}\right)\left(\frac{\xi_s}{\xi_{s-}}-1\right)\right)\right]ds\right\}\exp\left[-\int_0^t \left(r_s^f + r_{p,s} + r_{J,s}\right)ds\right]\mathbb{E}_0 C_t dt$$

$$=\frac{\chi}{1-1/\epsilon}\int_0^\infty\left\{\int_0^t \left[\frac{\partial\lambda_{2,s}}{\partial T_0}\left(\frac{1-1/\epsilon}{\alpha_2+1-\gamma}\right)\right]ds\right\}\cdot\exp\left[-\int_0^t \left(r_s^f + r_{p,s} + r_{J,s}\right)ds\right]\mathbb{E}_0 C_t dt$$

$$=\int_0^\infty\left\{\int_0^t \chi\left(\frac{1}{\alpha_2+1-\gamma}\right)\frac{\partial\lambda_{2,s}}{\partial T_0}ds\right\}\cdot\exp\left[-\int_0^t \left(r_s^f + r_{p,s} + r_{J,s}\right)ds\right]\mathbb{E}_0 C_t dt \qquad (15)$$

B   Numerical Results for the New Climate Regime (B)

Below we provide the numerical results for the risk-free rate and the risk premium in Regime (B), as a supplementary analysis for Section 4.2.

   We consider the case where under climate volatility risk the intensity of climate disasters increases while their frequency does not change. Call this regime (B). Since the SCC can be regarded as the current price of an asset which pays the amount of climate-induced future losses in consumption flow as "dividend" in each period, the calculation of SCC fits well into the regular asset pricing framework. Based on the analytical framework in Section 4, we provide the numerical results for the key components of the consumption discount rate, the risk-free rate and the risk premium. We consider three different cases of the disaster intensity in the new regime: $\mathbb{E}J_2^{(H)} = 4\mathbb{E}J_2^{(L)}, 2\mathbb{E}J_2^{(L)}$, and $\mathbb{E}J_2^{(L)}$.

B.1   Risk-free rate

The risk-free rate in the business-as-usual scenario   Figure 25 shows the decomposition of risk-free rates in the business-as-usual scenario, according to Equation (2). Panel (a) and (b) show the expectation effect and the risk effect of the stochastic climate volatility on risk-free rates, Panel (c) shows the effect of climate disasters on the risk-free rate, and Panel (d) plots the time paths of the risk-free rate itself. Both the climate disaster risk and the climate volatility risk negatively affect the risk-free rate, as can be seen in Panel (a), (b) and (c). Moreover, their magnitudes are larger under higher disaster intensity $\mathbb{E}J_2^{(H)}$, because the economy is subject to more climate risks when $\mathbb{E}J_2^{(H)}$ is larger. Besides, the sizes of all risks in Panel (a), (b) and (c) increase over time, because rising temperature leads to more frequent climate damages and the expected climate damage increases as the shock to climate volatility is more likely to happen in the future. The expected effect of climate volatility risk and the climate disaster effect are of the same order, while the risk effect of climate volatility risk is much smaller. The time path of risk-free rate is downward-sloping since the negative effects of both types of climate risks increase over time. Compared with Regime (A) in the BAU scenario, the magnitudes in Panel (a), (b) and (c) are larger under Regime (B), which therefore leads to lower time paths of the risk-free rate.

The risk-free rate under optimal abatement   Figure 26 shows the average risk-free rate and its decomposition under optimal abatement policies. Panel (a) and (b) measure the effects of climate volatility risk through the expectation and the risk channels, Panel (c) shows the effect of climate disaster risks, and Panel (d) shows the time path of risk-free rates under different climate disaster intensities in the new climate regime. Compared with the BAU scenario, both climate disaster risk and climate volatility risk have a smaller impact on the risk-free rate, because temperature rises more slowly under emission control and thus extreme weather events are less likely to happen. Climate volatility risk has a significant impact on risk-free rates. From Panel (a) and (b), we find that climate volatility risk affects the risk-free rate largely through the expectation channel. The risk effect of climate volatility risk is positive before the emission control rate reaches its maximum of 100% and declines below zero afterwards. As the climate volatility risk gradually resolves over time, the effect
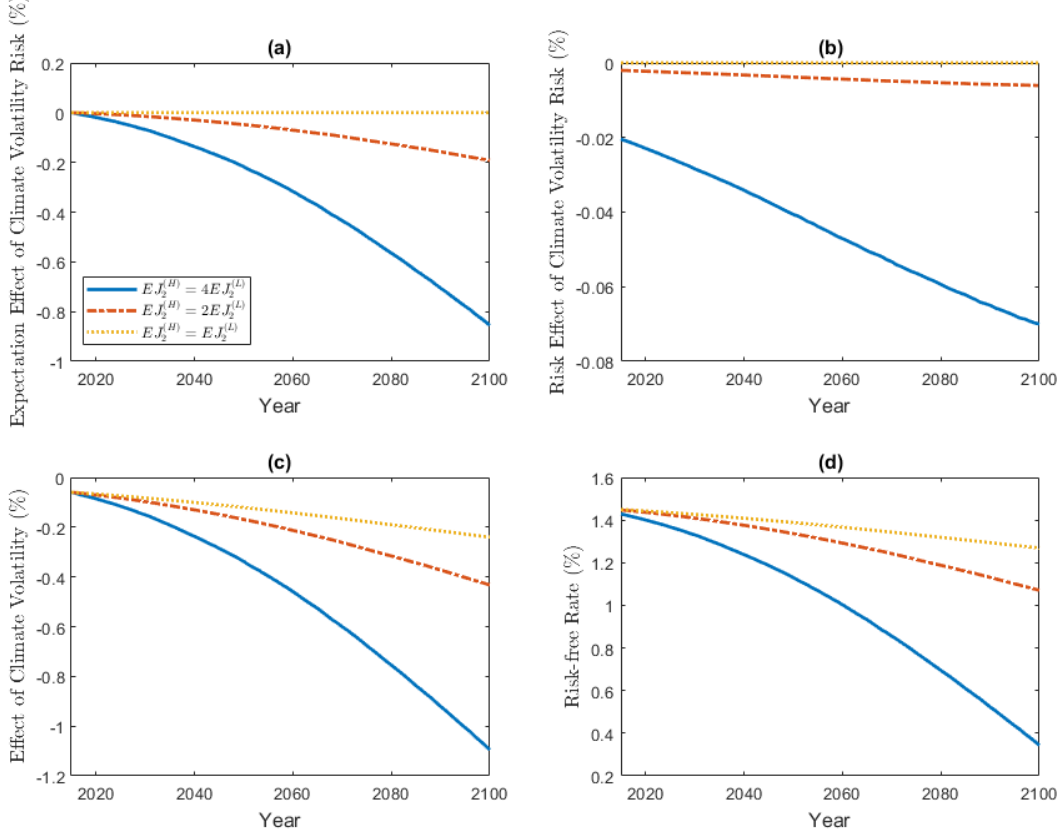
Figure 25: Decomposition of (average) risk-free rates in the BAU scenario under climate volatility risk (B). The expected size of one climate disaster in the new regime rises to $4\mathbb{E}J_2^{(L)}$, $2\mathbb{E}J_2^{(L)}$, or remains unchanged. Panel (a) and (b) show the expectation effect and the risk effect of the stochastic climate volatility on risk-free rates, Panel (c) shows the effect of climate disasters on the risk-free rate, and Panel (d) plots the time paths of the risk-free rate itself.

of volatility risk in Panel (b) will converge to zero, but this happens beyond our window of time displayed in the figures.

B.2 Risk premium

The risk premia in the business-as-usual scenario Figure 27 shows the risk premia and its climate-related components in the business-as-usual scenario in (B). Panel (a) and (b) shows the expectation effect and the risk effect of climate volatility risk, respectively. Panel (c) shows how much the risk premium is affected by climate disaster risk, and Panel (d) shows the time paths of risk premia. Compared with the BAU scenario in (A) (Figure 3), Regime (B) leads to a larger compensation for both climate disaster risk and the volatilty risk, as shown in Panel (a), (b) and (c). The expectation effect, the risk effect and the climate disaster effect contribute to risk premia in the same order of magnitude, which corroborate the main conclusion in the main body of this paper: climate volatility risk is as important
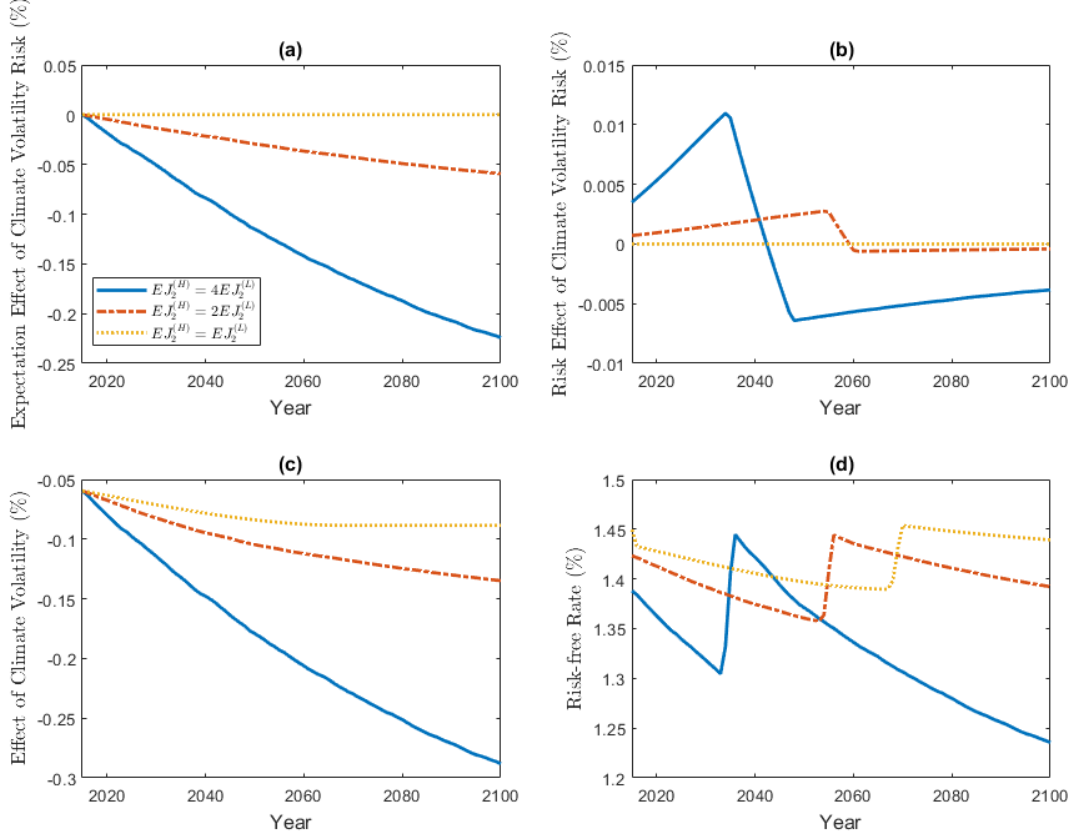
Figure 26: Decomposition of risk-free rates under optimal abatement policies under climate volatility risk (B). The expected size of one climate disaster in the new regime rises to $4\mathbb{E}J_2^{(L)}$, $2\mathbb{E}J_2^{(L)}$, or remains unchanged. Panel (a) and (b) show the expectation effect and the risk effect of the stochastic climate volatility on risk-free rates, Panel (c) shows the effect of climate disasters on the risk-free rate, and Panel (d) plots the time paths of the risk-free rate itself.

as the climate volatility itself in calculating the discount rate and the SCC.

Effects from climate volatility and the expectation effect of volatility risk rise over time, since the intensity of climate disasters increases over time and rising temperature leads to more disasters in the future. Expecting more intense natural disasters in the future, agents require higher risk compensation. The risk effect of stochastic climate volatility risk shown in Panel (b) increases in disaster frequency, because a new regime with more intense disasters poses larger threats to the economy and thus the risk compensation required by agents increases correspondingly. As the climate volatility risk gradually resolves over time, the effect of volatility risk in Panel (b) will converge to zero, but this happens beyond our window of time displayed in the figures.

The risk premia under optimal abatement Figure 28 shows the risk premium and its decomposition under optimal abatement. Panel (a) and (b) show the expectation effect and the risk effect of climate volatility risk, respectively. Panel (c) shows the effect of climate
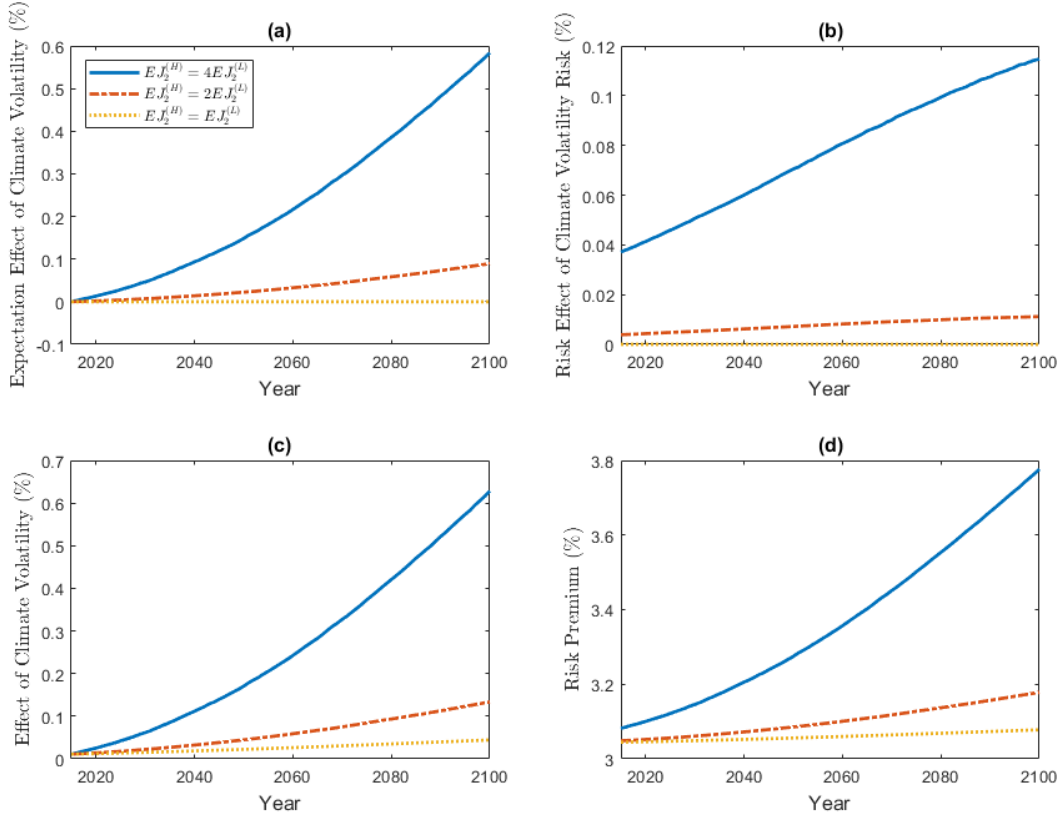
Figure 27: Decomposition of risk premia in the BAU scenario under climate volatility risk of Type (B). The expected size of one climate disaster in the new regime rises to $4\mathbb{E}J_2^{(L)}$, $2\mathbb{E}J_2^{(L)}$, or remains unchanged. Panel (a) and (b) shows the expectation effect and the risk effect of climate volatility risk, respectively. Panel (c) shows how much the risk premium is affected by climate disaster risk, and Panel (d) shows the time paths of risk premia.

disaster risk on risk premia, and Panel (d) plots the risk premia over time. The impact of climate volatility risk and climate disasters is smaller under optimal abatement than the BAU scenario because of the stringent abatement policies, but their sizes are of the same order of magnitude. This implies that climate volatility risk is as important as climate volatility itself when calculating risk premia and the SCC, regardless of abatement policy stringency.

Panel (a), (b) and (c) imply that the climate disaster risk and the climate volatility risk increase in $\mathbb{E}J_2^{(H)}$. Since the new climate regime poses larger threat to the economic condition, agents require higher compensation for the climate risk. In Panel (b), the initial and the long-run effects of climate volatility risk through the risk channel decrease over time as uncertainties about climate volatility resolve gradually, and the upward jumps happening in the middle of the century result from the kinked point in the emission control rate. Panel (d) implies that risk premia do not differ much under different climate conditions in the new regime, because emission control effectively decelerates global warming and postpones the
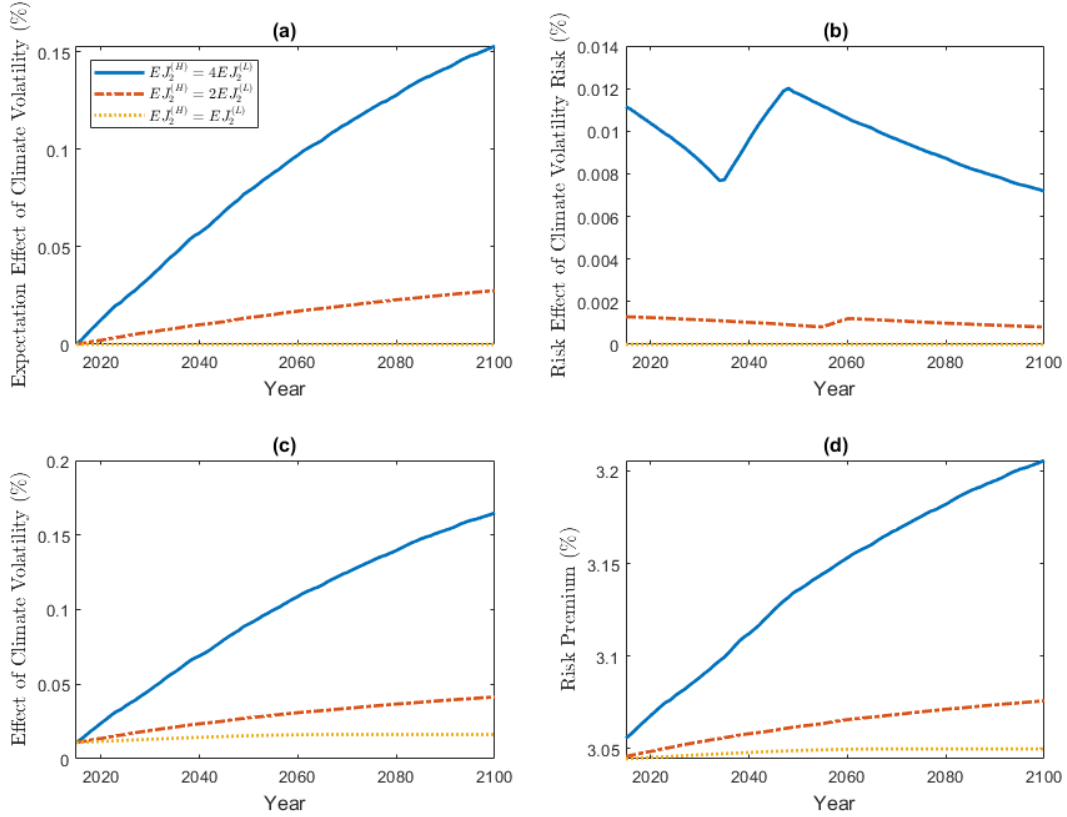
Figure 28: Decomposition of risk premia in the optimal abatement policy scenario under climate volatility risk of Type (B). The expected size of one climate disaster in the new regime rises to $4\mathbb{E}J_2^{(L)}$, $2\mathbb{E}J_2^{(L)}$, or remains unchanged. Panel (a) and (b) show the expectation effect and the risk effect of climate volatility risk, respectively. Panel (c) shows the effect of climate disaster risk on risk premia, and Panel (d) plots the risk premia over time

negative impact of climate change.

C Numerical Results under Different Arrival Rates of Climate Regime Shift

Due to the lack of time series data and credible models of climate volatility risk, it is difficult to calibrate the arrival rate of the new climate regime λ_0. In the main body of this paper, we set $\lambda_0 = 0.01$, so the expected arrival time of a new regime is 100 years which is consistent with the time horizon considered in the first IPCC reports. In this section, we consider different possible values of λ_0 (0.01, 0.02, and 0.05) in the BAU scenario under the assumption that the disaster frequency parameter in the new regime is doubled (i.e. $\bar{\lambda}^{(H)} = 2\bar{\lambda}^{(L)}$). Below we show how λ_0 affects the risk-free rate, the risk premium, and the SCC.

Risk-free rate Figure 29 shows the risk-free rate and its decomposition under $\lambda_0 = 0.01$, 0.02, and 0.05. Panel (a) and (b) show the expectation effect and the risk effect of the stochastic climate volatility on risk-free rates, Panel (c) shows the effect of climate disasters on the risk-free rate, and Panel (d) plots the time paths of the risk-free rate itself.
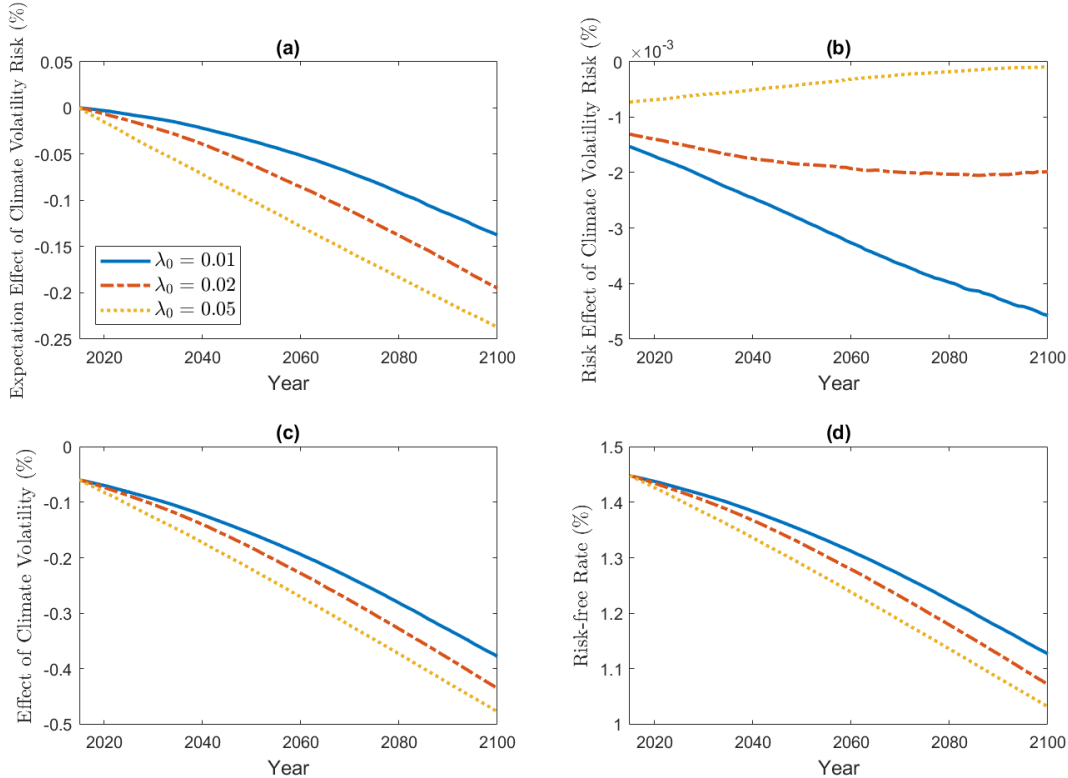

Figure 29: Decomposition of (average) risk-free rates in the BAU scenario under $\lambda_0 = 0.01$, 0.02, and 0.05, where $\bar{\lambda}^{(H)} = 2\bar{\lambda}^{(L)}$. Panel (a) and (b) present the expectation effect (Expression (3)) and the risk effect (i.e. the last term in Equation (2)) of stochastic climate volatility on the risk-free rate. Panel (c) shows the effect of climate disaster risk, and Panel (d) shows the risk-free rate over time.

Panel (a), (b) and (c) shows that both the climate disaster risk and the climate volatility

risk negatively affect the risk-free rate. Moreover, their magnitudes are larger under higher λ_0. This is because the economy is subject to more climate risks if the new climate regime arrives earlier. The magnitudes of the expected effect of climate volatility risk and the effect of climate disaster risk in Panel (a) and (c) increase over time, because rising temperature leads to more frequent climate damages and the expected climate damage increases under the stochastic arrival of the new regime. The expected effect of climate volatility risk and the climate disaster effect are of the same order, while the risk effect of climate volatility risk is much smaller.

The risk effect of climate volatility risk shown in Panel (b) is non-monotonic over time. When λ_0 is high, the uncertainty about climate regime shift is expected to be resolved in the near future and thus the risk effect converges to zero earlier. Under smaller λ_0, the uncertainty about climate regime shift is expected to be resolved later and thus the magnitude of the risk effect increases for a longer period and converges to zero in the farther future. Since the risk effect of climate volatility risk is relatively small, the risk-free rate shown in Panel (d) is largely determined by the expectation effect of climate volatility risk and the climate disaster risk. Therefore, the time paths of the risk-free rate are downward sloping.

Risk premium   Figure 27 shows the risk premia and its climate-related components in the business-as-usual scenario in (B). Panel (a) and (b) shows the expectation effect and the risk effect of climate volatility risk, respectively. Panel (c) shows how much the risk premium is affected by climate disaster risk, and Panel (d) shows the time paths of risk premia. All types of climate risks in Panel (a), (b) and (c) have positive impacts on the risk premium. The expectation effect of climate volatility risk and the climate disaster effect contribute to risk premia in the same order of magnitude, while the risk effect of climate volatility risk is smaller.

Panel (a) and (c) show that both the expectation effects of climate volatility risk and the disaster effect increase in λ_0, since agents would require higher compensation for climate risks if the new climate regime with more frequent extreme weathers is expected to arrive soon. The risk effect of stochastic climate volatility will converge to zero in the long run when uncertainty about climate volatility is resolved. In the short run, a smaller λ_0 means a later arrival of the new regime, and its effect on risk premia is larger and converges to zero in the farther future.

Social cost of carbon   Before looking at the SCC, we first present the time paths of the growth-adjusted consumption discount rate $r^{(CDR)}$ and the growth rate of expected consumption given in Equation (7). Since neither of them can be evaluated analytically, we show the numerical results from our simulation to show how climate volatility risk affects each term.

Figure 31 shows the expectation effect (Panel (a)) and the risk effect (Panel (b)) of stochastic climate volatility, the effect of climate disaster risk on the growth-adjusted consumption discount rate $r^{(CDR)}$ (Panel (c)), and the growth-adjusted consumption discount rate $r^{(CDR)}$ (Panel (d)). Negative values in Panel (a), (b) and (c) imply that both climate disaster risk and stochastic climate volatility reduce the growth-adjusted consumption dis-
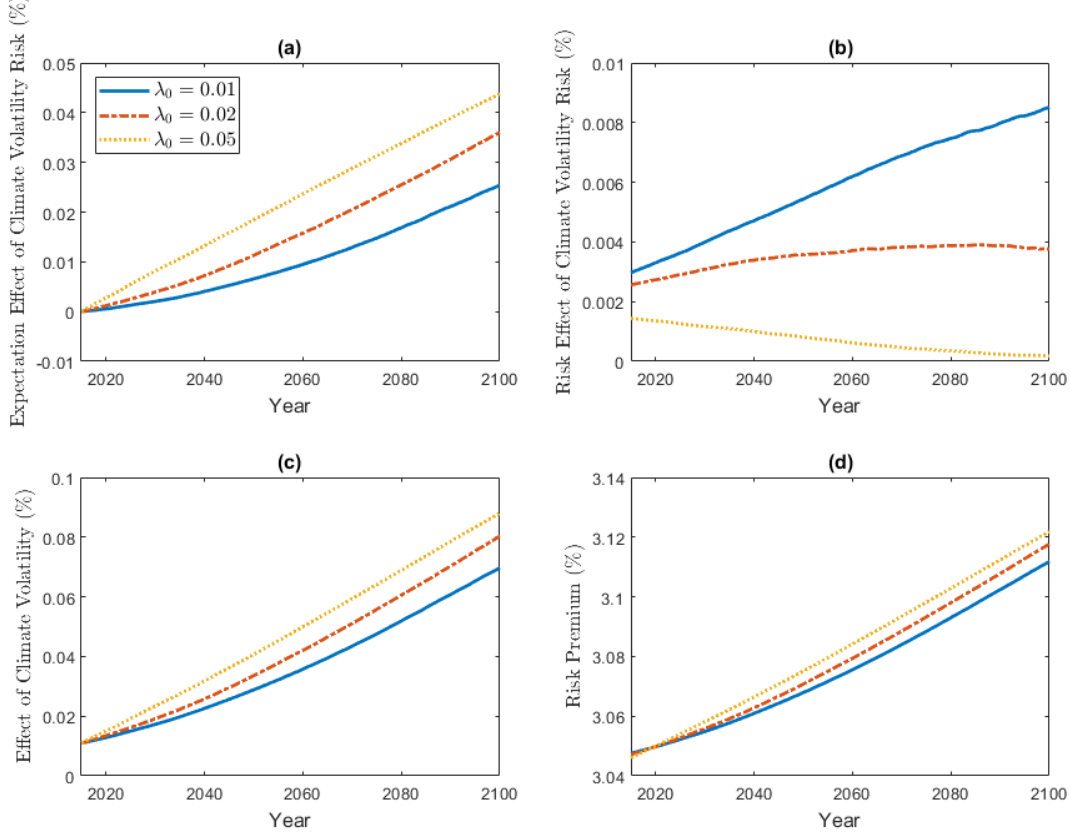
Figure 30: Decomposition of risk premia in the BAU scenario under $\lambda_0 = 0.01$, 0.02, and 0.05, where $\bar{\lambda}^{(H)} = 2\bar{\lambda}^{(L)}$. Panel (a) and (b) present the expectation effect (Expression (5)) and the risk effect (the last term in Equation (4)) of stochastic climate volatility on risk premia. Panel (c) shows the effect of climate disaster risk, and Panel (d) shows the risk premia over time.

count rate $r^{(CDR)}$, which drives up the SCC. The magnitudes of the climate disaster effect and the expectation effect of climate volatility risk increase over time under the irreversible global warming and the threat of a new regime with more severe climate conditions. Besides, the magnitudes of both effects increases in λ_0, since an earlier positive shock to the climate volatility leads to a faster deterioration of climate condition and a larger impact on the discount rate. The risk effect of climate volatility risk shown in Panel (b) converges to zero earlier under larger λ_0 when uncertainty about climate volatility risk is expected to be resolved earlier. Its magnitude is much smaller than those in Panel (a) and (c). Therefore, the downward-sloping time paths of $r^{(CDR)}$ in Panel (d) results from the climate disaster effect and the expectation effect of climate volatility risk.

Figure 32 shows the expected consumption growth over time. As suggested by Equation (8), it is affected by climate volatility risk only through the expectation channel. Under any possible value of λ_0, the expected consumption growth rate declines over time due to the deteriorating climate condition. Moreover, a higher λ_0 implies an earlier arrival of the new climate regime with more frequent disasters, which hinders the growth in aggregate
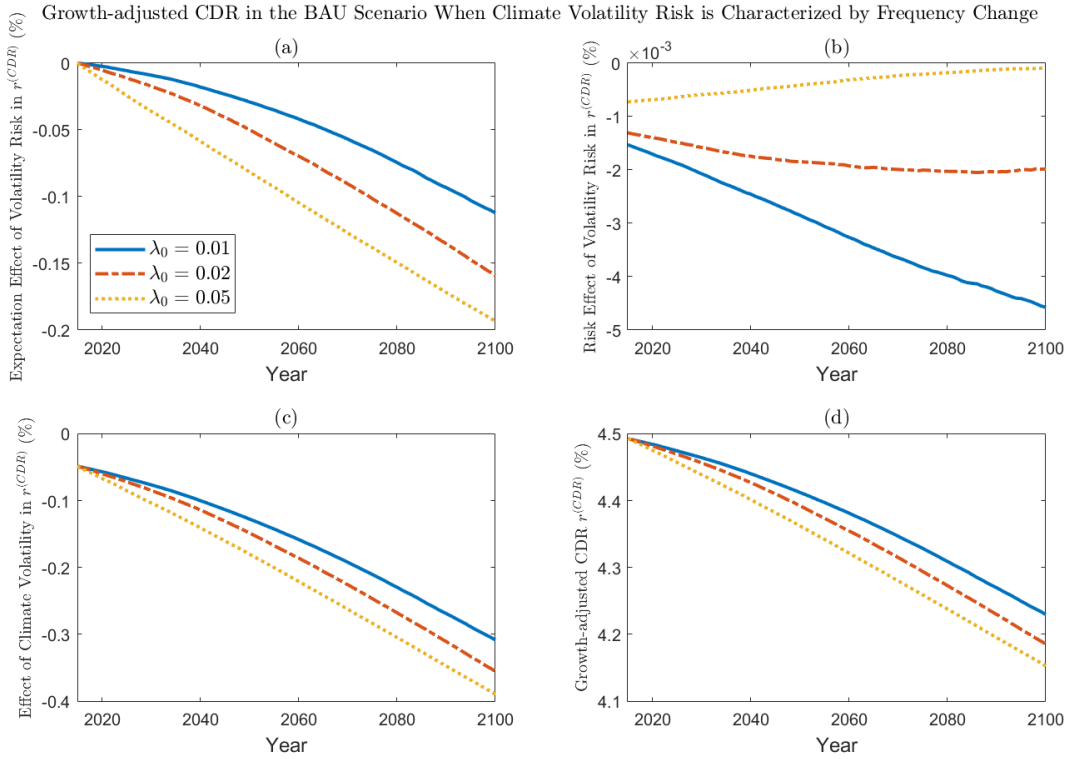
Figure 31: The expectation effect (Panel (a)) and the risk effect (Panel (b)) of stochastic climate volatility, the effect of climate disaster risk (Panel (c)) in the growth-adjusted consumption discount rate $r^{(CDR)}$, and the time paths of $r^{(CDR)}$ (Panel (d)) in the BAU scenario under $\lambda_0 = 0.01$, 0.02, and 0.05, where $\bar{\lambda}^{(H)} = 2\bar{\lambda}^{(L)}$.

endowment and consumption, and results in a lower time path of the expected consumption growth.

Figure 33 shows the average social cost of carbon and mean global surface temperature from Year 2015 to 2100 in the BAU scenario under different arrival rates of a new climate regime. Since carbon emissions are exogenously given and independent of the scale of climate damage in the business-as-usual scenario, changes in temperature is deterministic and same under all λ_0's, as shown in the right panel. The left panel shows the SCC, which is larger under a higher λ_0 but the difference is small under all λ_0's. This is because in the short run before the shock to climate volatility is realized, the welfare loss due to climate damages rises if more severe climate condition is expected to happen earlier (i.e. when λ_0 is large). However, as the uncertainty about climate regime shift is resolved in the long term, the difference in the arrival time of new climate regime is less important than the long-run climate condition in the new regime.
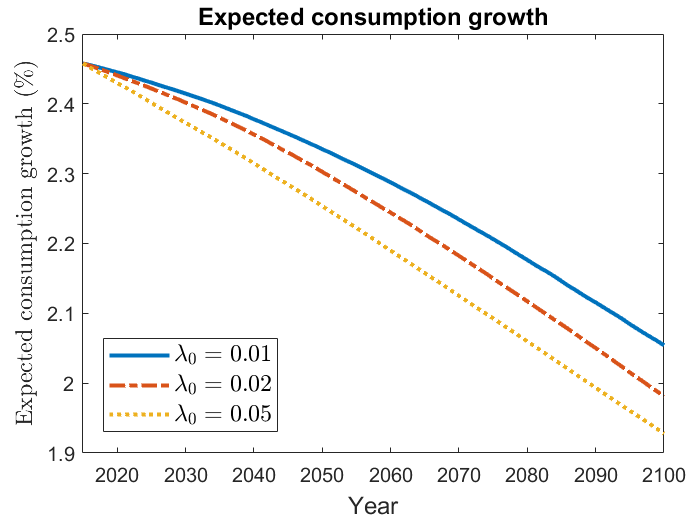
Figure 32: Expected consumption growth rate in the BAU scenario under $\lambda_0 = 0.01$, 0.02, and 0.05, where $\bar{\lambda}^{(H)} = 2\bar{\lambda}^{(L)}$.
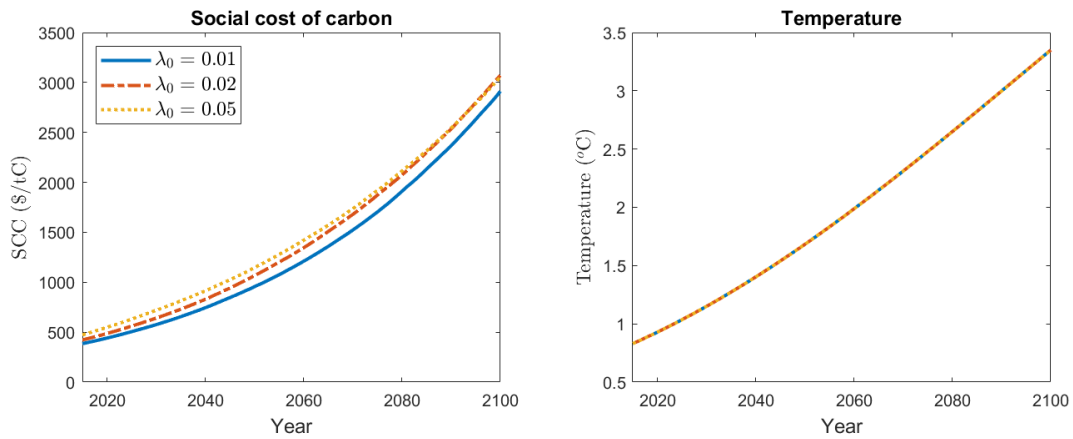

Figure 33: Social cost of carbon (US dollar per ton of carbon, or \$/tC) and mean global surface temperature ($^\circ$C) in the business-as-usual (BAU) scenario from 2015 to 2100 under $\lambda_0 = 0.01$, 0.02, and 0.05, where $\bar{\lambda}^{(H)} = 2\bar{\lambda}^{(L)}$.